TAMPEREEN TEKNILLINEN YLIOPISTO
TAMPERE UNIVERSITY OF TECHNOLOGY

ANTTI MAUKONEN

SHEATH DAMAGES OF MEDIUM VOLTAGE UNDERGROUND CABLES CAUSED BY ATMOSPHERIC OVERVOLTAGES

Master of Science Thesis

Examiner: Dr. Tech. Kari Lahti
Examiner and topic approved by the Faculty Council of the Faculty of Computing and Electrical Engineering on 9th October 2013.

ABSTRACT

TAMPERE UNIVERSITY OF TECHNOLOGY
Master's Degree Programme in Electrical Engineering
MAUKONEN, ANTTI: Sheath Damages of Medium Voltage Underground Cables Caused by Atmospheric Overvoltages
Master of Science Thesis, 81 pages, 1 Appendix pages
November 2013
Major: Power Systems and Market
Examiner: Dr. Tech. Kari Lahti
Keywords: Medium voltage, underground cable, atmospheric overvoltage, lightning, sheath fault

The investments on underground electricity distribution networks have increased fast during past few years due to new stricter regulatory terms of distribution reliability and quality in Finland. Though underground cables are usually considered totally weatherproof, in fact they have some weaknesses as well. The outer layer of modern distribution cables most usually consists of a polyethylene sheath which is designed to provide an excellent mechanical, chemical and UV-protection while still maintaining sufficient flexibility of the structure. Unlike the main electrical insulation of the cable the PE sheath is not designed primarily to take electric stress. However, in case of a lightning strike nearby the cable, a high fast front voltage stress may fall over the PE sheath.

The sheath damages caused by a lightning strike may be resulted by an electric breakdown in soil but it is not the only possible mechanism. The potential of soil always rises near the lightning strike point and it may lead to sheath punctures as well without a direct soil breakdown to cable. Three different aspects are considered in this study to evaluate the effects of lightning strikes on buried cables. In addition to the estimation of effective distances, also the levels of possible overvoltages over the sheath are estimated in this study. In the calculations of these complicated phenomena some simplifying assumptions have to be applied which cause uncertainties in the results. Especially, the assumption of homogenous electrical properties of soil is not valid in reality. As a rough estimation it can be said that the cables located closer than 10 meters from the strike point are in active danger zone.

The laboratory tests were done for cable types AXAL-TT PRO by Ericsson and AHXAMK-W and AHXCMK-WTC/PE by Reka to measure the impulse voltage breakdown strengths of the sheaths. The breakdown strengths of the sheaths are then compared to the results of theoretical estimations.

The unconnected cables with open ends should always be temporary grounded. The temporary grounding minimizes the transient wave reflections in the open ends of the cable. It is of great importance also in improving safety at work by discharging possible charge of the cable. Use of shielding ground wires above cables is a suggested preventive measure in the literature. Although the implementation of the method would increase the investment costs of the cable grid, it should be studied more. Also several other future research topics were pointed up during the study.

TIIVISTELMÄ

TAMPEREEN TEKNILLINEN YLIOPISTO
Sähkötekniikan koulutusohjelma
MAUKONEN, ANTTI: Ilmastollisten ylijännitteiden aiheuttamat keskijännitemaakaapeleiden vaippavauriot
Diplomityö, 81 sivua, 1 liitesivua
Marraskuu 2013
Pääaine: Sähköverkot ja -markkinat
Tarkastaja: TkT Kari Lahti
Avainsanat: Keskijännite, maakaapeli, ilmastollinen, ylijännite, salama, vaippavika

Sähkönjakeluverkkojen maakaapeli-investoinnit ovat kasvaneen nopeasti viime vuosien aikana johtuen uusista tiukemmista jakelutoiminnan laatua ja luotettavuutta ohjaavista valvontamalleista. Vaikka maakaapeleita usein pidetäänkin täysin säävarmoina verkkokomponentteina, todellisuudessa myös niihin liittyy omat heikkoutensa. Modernien maakaapeleiden uloimpana kerroksena on yleensä kaapelin mekaaniseksi, kemialliseksi ja UV-suojaksi suunniteltu polyeteenivaippa. Toisin kuin kaapelin sähköeristettä, PE vaippaa ei ole suunniteltu ensisijaisesti kestämään kaapelin ulkopuolelta tulevia sähköisiä rasituksia. Kaapelin metallisen kosketussuojan päällä olevaan PE-vaippaan voi kuitenkin kohdistua äkillisiä ylijännitteitä salamaniskun osuessa kaapelin läheisyyteen.

Salamaniskun aiheuttamat vaippavauriot voivat johtua suorasta läpilyönnistä maa-aineksen kautta kaapeliin, mutta myös maaperän potentiaalin nousun aiheuttama jännite ero vaipan yli saattaa rikkoa sen. Tässä työssä maahan osuvan salamaniskun vaikutuksia maakaapeleihin on arvioitu kolmesta eri näkökulmasta. Vaikutusetäisyyksien lisäksi myös vaippaan kohdistuvia jänniterasituksia on arvioitu. Monimutkaisten ilmiöiden arvioimiseksi laskennallisesti on täytynyt soveltaa yksinkertaistavia oletuksia, jotka aiheuttavat epätarkkuutta tuloksiin. Erityisesti oletus maaperän sähköisten ominaisuuksien homogeenisuudesta ei päde todellisuudessa. Karkeana arviona voidaan todeta että kaapelit jotka ovat alle 10 metrin päässä iskukohdasta ovat vaara-alueella.

Vaipan syöksyjännitekestoisuudet määritettiin seuraavista kaapelityypeistä: AXAL-TT PRO (Ericsson), AHXAMK-W (Reka) ja AHXCMK-WTC/PE (Reka). Työssä testituloksia verrataan maaläpilyönnin aiheuttaman kulkuaallon ylijännitteeseen ja maapotentiaalin nousun aiheuttamaan jänniterasitukseen vaipan yli.

Verkkoon kytkemättömät maakaapelit ovat haavoittuvia kulkuaalloille johtuen aaltoimpedanssin muutoskohdasta kaapelin päissä. Kulkuaallon heijastumisia kaapelin päissä voidaan ehkäistä kaapelin päiden väliaikaisella maadoituksella. Väliaikainen maadoitus on tärkeä myös työturvallisuuden kannalta, sillä se purkaa mahdollisesti kaapeliin kertyvän varauksen. Aiemmissa tutkimuksissa on suositeltu suojaavan maadoitusköyden käyttöä kaapelin ja maan pinnan välissä. Vaikka menetelmän käyttöönotto nostaisi kaapeliasennusten investointikustannuksia, sen toimivuutta tulisi silti tutkia suojausmielessä. Työn aikana nousi esille myös muita tulevaisuuden tutkimuskohteita liittyen keskijännitemaakaapeleiden vaippavaurioiden ehkäisyyn.

FOREWORD

This study was provided and coordinated by Elenia Oy, Ericsson Oy and Reka Kaapeli Oy together with Tampere University of Technology department of Electrical Engineering. The supervisor and examiner of the work was Research Manager Kari Lahti from the department. I would like to thank Kari for all the valuable effort and guidance during the work.

I also thank all the members of the project steering group for their expertise and interests towards the project. Special thanks go to research assistant Jouni Puikko who helped me with the cables during the laboratory tests. I would also express my gratitude to researchers of the high voltage research group at TUT for kind support.

Tampere, 22.11.2013

Antti Maukonen

TABLE OF CONTENTS

TERMS AND DEFINITIONS

Abbreviations

AC	Alternating current
CENELEC	European Committee For Electrotechnical Standardization
BD	Breakdown
CG	Cloud-to-Ground
DC	Direct Current
GPR	Ground potential rise
HDPE	High density polyethylene
HV	High Voltage
IEC	International Electrotechnical Commission
IEEE	Institute of Electrical and Electronics Engineers
LDPE	Low density polyethylene
LLDPE	Linear low density polyethylene
MDPE	Medium density polyethylene
MV	Medium voltage
PE	Polyethylene
PVC	Polyvinyl chloride
SD	Standard deviation
SF_6	Sulfur Hexafluoride
SFS	Finnish Standards Association
XLPE	Cross-linked polyethylene
TUT	Tampere University of Technology
UV	Ultraviolet

Notation

C	Capacitance
C_{HV}	Capacitance of HV capacitor
E	Electric field strength
E_0	Critical electric field strength
I	Lightning current
I_{ca}	Impact current to a cable
$I_{leakage}$	Leakage current per kilometer

I_{load}	Load current
I_m	Maximum current injected into soil
i_1	Current before the point of discontinuity of the characteristic impedance
i_2	Current after the point of discontinuity of the characteristic impedance
i_{1r}	Current of a reflecting wave
J	Current density
L	Inductance
l_{cable}	Length of a cable
P_{loss}	Effective power losses
R_D	Discharge resistance
R_E	External resistance
R_g	Ground resistance
R_I	Internal resistance
R_{sheath}	The resistance over the sheath
r	Radial distance
r_0	Hemispherical radius of soil ionization
r_1	Arcing distance
$r_{1,max}$	Maximum arcing distance
U_r	Ground potential at distance r from lightning strike point
U_{sheath}	Voltage over a cable sheath
u_1	Voltage before the point of discontinuity of the characteristic impedance
u_2	Voltage after the point of discontinuity of the characteristic impedance
u_{1r}	Voltage of a reflecting wave
Z_{ca}	Characteristic impedance
$Z_{ca,1}$	Characteristic impedance before the point of discontinuity
$Z_{ca,2}$	Characteristic impedance after the point of discontinuity
ρ_s	Soil resistivity
ΔU	Change of potential
ΔR_g	Change of ground resistance
Δr	Change of radial distance

1 INTRODUCTION

The Finnish electricity distribution infrastructure is facing major reforms during next years and decades. Investments to the grid have being speed up by the electricity market law which newly came into effect in Finland in September 2013. After the period of transition in December 2019 the network owners must achieve the new level of power distribution quality required by the standards stated on law. To be able to satisfy the new stricter standards of distribution quality and tolerated electricity outage lengths the network owners are investing vastly to underground distribution networks. This is the main reason to invest also in studies on the buried cables. Even the large scale use of buried cables is an excellent step forward towards the weatherproof electricity distribution system the underground cables also have some drawbacks.

Finnish Energy Industries forecast the total investments to the Finnish electricity distribution network to reach four billion euros during next five years. Investments by network owners during year 2013 will be almost 700 million euros. The largest single factor resulting to the growth of total investments is the increase in network underground cabling. Especially the investments to the medium voltage underground cables are expected to grow over 200% between the years 2012 and 2019 (Energiateollisuus 2013.)

In electricity distribution business these acts are generally called smart grid development which includes many aspects from markets and communication improvements to acts that enable better quality, efficiency and reliability in the electricity distribution system. Though information technology has a crucial role in the future system, many of these development goals also require large investments to the core structures of the future electric grid, such as underground cables. Today large majority of the Finnish electricity distribution network consists of overhead lines. After the last major disturbances in 2010 and 2011 network companies have hasten the building of underground network to improve the reliability of the power distribution. Some companies like Elenia have decided to build all new parts of network underground.

Usually, the larger scale the investments, the more there should be done research and gain knowledge about the objects of the investment. Although the underground lines are safe from snow, trees and wind and therefore considered a very reliable way for electricity distribution, they can still be evidently harmed by atmospheric overvoltages. Interest to this study is based on some experiences of sheath damages of underground cables not yet connected to the grid. The damages were evidently resulted by atmospheric overvoltages. Propagation of lightning currents in soil is difficult to predict because of combined effects of statistical nature of electrical breakdown process and electrically unstable and inhomogeneous characteristics of soil material.

This study was launched and coordinated by network company Elenia together with cable manufacturers Ericsson and Reka. The aim of the study is to evaluate the possibility of sheath faults of medium voltage underground cables. The impulse voltage breakdown strengths of the test cables were measured in the laboratory tests. The possibility of perforation of the cable sheath is then estimated based on the theoretical calculations. The sheath fault case of Viitasaari is used as an example case during the study. In wider perspective the harmful effects of lightning strikes are not limited to electricity distribution cables only. Telecommunication cables may get punctured as well since they have conductive layers below the sheath too.

In the second chapter the structure of modern medium voltage underground cables is presented. The cable types chosen for the laboratory tests are also introduced as well as some installation practices and regulations. Lightning phenomenon in general and flash density in Elenia operational area are discussed in the third chapter. After that in the fourth chapter there are theoretical calculations and estimations of the effects of lightning strikes on buried cables. The calculations cover three different aspects. First one is based on presumption of a soil breakdown occurrence. However, puncturing of the sheath may be possible without a soil breakdown as well. That is why there is also an evaluation of puncturing occurrence without a soil breakdown in the ground potential rise-chapter. As the third aspect, the dependence of the maximum lightning current injected to soil on soil resistivity is discussed based on some experimental studies available in literature. Last few other aspects, like behavior of travelling waves in the cable shield, are pondered without further calculations. In the fifth chapter the setup and results of the breakdown strength tests are presented. The example sheath fault case is presented in the sixth chapter. There is also discussion on the sheath fault detection method used by Elenia and preventive measures for protecting the underground cables from sheath punctures. At last the conclusions of the study and topics for the future research are discussed.

2 MEDIUM VOLTAGE UNDERGROUND CA-BLES

In this chapter, there is an introduction to MW underground cables in general and losses occurring in the cables. Their structure is presented in more detail. After that the cable types used in this study are introduced. Lastly the regulations and practices of cable installations are discussed.

In Finland we have established practice to use 20 kV phase to phase nominal voltage level as a main MV distribution voltage level. The highest voltage for equipment (U_m) is actually 24 kV in those networks according to IEC- 60071-1 standard while the corresponding power frequency test voltage (1 min) is 50 kV and lightning impulse test voltage 125 k (1,2/50 µs) (IEC 2006). Anyhow, some other MV voltage levels like 10 kV can still be found in old regional parts of the distribution network. In safety at electrical work standards, Finnish SFS 6002 and international CENELEC EN 50110, the term MW is not defined as well as in many IEC standards. Thus, phase to phase nominal voltage levels over 1 kV AC and 1.5 kV DC are widely treated as HV voltage levels in Europe. The term medium voltage is still generally used in Finland and will be used also in this thesis. IEEE uses the term for voltage levels between 1 kV and 35 kV (IEEE 2002). In Finnish SFS 6001 (SFS 2009) standard underground cables having equal or less than 45 kV nominal voltage (52 kV largest operating voltage) are called medium voltage underground cables.

MV voltage level is designed for transferring electrical energy from a substation closer to end-users. This function is reasonable to carry out by using a high voltage level to minimize effective power losses caused by the current flowing in the conductor. Effective power losses are directly proportional to the square of the load current and can be written as

$$P_{loss} = RI_{load}^{\ 2}, \tag{2.1}$$

where P_{loss} is the effective power loss and I_{load} is the load current. R is the resistance of the cable or the conductor where the power losses turn into dissipated heat.

On the other hand, the higher the voltage level is, the higher are the system requirements for the electrical insulation. Even if the implementation of high voltage level reduces effective power losses, required insulation materials and elements usually make the network investment a lot more expensive. In addition to the required distribution line length, the total resistance of the line also depends on the chosen cable type and its conductor's cross-sectional area. That is why the decision of the appropriate voltage level has to be done by taking the required distribution distance into account as well.

Highly capacitive nature of underground cables also inflicts power losses due to capacitive current. In addition, conductivity and polarization phenomena of the cable insulation causes dielectric losses, but these are usually negligible compared to other loss mechanisms. Load current also creates a magnetic field around the conductor. If the cable has a metallic shied that is grounded in several points forming an electrical loop, the magnetic field induces a current to flow also in the shield. That current causes shield losses. In addition to economic harms, the losses decrease load carrying capacity and increase voltage drop in the cable. (Thue 1999.) Because this study concentrates mainly on lightning damage mechanisms in the cable, these loss phenomena will not be discussed in more detail.

2.1 General structure

A modern MW underground cable consists of several components designed for different purposes. The structure and form of components can vary between different cable types, although the basic function of at least the most crucial components remains same. The general structure and the components of a MW cable are presented below in the figure 2.1. Cable type AHXAMK-W is used as an example in the figure. Although the structure may slightly differ between cable types, they all have mainly the same components included within. More detailed introduction to these main components of the MW underground cable is given in the following.

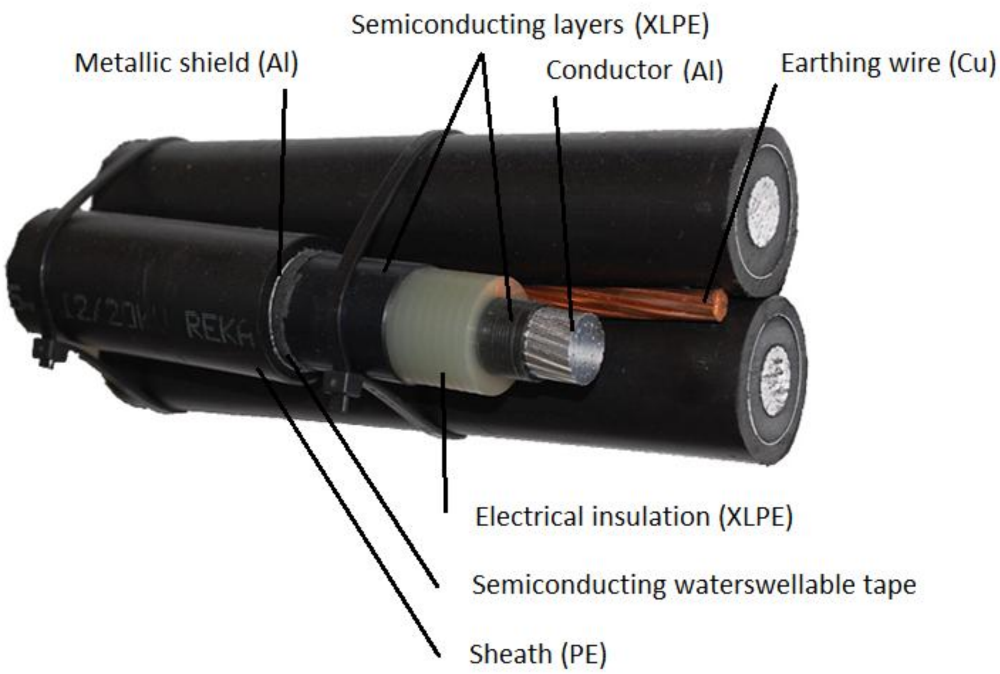

Figure 2.1. *Structure and components of a MV underground cable (AHXAMK-W).*

2.1.1 Conductor

The inner core of the cable is the conductor, which is designed to provide a path for the load current. The conductor is usually composed of small wires that are stranded together to prevent the skin effect and to make the cable more bendable. Different stranding forms or methods are: concentric, compressed, compacted, segmental and annular (Thue 1999). The skin effect forces the current to flow near the edges of the conductor at AC but using several wires instead of one solid conductor, its effect can be reduced. There is also a practical reason for stranding: When the cross-sectional area of the conductor rises, a solid conductor becomes too rigid for installation needs. The cable must be also flexible enough to be transported on cable reels.

As the name indicates, material used in conductor must have a good conductivity. In the modern cables used in electricity distribution, the conductor material is either copper or aluminum. Aluminum is the most used conductor material in MV cables because of its significantly lower market price when compared to other highly conductive metals like copper. The cost of the material is the main reason that prevents even more conductive materials to be applied in electricity distribution cables.

2.1.2 Insulation

The insulation is a highly resistive component that is included in the cable structure to keep the current in the conductor. In modern MV cables various types of polymers are often used as an insulation material. In every cable type chosen for this study cross-linked polyethylene is used as an insulation material. The abbreviation of cross-linked polyethylene is XLPE. In this context cross-link means chemical bond that joins two polymer chains together. As for polyethylene, it is the most manufactured plastic in the world that is also called polyethene or polythene. The abbreviation of polyethylene is PE. Since polyethylene is used also in the sheath, there will be closer look at it later in this chapter.

2.1.3 Shield

According to Thue (1999) the main functions of the metallic shield in a cable are to provide a low resistance path for charge and fault currents. In addition to that the shield is useful for preventing electrical accidents. That is why in Finland the shield is also called generally a protection against accidental contact. Like the conductor, the shield is usually made of aluminum or copper and is wrapped around the insulation in form of foil or wires. The metallic shield made of aluminum-plastic laminate often works also as a radial waterbarrier and protects the inner parts of the cable from the moisture (Reka Cables 2013).

2.1.4 Sheath

The outer jacket, usually called the sheath, is the most crucial component of the cables in this study. The main function of the sheath is to protect the cable against mechanical and chemical stresses and moisture.

Because most of the modern cables have a polyethylene sheath, it is the only sheath material under further discussion. Polyethylene (PE) has been a popular sheath material since its commercial breakthrough in about 1950. PE has the best moisture resistant abilities of all non-metallic sheath materials (Thue 1999). In modern cables carbon black polyethylene compound is often used, because of its good sunlight protection properties. Even if the majority of the cable length is underground away from sunlight, there is often part of the cable exposed to ultra-violet degradation for example near cable terminations. In table 2.1 the PE sheath materials are categorized in three different classes according to their densities. (Thue 1999.)

Table 2.1. *PE sheath materials categorized with the density.*

class	density (g/cm^3)
low density PE (LDPE)	0.910 – 0.925
medium density PE (MDPE)	0.926 – 0.940
high density PE (HDPE)	0.941 – 0.965

Traditionally low and medium density polyethylenes have been manufactured in high pressure and high density polyethylenes in low pressure. While the manufacturing processes have been developed further it has become possible to manufacture low and medium density polyethylenes by low pressure process as well. This modern PE sheath material is called linear low density polyethylene LLDPE. It is the most popular modern sheath material since it has better stress-crack abilities than MDPE and HDPE (Thue 1999.)

According to Thue (1999) density of the sheath material affects the crystallinity, hardness, melting point, and general physical strength of the sheath. Also molecular weight distribution influences the processing and properties of the polymer. Polyethylene has the best moisture resistivity properties of all non-metallic sheath materials. That is one of the main reasons for its popularity in the field. (Thue 1999.)

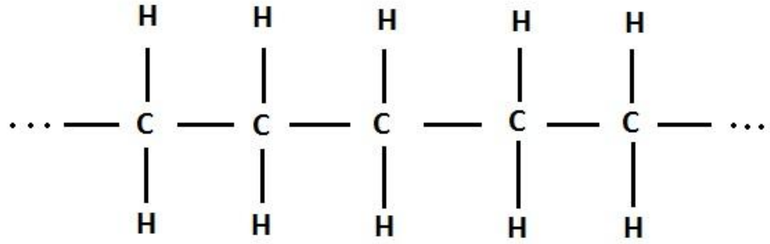

Figure 2.2. *Simplified chemical structure of PE chain.*

Polyethylene is hydrocarbon polymer, which means it is comprised of carbon and hydrogen. It can be processed by chaining together ethylene molecules as in the simplified presentation above. True nature of PE is more complex than shown in the figure 2.2. (Thue 1999.)

2.1.5 Semiconducting layers

There are usually two separate semiconducting layers in a cable. They are mostly made of semiconducting plastic. The first one is called the conductor screen. It is extruded around the pale conductor. Its purpose is to afford a smooth interface between the conductor and the insulation. Without the conductor screen even a small sharp angle in the conductor would distort the electric field and cause local electrical stress concentration. (Thue 1999.)

Another one of the two semiconducting layers is extruded around the main insulation and is generally called an insulation screen and “hohtosuoja” in Finnish. It is basically made to serve the same function as the conductor screen, to smoothen the electrical field and the interface of the two surrounding components (Thue 1999).

In addition to these two semiconducting screens, the cables also include a component, which is designed to assure the longitudinal waterproof abilities of the cable. In Reka cables it is called a semiconducting waterproof band and in AXAL-TT by Ericsson the same ability is achieved by means of swelling powder and swelling yarn (Ericsson 2013a).

2.2 Cables chosen for tests

The choice of cable types used in laboratory test was made by the orderers of the study. All of the following types are commonly used in Finnish medium voltage distribution network. AXAL-TT by Ericsson is mainly used by Elenia and it is the cable type damaged in "Viitasaari case" described in the sixth chapter. However, it is reasonable to include few more usual cable types to the study since the failure phenomenon is not limited to any particular cable type.

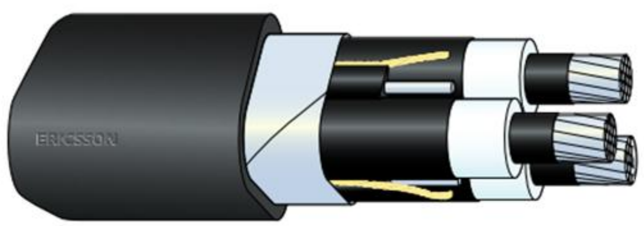

Figure 2.3. *AXAL-TT PRO by Ericsson (Ericsson 2013a)*

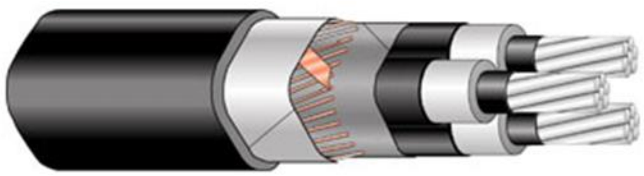

Figure 2.4. *AHXCMK-WTC/PE by Reka (Reka Cables 2013)*

Figure 2.5. *AHXAMK-W by Reka (Reka Cables 2013)*

In figures 2.3, 2.4 and 2.5 the medium voltage cable types chosen for the study are presented. The upmost is AXAL-TT PRO produced by Ericsson. In this type as well as in AHXCMK-WTC/PE by Reka there is a shared shield and sheath for all three phases. In the beginning of the project, the AHXAMK-WP was chosen for the tests as well. In both AHXAMK-W and its variant AHXAMK-WP by Reka all three phase conductors are sheathed and shielded separately. The fully protected phase conductors are then stranded together. However, the only difference between these two models is the earthing conductor made of circular stranded copper that is included only in the AHXAMK-W.

Unlike the other cable types that have an aluminum foil as a shield, the metallic shield of AHXCMK-WTC/PE consists of helically applied copper wires with a copper tape counter helix. Since AHXCMK-WTC/PE has copper wires as shield components, it lacks radial waterproof ability usually provided by a foil formed shields. Thus AHXCMK-WTC/PE is not the best option for wet underground conditions. However, it is better than for example AHXAMK-W to surface installations because of its stronger structure against the forces of short circuit (Simonen 2009). The three other cables with an aluminum foil as a shield are both longitudinally and radially waterproof and suit excellently in wet conditions as well. They are also excellent for plowing because of the hard water resistant PE outer sheath. However, none of these cables are meant for permanent submarine installation. PE sheathed cables are generally not suitable for public indoor installations either because of the poor fire and heat resistant abilities of PE. The exact composition of sheath material is usually a commercial secret and not available publicly.

According to Mutru (2013) the outer sheath thickness of a cable may vary for example between 3.0 and 3.2 mm when the nominal thickness is 3.0 mm. During the manufacturing process it is ensured that the sheath thickness is at least at its nominal level. The PE material is extruded around the cable. The sheath thickness values of the cross-section are measured from six points at intervals of 60 degrees starting from the thinnest point. The average values must not be under the nominal value of thickness. In longitudinal direction the thickness of the sheath does not vary as much as in the different points of the cross-section. (Mutru 2013.)

The further definition of standard measuring methods of sheath thickness is presented in the CENELEC standard HD 605. Allowed deviation from the nominal thickness for a XLPE insulated medium voltage power cable is quantified in the standard SFS 5636 (SFS 2008). The tolerance is dependent on the shape of the surface where the sheath material is extruded. On smooth cylindrical surfaces the thickness must not differ more than 0.1 mm + 15% of the specified value. However, the average thickness shall not be less than the specified value of the cable. For the sheath applied over a cable with uneven surface the maximum difference is limited to 0.2 mm + 20 % of the specified value. On these geometrics the average thickness must still not be lower than the specified value of the cable. (SFS 2008.)

Table 2.1. *Standards sheath thicknesses on cables with irregular and smooth cylindrical surface*

	AHXAMK-W 3x95+35CU	AHXCMK-WTC/PE 3x95+25CU
Maximum difference from the nominal value	0.1 mm + 15% of nominal value	0.2 mm + 20% of nominal value
Nominal value (mm)	2.9	3.0
Thickness max (mm)	3.435	3.8
Thickness min (mm)	2.365	2.2

The surface of AHXAMK-W is obviously a smooth and cylindrical by the sheath extrusion structure. The nominal sheath thickness of AHXAMK-W 3x95+35 is 2.9 mm. The thickness at any place is then allowed to be 3.435 mm as maximum and 2.356 mm as minimum. AHXCMK-WTC/PE has uneven irregular cylindrical surface when looked at cross-section. For example the average thickness of AHXCMK-WTC/PE 3x95+25 can be 3.8 mm as maximum and 2.2 mm as minimum for the nominal thickness of 3.0 mm. For the both geometries the average thickness still must not be below the nominal value (SFS 2008). However, the manufacturing tolerances set by manufacturers may be narrower than the standardized limits.

AXAL-TT is also classified as an irregular cylindrical surfaced cable. The sheath of AXAL-TT is made of two PE layers. The thinner one of them, outer HDPE layer, is mechanically very strong while the inner one is composed of more traditional LLDPE material. The nominal thicknesses are 3.6 mm for the inner and 0.5 for the outer sheath layer. Thus the total nominal thickness of AXAL-TT sheath is 4.1 mm. This is significantly more than the sheath thicknesses of AHXAMK-W and AHXCMK-WTC/PE. (Jägerskiöld, 2013.)

2.3 Underground installation regulations and practices

Requirements for MV cable installations in Finland can be found in SFS 6001 + A1 + A2 (SFS 2009) standard for high-voltage electrical installations. An advisable laying depth of a MV cable is 0.7 m, which is the same for low voltage cables as well (SFS 2009). Mechanical protection of MV cables is recommended to be made similarly as for unshielded low voltage cables defined in standard SFS 6000-5-52. That means usage of plastic pipes or half pipes as conduits for the cables in installation conditions where extra mechanical protection is needed. However, the need of mechanical protection can be evaluated case-specifically. The cable laying itself can be done in couple of different ways. The choice of the applied method is done in advance during the work planning.

Today the plowing technique is the most common way to lay a MV cable into ground. This is because of the usually high cost efficiency of the method when the site and circumstances are suitable. The cost efficiency comes as a result of a faster excavator work compared to the digging method. In this method the cable is laid using a cable plow as a special tool for this purpose. The plow is usually installed to an excavator and it opens the soil enough for the cable to be laid. However, this method may be violent for the cable since it increases the mechanical stress focused to the outer sheath of the cable. That is why the sheaths of the cables designed for plowing are made of harder material that can take more stress during installation and usage. The exact conditions of the soil where the cable is plowed are often more or less unknown. There may be sharp objects that wear down the surface of the sheath. To make the plowing smoother the cable route can be first preplowed without the cable attached. This is a procedure also to confirm that the required laying depth is reached. Best sites for plowing are fields, sides of the roads and other soft enough terrain.

As an alternative the digging method can be used. In this method the conditions in the cable trench are visible. Since the trench must be opened and closed, the stage of excavator work is usually significantly slower and more expensive. This is why it is mainly used in cases where the plowing is not possible for some reason. If the cable route is taken across bare cliffs, neither of previous methods can be used. In these cases the cable is usually covered with concrete.

3 ATMOSPHERIC OVERVOLTAGES

Haluza (1996) determines lightning as “an abrupt transient high current electrical discharge in the atmosphere”. In this chapter this natural phenomenon closely related to the aim of the study is discussed. At first the cloud to ground (CG) lightning phenomenon is described and discussed. In this case there is no interest towards other flash types like intra-cloud or cloud to cloud lightning strikes since they have no effects on the objects on the ground. After formation of CG lightning strike is described the annual lightning activity is roughly estimated in Elenia operational area.

Generally overvoltages can be generated due to either external or internal action. External reasons are often atmospheric discharges, while internal ones refer to system fault initiation or extinction in electric grid (Kuffel et al. 2000). Overvoltages are recommended to be categorized according their form. However, in this study only fast-front overvoltages that usually are caused by a lightning strike are examined. Other types of overvoltages are temporary, slow front and very fast front overvoltages. (Aro et al. 2003, p. 243.) Generally the birth of atmospheric overvoltage caused by a lightning discharge is divided in three mechanisms: direct strike mechanism, back flashover mechanism and induced overvoltage mechanism (Aro et al. 2003). This classification fits best for atmospheric overvoltages in overhead lines. Lightning may cause overvoltages also in the underground cables either due to lightning strikes hitting close to the cable or in the form of surges travelling to the cable from the overhead network.

Although lightning usually occurs in and around thunderstorms it can be associated with different natural phenomena like sandstorms and volcanic eruptions as well (Haluza 1996). In terminology a lightning flash refers to a lightning discharge which may consist of multiple subsequent lightning strikes via the same discharge channel.

3.1 Cloud to ground lightning

In this context only lightning in the form of cloud to ground (CG) strike is interesting, despite of the fact that only a minority of lightning strikes finally hit the ground. The majority of lightning discharges occur between clouds or within a cloud. In Finland this majority is about 60-70 percent and in tropical area about 85 percent (Aro et al. 2003). Although a lightning flash looks like a single discharge to the eye, there are actually repeat or multiple discharges in most cases. The first strike is usually followed by repeat strikes that follow the same discharge channel opened by the first strike. They can be captured with a high-speed photography. The later strikes do not branch like the first one. Although a lightning strike has huge power due to its high voltage and current levels, the energy content of it is relatively small because of the short duration of each strike discharge. The duration of main strike and any subsequent strike is on the order of 100 µs. Majority, about 98 % of the energy of the strike is used to an explosive expansion of the air in the discharge channel. (Aro et al. 2003.)

Lightning discharges are usually classified according to their polarity and direction of propagation. In this context the direction refers to the stepped leader not to the main strike. These are always opposite to each other in direction. As it is told below in more details, the stepped leader is the discharge that forms the discharge channel for the use of the following main strike. The polarity is determined by the polarity of charge distributed from cloud to the discharge channel. Hence, there are four different possible combinations of lightning polarity and direction of propagation. The combinations are showed in figure 3.1. However, only the two combinations in upper fourths are actually interesting because upwards propagative lightning strikes are typically induced only by extremely high structures like telecommunication towers. In Finland upwards initiated strikes are not a threat for electricity distribution system, since there are no overhead lines or underground cables in high enough conditions. (Aro et al. 2003.)

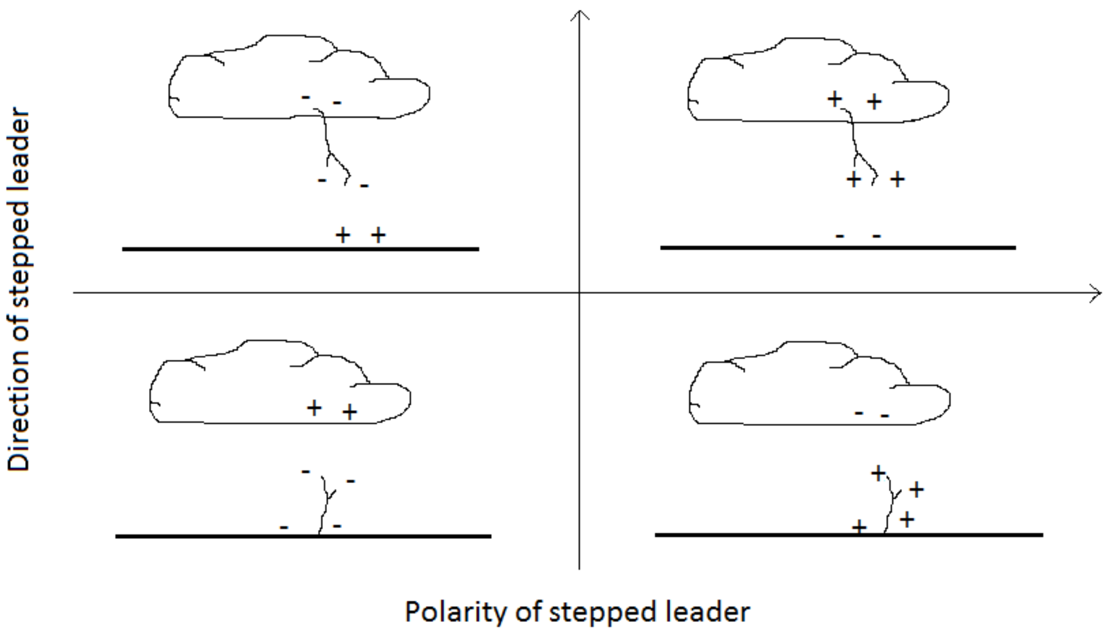

***Figure 3.1**. The four combinations of flash classified according to direction and polarity.*

In Finland majority of about 80 percent of downward directed CG flashes are initiated from negative charge (Mäkelä 2012, 2011). About 45-55 percent of these consist of only one strike. The number of subsequent strikes of the rest can differ radically. The average number of subsequent strikes three (Aro et al. 2003.)

Positive CG lightning strikes are typical in the final stage of a thunderstorm and can be detected during all seasons (Aro et al. 2003). In Finland thunderstorm activity in winter is low. Positive CG discharges are relatively rare in summertime, when most of the damages by thunderstorms usually take place. Still a positive strike has more potential to cause damage to electricity distribution infrastructure due to its usually higher peak current. Lightning strikes with positive polarity are more rarely followed by subsequent strikes than negative strikes. During 2011 about 88 and 2012 about 85 percent of positive strikes were single strikes in Finland (Mäkelä 2012, 2011). Six different stages can be recognized in the cloud-to-ground lightning incident. These stages are indicated in figure 3.2 for the most typical, negative polarity strike. A negative polarity flash is used as an example in following. The positive polarity can be described similarly.

During the first stage (a) of a negative cloud to ground lightning, a negative leader discharge moves rapidly downwards from a negative charge center of a cloud. It is called a stepped leader according to its tendency to proceed in steps of 50 m to 100 m. In the tip of the discharge goes a pilot streamer that is followed by the stepped leader. An average velocity of both is about 0.1 m/μs. The leader carries some 100 A current, when the pilot streamer carries only few amperes. When the leader comes closer to earth (b) the magnitude of the electric field increases and positive point discharges from tall objects start to form. The final destination of the strike on the ground is not determined until the discharge is about 100-150 m away from the ground (Aro et al. 2003). With a high enough charge concentration in the earthed object, a positive pre strike is initiated upwards, towards the negative discharge channel. When the discharges meet, a heavy return streamer from earth to cloud forms (c). It is generally called a main strike or a return strike. It has speed of about 100-250 m/μs and its current varies from few amperes to hundreds of kiloamperes (Aro et al. 2003). Glowing plasma in the discharge channel makes the lightning luminous and is responsible for the visible effect we are used to call a lightning. The temperatures within the discharge channel are between 15 000 °C and 20 000 °C. (Kuffel et al. 2000.)

When the first, previously negative charge center of the cloud is now completely discharged via the main strike, a positive charge center is formed in its place (d). There can be discharges between the positive charge center and other negative discharge centers of the cloud, that leads to a new discharge from negatively charged cloud to positive ground via the same discharge channel (e). Compared to the first strike there is no need for stepped leader anymore when the discharge channel is once opened. Instead of stepped leader the initiator of subsequent strikes is called a dart leader because of its dart-like appearance. It follows the opened discharge channel without branching and distributes negative charge along its path. The dart leader is much faster than the stepped leader which once opened the discharge channel. Then a subsequent strike can end up to a heavy return streamer (f) and a return strike from ground to cloud that distributes positive charge to the charge center of the cloud. Thus the first discharge can be followed by several other discharges called subsequent strikes. (Kuffel et al. 2000, Aro et al. 2003.)

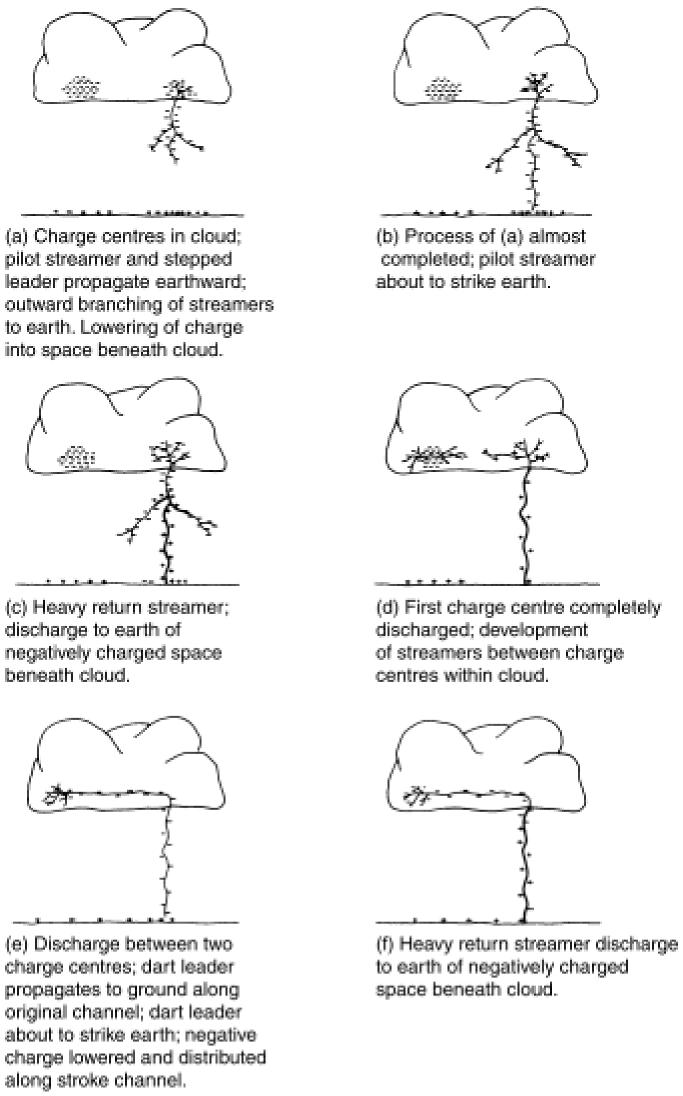

Figure 3.2*. Schematic representation of various stages of lightning strike between cloud and ground (Jolly 1972, cited in Kuffel et al. 2000)*

3.2 Flash density in Finland and Elenia operational area

The Finnish meteorological institute gathers and governs data of annual lightning statistics in Finland. Today the lightning data is gathered in cooperation with Sweden Norway and Estonia. The countries still have their own location networks but when joined together they form the Nordic Lightning Information System, NORDLIS. This collaboration makes the system performance significantly better in many ways. In 2002 there were 30 lightning location sensors in the system (Mäkelä 1012).

In figure 3.3 the area of Finland is presented in regional squares to illustrate the annual national distribution of lightning strikes during years 2010, 2011 and 2012. The numbers in the squares refer to the number of first strikes in that area. The subsequent strikes are not counted in. The regional numbers are reported per 100 km^2 in the picture.

For example in Hanko area, in south coast of Finland, a total of 1136 flashes were located in 2012 which corresponds to 90 flashes per 100 km^2 since the area of Hanko is 1257 km^2 (Mäkelä 2012). The total numbers of flashes on the map areas were 167 712 in 2012, 180 539 in 2011 and 78 000 in 2012. (Mäkelä 2012, 2011, 2010) Åland islands have been left out from the maps of figure 3.3 to save space but they are included in the calculation of total number of located flashes over the map areas. From the figure below it can be seen that the number of annual flashes is varying significantly both locally and nationally.

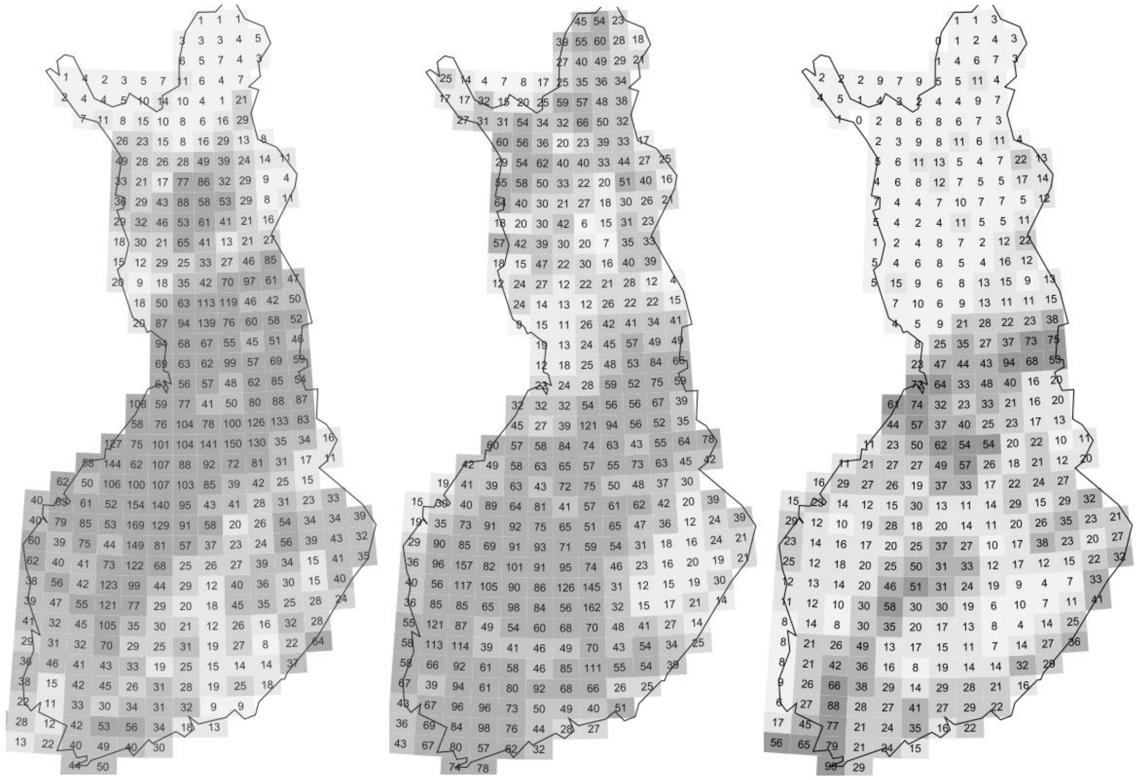

***Figure 3.3**. Located flashes per 100 km^2 in 2010 (left), 2011 (middle) and 2012 (right) (Mäkelä 2012, 2011, 2010).*

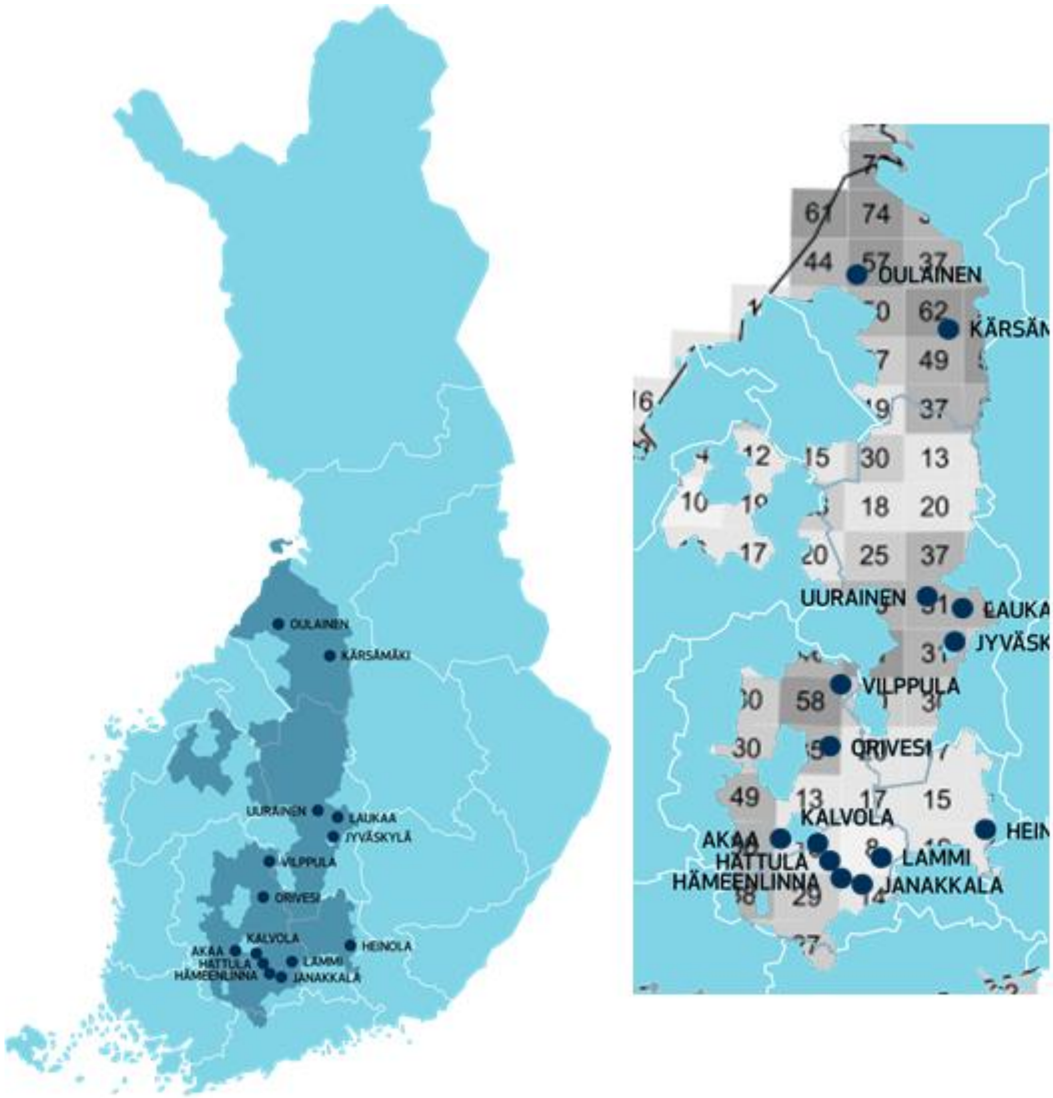

Figure 3.4. *On the left: Operational area of Elenia (www.elenia.fi/yritys/toimialuekartta). On the right: Located flashes per 100 km^2 in Elenia area in 2012.*

In the figure 3.4 above the operational area of Elenia is shown on the dark blue color in the left picture. Since Elenia has a wide operational area reaching from Tavastia to Northern Ostrobothnia, the characteristic weather conditions differ significantly between different places. The amount of annual flashes in Elenia operational area can be estimated by laying these annual lightning statistics on the operational area map. The statistics of the year 2012 are positioned on the operational area map in the right picture of figure 3.4. During the year 2012 the lightning activity was highest in the regions near Oulainen, Kärsämäki and Vilppula where the number of located flashes reached the frequencies of over 50 flashes per 100 km^2.

However, statistically more interesting data can be found in the figure 3.5 below. Here the surface area of Finland is divided to the squares of 10 km x 10 km to examine the local lightning activity more precisely. The statistics of 14 years instead of one give more valuable data when examining the local flash densities because annual flash densities vary significantly as seen in the figure 3.3.

Now the flash densities can be examined more accurately because the mean location accuracy is sufficient by the squares of 10 km x 10 km. However, when the number of flashes per square is reduced, the noise is caused not only by climatic and topographic variation but also random weather variation starts to take effect. This random noise is not totally smoothed by 15-year averages. (Mäkelä 2012.)

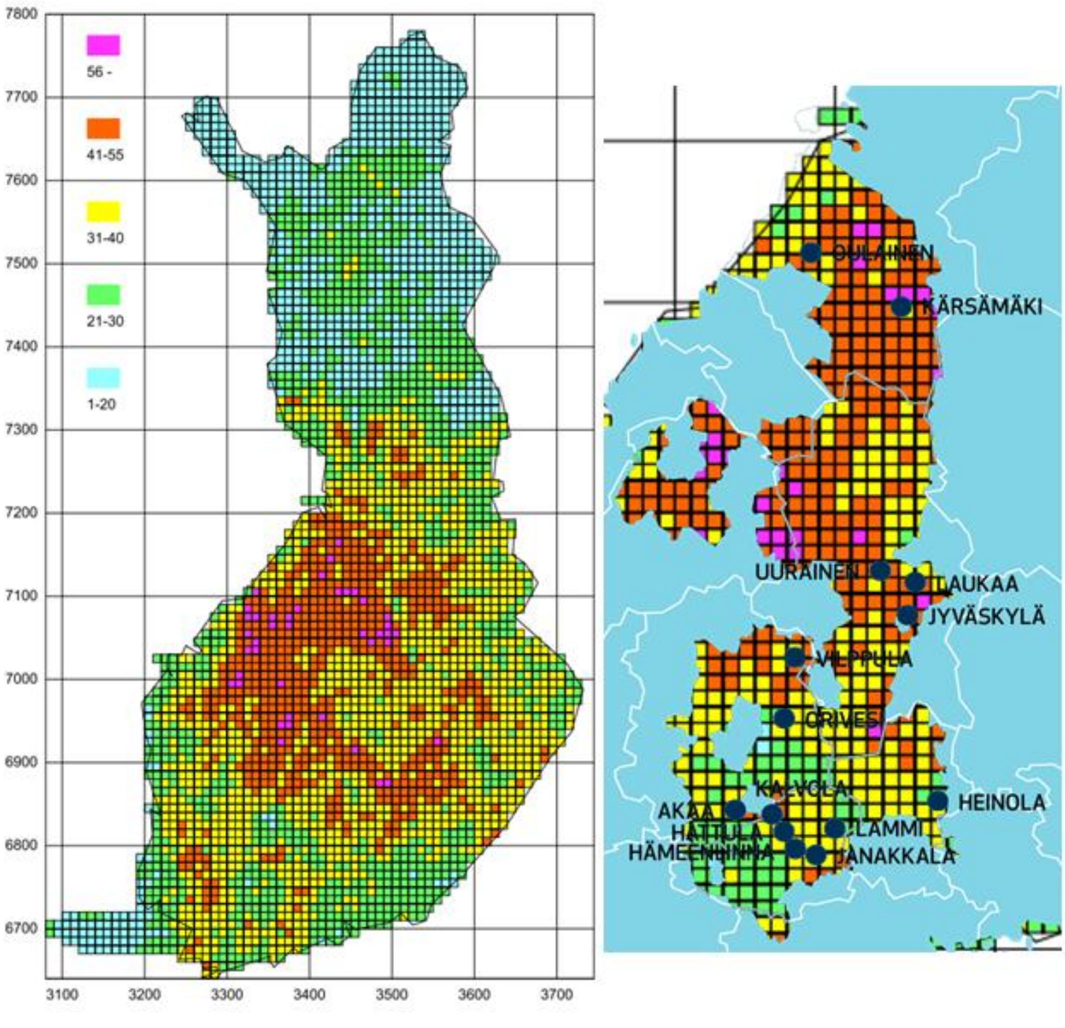

Figure 3.5. *On the left: Annual flashes on 10 km x 10 km squares during years 1998–2012 (Mäkelä 2012). On the right: The picture on the left positioned on the Elenia operational area.*

Based on the figure 3.5 the average annual lightning activity in Elenia operational area can be estimated. In the table 3.1 below a rough calculation of the number of different flash density squares in Elenia operational area is given. Based on the average number of flashes per squares and the number of squares with different densities a calculation of the approximate total amount of flashes in the whole Elenia area is given. For the purple squares the average of flash number is set conservatively to the lowest value.

Table 3.1. *Approximated annual flash activity in Elenia operational area.*

Colour	Flash number	Flash number in Av.	Squares	Flashes in Elenia area
Purple	56–	56	22	1232
Orange	41–55	48	54	2592
Yellow	31–40	35.5	172	6106
Green	21–30	35.5	193	6851.5
Blue	1–20	10.5	2	21
Total			443	16802.5

The operational area of Elenia is approximated to be roughly 44300 km^2 based on the number of squares. In table 3.2 the flash activity in the vicinity of MV cables over the operational area is approximated. When the total number of flashes in operational area is distributed equally to the area the average density of flashes can be evaluated. To take the approximation further a percentual part of the area close to the MV cables is estimated. Although only about 0.12 percent of Elenia operational area is 10 meters away or closer to a MV cable there is annually about 20 flashes in that area. The approximative characteristics of this number cannot be overemphasized but it is evident that some flashes hit the ground close to MV cables every year.

However, lightning usually strikes to tall objects like trees instead of flat ground. In these situations the roots of the tree may drive the current in several direction.

Table 3.2. *Approximated annual flash activity near MV cables in Elenia operational area.*

Flashes in operating area	16800
Elenia area (km^2)	44300
Flashes per 1 km^2 in average	0.38
Flashes per 100 km^2 in average	37.92
Total lenght of Elenia MV grid (km) (12% cabled)	22700
Lenght of Elenia MV grid, cabled (km)	2724
Area in the vicinity of MV cables (km^2, ≤10 m from the cables)	54.48
Part of operational area near to cable (%)	0.12
Flashes in the cable area in average	20.66

Table 3.3. *Flash activity in the Elenia future grid with 70 % cabling rate.*

Length of future MV grid, cabled (70 % cabling rate)	15890
Area of max. 10 m away from MV cable (km^2)	317.80
Part of operational area near to cable (%)	0.72
Flashes in the cable area in average	120.52

Elenia has set their goal to raise the rate of cabling to the 70 percent during next 15 years. A dramatic change like this naturally raises the probability of flashes to hit the ground near underground cables. In table 3.3 an evaluation of the flash frequency near the MV cables in the future grid of Elenia is given. The total length of MV grid is assumed to remain static while cabling rate is raised from 12 % to 70 %. In reality the length likely varies because the new cable grid is built for example to new residential areas where old grid does not exist. New MV cable line is not always constructed to the place of disassembled overhead line. However, this speculative rise of cabling rate would increase the area of 10 m or closer to a MV cable to about 0.72 %. This would also multiply the amount of flashes expected to strike to area by six. Even if only part of these 120 flashes strikes to flat ground, the total amount of punctured cables likely rises proportional to the rise of the cabling rate.

Even the probability of cable to get struck by a lightning strike rises along the cabling rate it still stays at relatively low level. In practice, majority of the strikes in the area near the cable most likely hit for example tree and do not necessarily damage the cable. Also, about half of the lightning strikes are low current strikes (< 10 kA) which will damage only the cables lying very close to the strike point in normal soil conditions (< 5 m distance). More details of the lightning strike currents will be presented in chapter 4.1.2. All in all, the speculative numbers given in the tables 3.2 and 3.3 are thus much greater than the realized fault frequency.

4 EFFECTS OF ATMOSPHERIC OVERVOLTAGES ON BURIED CABLES

Previous chapter focused on the lightning phenomena and lightning density in Finland. In this chapter the effects of lightning current are evaluated when current proceeds into soil. Breakdown strength tests for the chosen cable types were one important part of this study. However, in order to be able to evaluate the sheath failure tendency also the lightning induced stresses had to be evaluated. This has been done by certain theoretical calculations and estimations. Some studies can be found in the literature concerning the effects of lightning strikes to buried cables. However, most of the studies are limited to low resistivity soils only.

Buried electric cables naturally contain always metallic parts. As excellent conductors cables typically represent the far away ground potential in the strike point area soil and this way disturb the electric field in the soil of strike point area. This is because the cable will be capacitively coupled to the surrounding soil and the main part of a cable in a soil with a potential of the far away ground. As conductive parts of the cable, both the conductor and the metallic shield provide a low resistant path for movement of electric charge. The local disturbance of electric field can be seen as a potential difference between surrounding soil and outer sheath of the cable. If the metallic shield was in straight contact with surrounding soil the disturbance and potential difference would be mitigated (Haluza 1996). However, to ensure mechanical and chemical protection of cables as well, the outer sheath is regularly made of insulating plastics like PE. Like mentioned before, this structure unfortunately allows a formation of potential difference between surrounding soil and the metallic part nearest to the ground, the metallic shield. The voltage stress is then formed over the sheath of the cable.

In the figure 4.1 the evaluation of lighting stresses to cables is illustrated in a form of a block diagram to create an overall picture of the topic. A lightning strike to ground causes the potential of the ground to increase locally. This is called ground potential rise (GPR). Close to the strike point an equipotential region is always formed where the soil is ionized. Inside this region the electric field strength created by a lightning strike exceeds the critical electric field strength E_0 of the local soil. The ionization in this case means that the air in the voids between the soil particles form ionized highly conducting plasma channels and can be described as a local breakdown itself.

However, the electric field strength in soil is increased outside the ionized region as well. If a cable is close enough to the ionized region, the strength of electric field exceeds the breakdown strength of soil and a soil breakdown to cable takes place. In this case a remarkable part of the lightning current is conducted into the cable and proceeds along the metallic shield or conductors in form of a travelling wave. If the breakdown to cable channel extends to the cable, the cable is punctured once at that point. If the peak voltage of the travelling wave exceeds the withstand voltage of the cable sheath, the sheath punctures over the cable length multiple times. Even if the cable is too far away from the lightning strike point for the soil breakdown to occur, the ground potential rise may still be high enough to exceed the withstand voltage of the sheath. The sheath is then punctured with a very limited current injected to the cable since highly conducting breakdown channel to the cable is not formed. The calculation of ground potential rise is discussed in more detail in the subchapter 4.4. The electric breakdown calculations presented in the subchapter 4.2 are based on the Song's model (Song et al 2002, Song 2004). As seen in the figure 4.1, both electric breakdown calculations and ground potential rise calculations are based on the fundamental electric field calculations in soil.

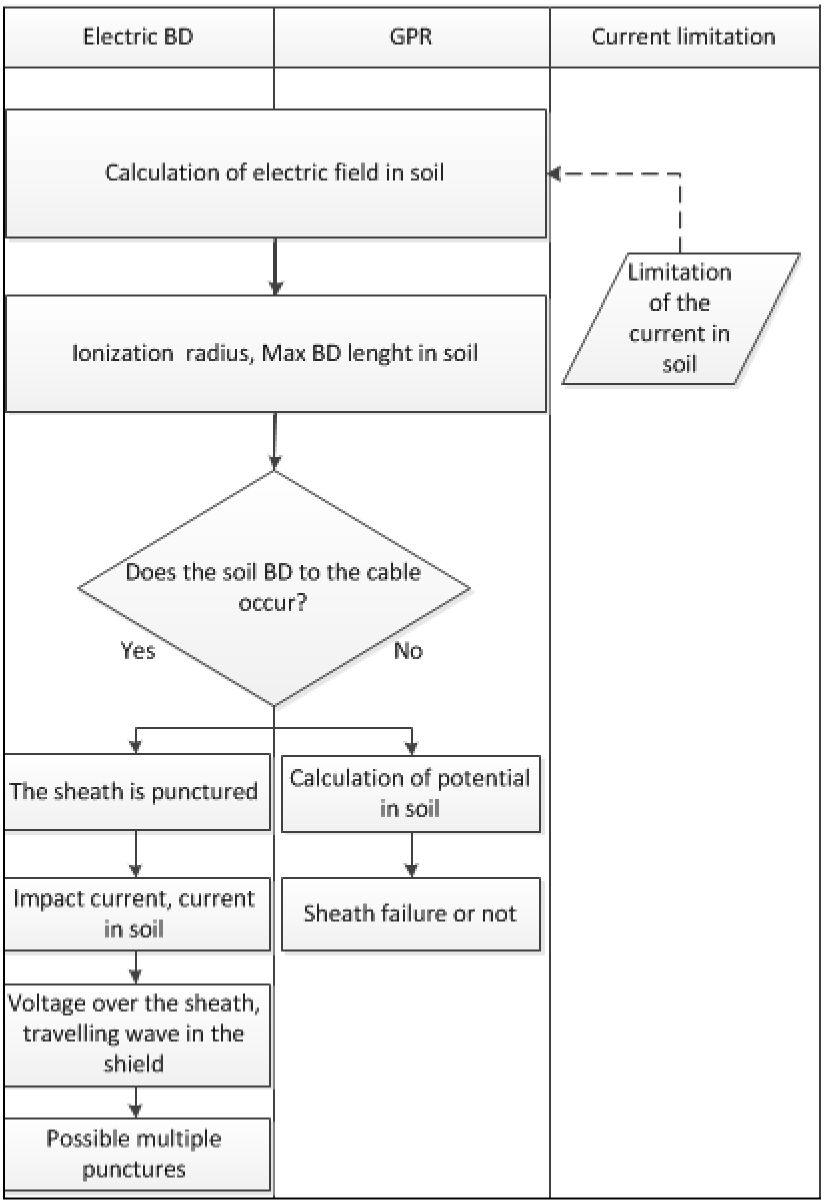

Figure 4.1. *A block diagram for calculating the lightning effects on the cable.*

In addition to the electric breakdown calculations the possibility of sheath damages without electric breakdown in soil is considered as well in the subchapter named Ground potential rise. Before that in subchapter 4.3 the electric breakdown in soil is discussed taking one experimental point of view into account. In this approach the limit of current injected into soil is dependent on the soil resistivity. Last the few other aspects, like effects of an open end of an unconnected buried cable, are shortly discussed. However, in the first subchapter the most important concepts and affecting factors in the estimations are presented.

All the results of the calculations shown in this chapter are presented and discussed in a graphical form. This is the most reasonable way of doing it because the inaccuracy of the simplified models and significant role of chosen parameter values make it irrelevant to examine exact values of results. It is of relevance to do the examinations only in the magnitude level based on the graphs, although the calculation was carried out with Excel spreadsheet program and there are exact values of data points available as well.

4.1 Affecting factors

The concepts and affecting factors presented next are applied in all three models or considerations of subchapters 4.2, 4.3 and 4.4. However, they are now presented as parameters of the electric breakdown model since it is the first one under discussion. A diagram of this model illustrated by Song et al. (2002) is presented in appendix 1. The model itself is discussed in more detail in subchapter 4.2. In this model soil resistivity and critical electric field strength of soil are needed as parameters together with lightning current and location of the cable compared to the strike point. These parameters can be used in calculation of ground resistance of breakdown channels. The first stage of calculation is called electric field model in the diagram. In the second stage the characteristic impedance of the cable is needed in calculation of impact current to the cable. In this calculation an equivalent circuit modified by Song et al. (2002) from the original equivalent circuit of Perala (1982, cited in Song et al. 2002) is used. The equivalent circuit distributes the total lightning current into the impact current that goes to the cable and the part that diffuses into surrounding soil. Finally the magnitude of overvoltage over the sheath can be calculated when the impact current is known. A closer look to the parameters previewed above is given in the following.

4.1.1 Soil resistivity

Resistivity of soil varies significantly depending on type, coarseness, density and humidity of the soil. Soil resistivity is one of the factors affecting the harmfulness of the lightning strike. Characteristically the average soil resistivity in Finland is high which results to difficult grounding conditions. This sets some additional requirements also for the sufficient grounding structures of electric network. However, the soil is very diverse and inhomogeneous containing different layers with different resistivity. Humidity of soil is not constant but strongly affected by local weather conditions like rain. In the table below there are listed usual soil resistivity values in Finland.

Table 4.1. *Soil resistivity values in Finland (Tiainen 2001).*

Type of soil or water	Typical resistivity (Ωm)	Usual limit (Ωm)
Clay	40	25–70
Clay and sand mixtures	100	40–300
Peat, loam, mud	150	50–250
Sand, fine sand	2000	1000–3000
Moraine gravel	3000	1000–10 000
Ridge gravel	15 000	3000–30 000
Solid granite	20 000	10 000–50 000
Lake and river water	250	100–400
Sea water (Gulf of Finland)	2.5	1–5

4.1.2 Lightning current

The peak value of the lightning current is used as a one main parameter in the model. The figure 4.2 and table 4.2 below taken from Finnish lightning observation reports (Mäkelä 2012, 2011) indicate the distribution of flash parameters. Lines in the figure indicate the percentage of the recorded strikes exceeding the current value. The solid lines indicate the first strikes and the dashed lines subsequent strikes. The figure together with the table shows the unlikeness of very high currents. Only 51 strikes with the peak current over 160 kA were recorded during year 2012 which was 0.07 percent of the total strikes. The amount was the same as in 2011 but with the percentage of 0.03. Strikes with a current exceeding 100 kA were also relatively unlike with percentual share of 0.57 and 0.36.

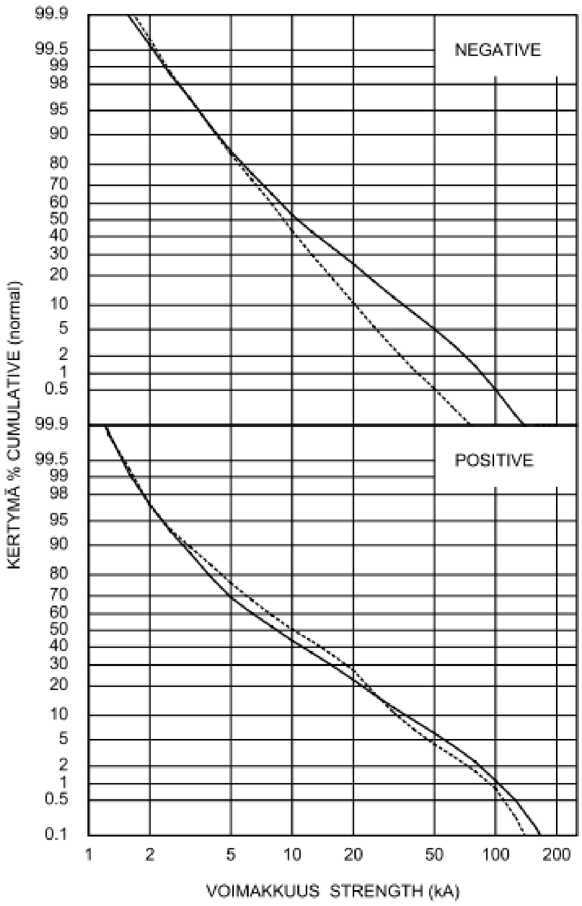

Figure 4.2. *Cumulative distribution of lightning strike strengths (kA) in Finland 2012 (Mäkelä 2012).*

Table 4.2. *Statistics of flash parameters in Finland in years 2012 and 2011 (Mäkelä 2012, 2011)*

	2011			**2012**		
	Neg	Pos	All	Neg	Pos	All
Peak current [kA]						
Median	-10.1	6.2	9.3	-10.4	8.0	10.0
Mean	-15.4	11.5	14.7	-16.1	15.4	16.0
Multiplicity	2.2	1.2	2.0	2.2	1.2	2.0
Single strike [%]	49.1	88.1	56.6	50.4	85.3	57.4
Polarity [%]	80.9	19.1		80.0	20.0	
>100 kA [#/%]	458/0.33	163/0.49	621/0.36	254/0.43	171/1.15	425/0.57
>160 kA [#/%]	27/0.002	24/0.07	51/0.03	29/0.05	22/0.15	51/0.07

The table 4.2 lists both mean and median values of the peak current. The mean current values are larger because of the few very high current strikes that weight the arithmetic mean larger. The median describes statistically better the actual level of currents without giving a dominant role for the strikes with the highest currents. Multiplicity means the average number of stokes which were two in both years. Tendency of single strikes is typical for the positive strikes especially but roughly half of the negative strikes were singles as well. About 20 percent of the strikes were recorded with positive polarity.

4.1.3 Critical electric field strength in soil

The critical electric field strength E_0 needed for the breakdown in soil is also called the breakdown gradient of soil. In the electric breakdown model used in this study the values of breakdown gradient are chosen based on the estimates of Chang (1980). Because the breakdown of soil is initiated in the air voids between the soil particles, the breakdown gradient is also governed by soil ionization in the air voids. However, the soil resistivity is governed by electric current flowing in the water which coats the soil particles. Mousa (1994) emphasizes that although the increasing of water content in soil decreases both breakdown gradient and soil resistivity, there is no direct correlation between the soil resistivity and the breakdown gradient. This can be reasoned as follows: If the water content in soil particles was fixed, the breakdown gradient would be constant as well. However, soil resistivity can still vary following the amount of salts dissolved to water content. Because the salt content in natural soils varies, the above conclusion is valid in natural circumstances. (Mousa 1994.) In the table 4.3 the values of internal breakdown gradient are presented for different soil values.

Table 4.3. *Internal breakdown gradients of different soil materials (Hays & Bodle 1958 cited on Chang 1980).*

Soil Category	Gradient (MV/m)
Gravel, moist	1.2 – 1.9
Gravel, dry	2.1 – 2.3
Sand, moist	1.3 – 2.3
Sand, dry	1.7 – 1.9
Mixture (75% clay, 25 % fine sand), moist	2.1

4.1.4 Characteristic impedance

Characteristic impedance is a term generally used in transmission line theory. In this context the cable can be seen as a transmission line where the lightning current proceeds. The current or signal encounters some electrical impedance in every differential cable length (Bogatin 2000). This is called the characteristic impedance Z_{ca}. It depends on the cable structure but not on the cable length. It also depends neither on applied voltage nor current (Aro et al. 2003).

According to Aro et al. (2003) a characteristic impedance of a medium voltage power cable is between 10 and 40 Ω. For overhead lines it is approximately ten times higher because of capacitive characteristics of cable structure. For a lossless transmission line the characteristic impedance Z_{ca} can be approximated by

$$Z_{ca} = \sqrt{\frac{L}{C}} \tag{4.1}$$

based on the transmission line model where L is inductance and C is capacitance of the line.

4.2 Model of electric breakdown in soil

In this subchapter the lightning effects are estimated by calculating the possible breakdown path lengths in soil and the voltage stress over the sheath caused by the travelling wave in the cable shield. This is done by combining basic electric field calculations and travelling wave theory to an equivalent circuit model illustrating the current dissolution in soil. Idea of combining these three already existing models of the figure together was made by Song et al. (2002). Song also examined the topic further in his doctoral thesis (2004). The basic idea applied in this study is the same as in his model shown in the block diagram in the appendix 1.

In this study the model based on the Song's model is called an electric breakdown model, since it is based on an assumption of an electric breakdown occurring in soil. The final calculation of impact current in the cable and overvoltage over the sheath is done using the general equations instead of circuit simulation with transient calculation software. This decision was done to limit the work in the theoretical basis of this particular model. Instead it was decided few other aspects to be included into the study to evaluate the validity of this model. However, the results of electric breakdown calculations shown later on this chapter are close to the ones of the Song's simulations.

Soil ionization and formation of electric field in the soil can be estimated with an electric field model (Chang 1980; Song et al. 2002), where ionized region is simplified as a perfect conductor. In essence the ionized region still has some resistivity. This has been tried to be taken into account by some researchers in their models. (Cooray 2010.) This unfortunately adds more additional parameters into the models. Advantage of the Chang's electric field model is its low number of required parameters compared to other models. This also makes it more applicable in different situations. In this study only the Chang's model is used in calculation of soil ionization.

In the model it is assumed that the lightning current is distributed into homogenous soil. The electric field strength E at the distance r from the lightning strike point is given by

$$E(r) = \rho_s J(r) = \rho_s \frac{I}{2\pi r^2}, \tag{4.2}$$

where ρ_s is the resistivity of soil and J is the current density. Since all of the injected current diffuses uniformly into the surface area of a hemisphere at the radius of r, the current density can be stated with the current I and the surface area of a hemisphere $2\pi r^2$. (Chang 1980, Song et al. 2002.)

Near the strike point an electric field strength caused by high enough lightning current creates a hemispherical volume where the soil is ionized (Chang 1980, Song et al. 2002, Klairuang et al. 2004). Electric breakdown strength of soil can be expressed as an internal breakdown voltage gradient of soil, E_0. The breakdown in the soil occurs if the electric field strength $E(r)$ is greater than the internal breakdown voltage gradient E_0. In other words E_0 represents critical electric field strength for soil ionization. When the internal breakdown voltage gradient E_0 is known the hemisphere radius of soil ionization r_0 is given by

$$r_0 = \sqrt{\frac{I\rho_s}{2\pi E_0}} \tag{4.3}$$

A principal illustration of the soil ionization is presented in the figure 4.3, where I is lightning current injected to strike point, r_0 is hemispherical radius of soil ionization and r_1 is the arcing distance to the buried cable.

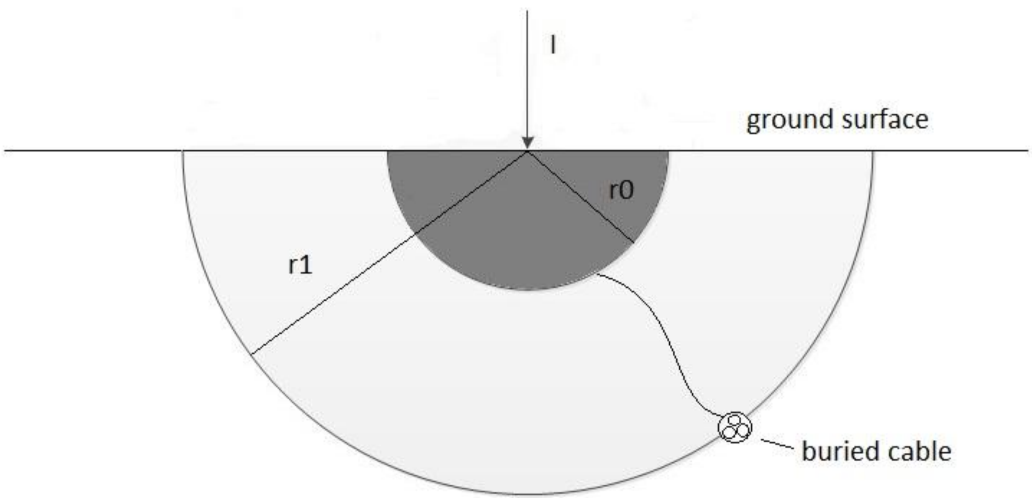

Figure 4.3. *Cross-sectional presentation of soil ionization and breakdown.*

The breakdown distance r_1 is an important factor in the model because if the lightning current is assumed to act like in the Chang’s model (1980) r_1 determines how far the lightning effect reaches from the strike point. According to Chang (1980) the minimum breakdown distance r_1 is given by

$$r_1 = r_0 \left(\frac{E_0}{E_1}\right), \tag{4.4}$$

where E_1 is the average strength of electric field required for soil breakdown between the outer boundary of ionized equipotential region at r_0 and an object located at r_1. The presence of a cable disturbs the electric field at r_1. According to Chang (1980) the potential of the cable may be less than 20 percent of the potential of the soil at same point without the cable. When the largest arcing distance is estimated, the cable is assumed to have a zero potential. Then the equation of maximum arcing distance is written as

$$r_1 = r_0 \left(1 + \frac{E_0}{E_1}\right). \tag{4.5}$$

Chang (1980) refers to earlier studies in which the measurements of the effective corona radius of a conductor in air and arcing between two conductors in air showed that ratio of E_0/E_1 is 1.4. Based on that Sunde (1968, 1945, cited in Chang 1980) suggested an adequate ratio of E_0/E_1 in soil to be 2. The maximum and minimum arcing distances in soil then vary from two to three soil ionization radii according the equations 4.4 and 4.5.

Thus the maximum breakdown distance $r_{1,max}$ used in this model is

$$r_{1,max} = 3\, r_0, \tag{4.6}$$

where r_0 is the hemispherical radius of soil ionization. Next the ground resistance can be calculated. According to Song et al. (2002) the ground resistance of the breakdown path R_g is presented as

$$R_g = \frac{\rho_s}{2\pi r} \tag{4.7}$$

based on Chang's model if the distance r between the lightning strike point and the cable is less than or equal to r_0 maximum ($r \leq r_0$). Song et al. (2002) approximated the cable to be in a zero potential. Hence the resistance R_g is now formed between the hemispherical electrode of radius r and ground far away from the strike point. If the cable lies at $r_0 \leq r \leq r_{1,max}$, the resistance is calculated as

$$R_g = \frac{\rho_s}{2\pi r_0}, \tag{4.8}$$

when the resistance R_g is between the hemispherical electrode of radius r_0 and far away ground. After the ground resistance is known, the impact current I_{ca} to the cable can be calculated from the equivalent circuit using current division rule derived from Ohm's and Kirchhoff's laws

$$I_{ca} = I \; \frac{R_g}{R_g + Z_{ca}/2}. \tag{4.9}$$

In the equation R_g is the ground resistance, I is the lightning current and Z_{ca} is the characteristic impedance of the cable.

According to Song (2004, p 85) impact current can be calculated using an equivalent circuit presented in the figure 4.4, where I is lightning current that is divided to current components I_g spreading into the ground and I_{ca} proceeding into the cable. R_g is ground resistance and Z_{ca} is the characteristic impedance of the cable.

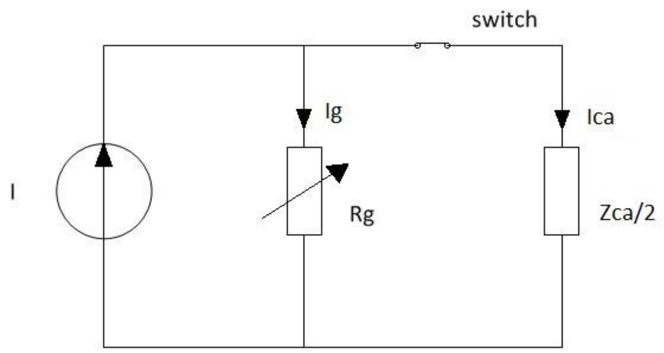

***Figure 4.4**. Equivalent circuit for the estimation of current impacting cable (Song 2004).*

Next the overvoltage U_{sheath} over the cable sheath caused by the travelling wave can be calculated according Song et al. (2002) as

$$U_{sheath} = I_{ca} \frac{Z_{ca}}{2}, \tag{4.10}$$

when the impact current propagates in two directions after getting into the cable. In the study by Song et al. (2002) the cables discussed were unshielded. The same equation can be still used for the overvoltage if the voltage is between surrounding soil and the shield as it was if the voltage was between phase conductor and soil. This is because even if the outer sheath is penetrated by the lightning current the electric insulation itself may remain unharmed. The overvoltage U_{sheath} calculated with this method is the overvoltage the current propagating in the shield creates over the cable sheath. In other words, if the lightning impulse voltage strength of the sheath is higher than the overvoltage the sheath is not punctured by it. Even in that case the sheath is already once punctured if the breakdown channel extends into the cable and impacting current proceeds to the shield. In case the overvoltage high enough to puncture the sheath the travelling overvoltage will puncture the sheath in several points along the cable until it is attenuated enough.

4.2.1 Results

In all figures presented later the value of critical electrical field strength used in calculations is chosen as follows. For 3000 and 5000 Ωm value 2.00 MV/m is used. For 500 and 1000 Ωm the used value is 1.00 MV/m. In reality critical electric field strength is hard to measure or quantify accurately because it is not only dependent on the soil resistivity but also to the dielectric constant of soil (Asimakopoulou et al. 2009). In addition there are also some difficulties in the determination of the dielectric constant of soil. Asimakopoulou et al. (2009) compared few methods of calculating the critical electric field strength in soil. The comparison shows that the resulted values vary significantly depending on the applied method. Thus in this examination the chosen values are 1.00 and 2.00 MV/m. With this selection the more complicated examination of soil material can be avoided without significant loss of validity. Chang (1980) and Song et al. (2002) used constant value of 1.00 MV/m for critical electric field strength in their studies for resistivity of 1100 Ωm and lower. However, Chang indicates that the value for higher resistivity soil types like rocky regions could be closer to approximately 2.00 MV/m. The following figures are plotted with the calculated values of lightning current points from 20 to 200 kA with steps of 20 kA. Because of the many approximations included in model, there is no reason to give the exact values for examination.

As mentioned before the resistivity in different soil types can vary in huge margin. In the studies of Chang (1980) and Song et al. (2002) the soil resistivity of 1100 Ω and lower are examined. This may be an adequate scale for the most common soil materials in some countries. As mentioned before, in Finland however the resistivity can be much higher because of the rocky base material of the soil.

Theoretical maximum breakdown distance of lightning current in soil can be approximated using equations 4.2, 4.3. and 4.6. In the figure 4.5 the maximum breakdown distance is presented as a function of lightning current with four different soil resistivity values. If the soil resistivity value of 3000 Ωm is examined the moderate 20 kA lightning current can cause a soil breakdown of about 7 m from the strike point in the soil. According to the lightning statistics reports less than 1 percent of either positive or negative clound-to-ground lightning strikes in Finland exceeds to the current level of 100 kA (Mäkelä 2012; 2011). Thus the breakdown distances of 15 meters or more are very unusual. For more average lightning current of 15 kA, the breakdown distance is supposed to be less than 5 meters.

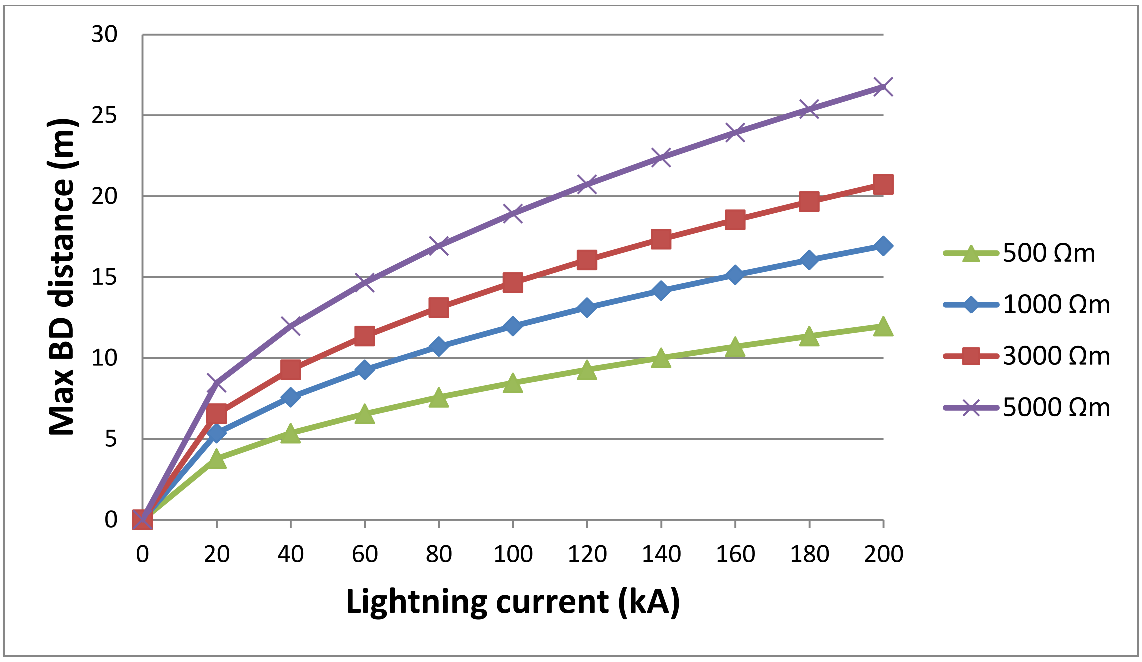

Figure 4.5*. Maximum BD distance with different soil resistivities as a function of lightning current.*

According to this approximation the distance between the strike point and the cable should be more than about 27 m to ensure that any lightning current up to 200 kA is unable to form a BD channel across the distance with soil resistivity up to 5000 Ωm. However, even this cannot be assured because the largest chosen value of soil resistivity for the approximation is not anyhow the maximal soil resistivity. There can be regions where the resistivity can reach 10 000 Ωm and even higher (Tiainen 2001). These can be for example bare cliffs and rocky mountain regions. It can still be said that BD distances of about 25 m and more are very unlike and require extremely high soil resistivity combined with very high lightning current.

In the equivalent circuit of figure 4.4 and equation 4.9 the lightning current splits in two components: the one that diffuses to surrounding soil and the other that proceeds into the nearby cable through the BD channel. The required ground resistance is calculated from equation 4.8 if the cable lies further away from the strike point than ionization radius. Otherwise the equation 4.7 is applied.

As seen in the figure 4.6 more lightning current is injected into the cable in higher resistivity soil. The effect of chosen value of critical electric field strength can be seen graphically as a slightly greater angular coefficient for the two higher resistivity soils. The limiting factor in the lower lightning current values is the breakdown distance. That is why there is no data points plotted at 20 kV in horizontal axel. In other words, in this case the breakdown channel does not extend to 10 meters from the strike point. Not even in soil with 5000 Ωm resistivity. By the same token there is no data at 500 Ωm resistivity soil until the lightning current reaches 140 kA. Below that level all of the lightning current diffuses to the surrounding soil and the BD channel does not reach the cable. The ratio between diffusing current and impact current to the cable is significantly dependent on the soil type and resistivity but lightning current also. In the soil of 3000 Ωm resistivity the ratio varies from about 89 % at 60 kA lightning current to about 82 % at 200 kA lightning current. In well conducting 500 Ωm soil the percentage is from about 61 % at 140 kA to 57 % at 200 kA. All in all, if the cable lies 10 m away the strike point very high ratio of total current may proceed to the cable. In extremely low conducting soil the ratio can be easily over 90 %.

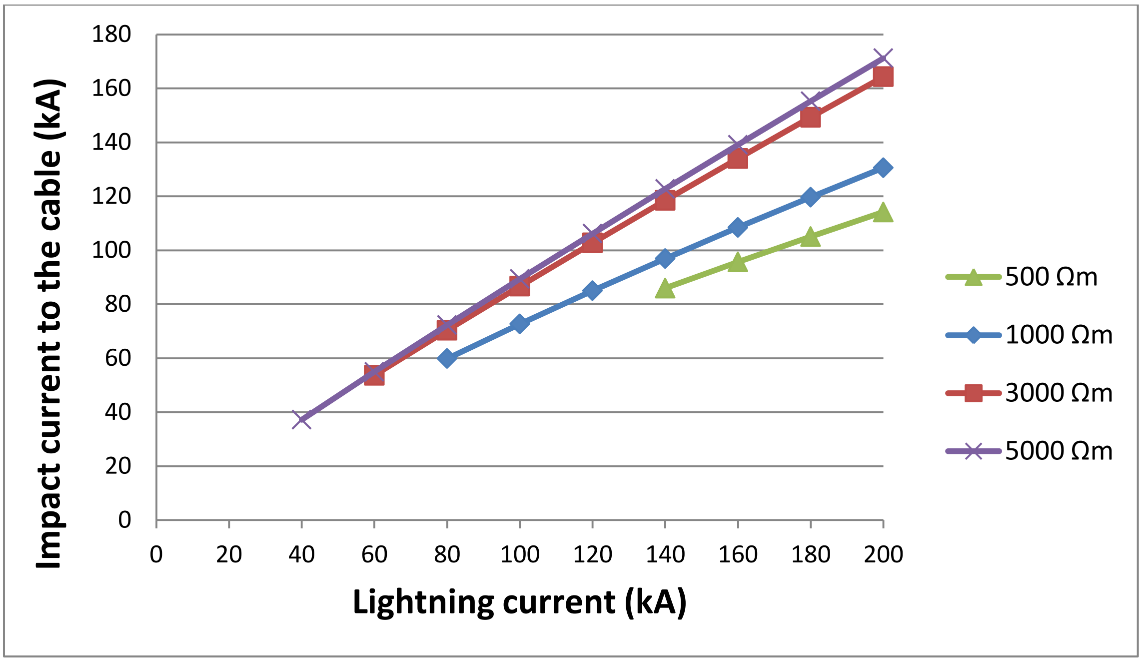

Figure 4.6*. Impact current to the cable at distance of 10 m from strike point.*

The approximated voltage stress between the cable shield and ground when impact current travels in the cable is given in the figure 4.7. Some of the data points are left out similarly as in figure 4.6 because of insufficient breakdown distance. The figure indicates that overvoltages are high enough to break any regular cable sheath whenever the arcing channel reaches 10 meters distance. In soil of 3000 Ωm resistivity the lightning current must however reach a peak value of about 50 kA to form the breakdown channel that reaches the cable. This is already much greater current than lightning strikes have in an average. The overvoltage for this case would be about 700 kV as seen from the figure 4.7.

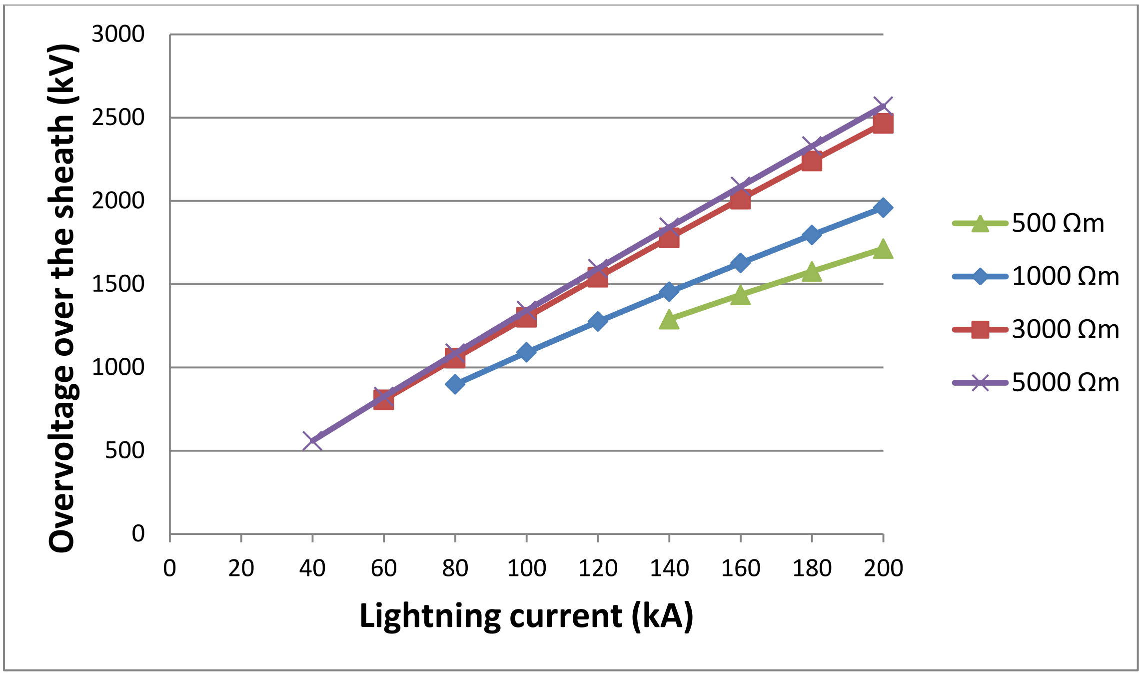

***Figure 4.7**. Overvoltage between the cable shield and ground when the cable is 10 m from strike point.*

As mentioned earlier, breakdown distances of 15 meters or more would require high lightning current of about 100 kA. These high current strikes are uncommon but still not totally exceptional in Finland (Mäkelä 2012; 2011). In the figure 4.8 there is the same examination for the cable lying now at 5 m from strike point. Compared to earlier examination with 10 m distance in figure 4.6 lower lightning currents can now reach the cable. That is indicated already in the figure 4.5 where only at resistivity level 500 Ωm 20 kA lighting current does not reach 5 m distance. The same conclusion can be done based on figure 4.8. However, if the lightning strike has a higher current level of for example 100 kA, the magnitude of impact current is exactly the same as it was for 10 m distance. That is because in the applied method the length of breakdown channel between the outer border of the ionization radius and the cable does not have an influence on the impact current. In this simplified version of the Song's model (Song et al. 2002) the resistance between the breakdown channel and the ground is not taken into account. In other words, the breakdown channel can be described as an insulated conductor.

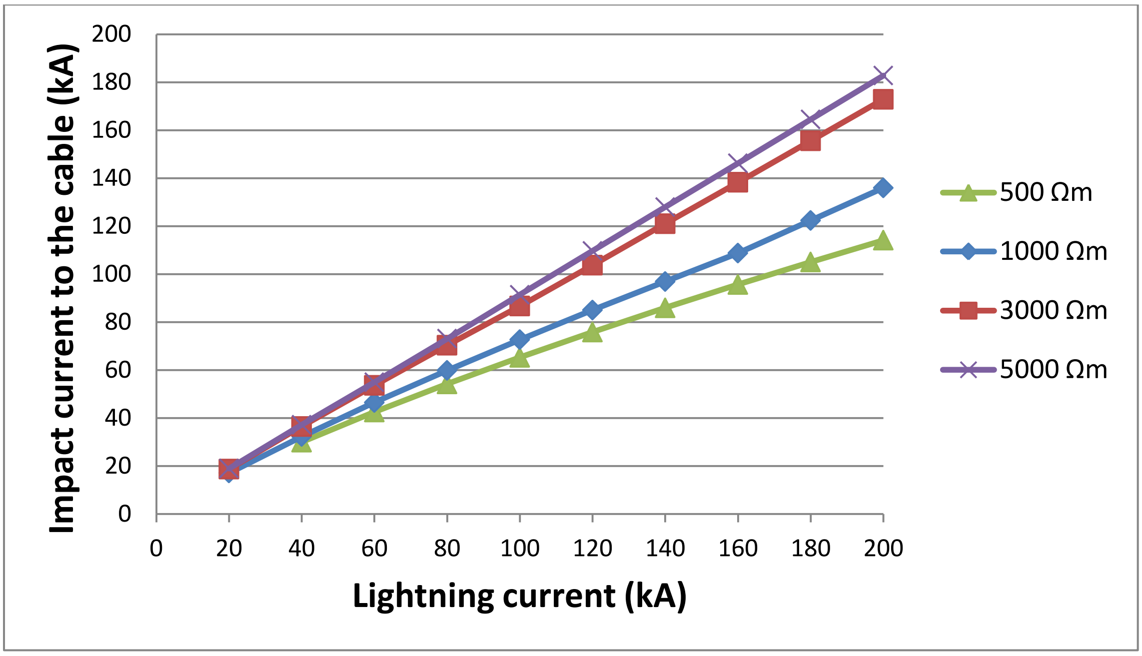

Figure 4.8. *Impact current to the cable when the cable is 5 m from strike point.*

When comparing the two different breakdown distances 5 m and 10 m, the lightning current level 120 kA is a critical point. It is the first step where the ionization radius exceeds 5 m. Now there is a situation where the ionization radius r_0 is larger than supposed breakdown distance r_1, in other words the distance between the strike point and the cable. As shown earlier with equations 4.7 and 4.8 the calculation of ground resistance R_g is different in this situation. The change in ground resistance affects the determination of impact current and the overvoltage as well. Thus, actually from 120 kA lightning current level the impact current and overvoltage (figure 4.9) are slightly higher for 5 m breakdown distance compared to 10 m distance because of greater ground resistance R_g values.

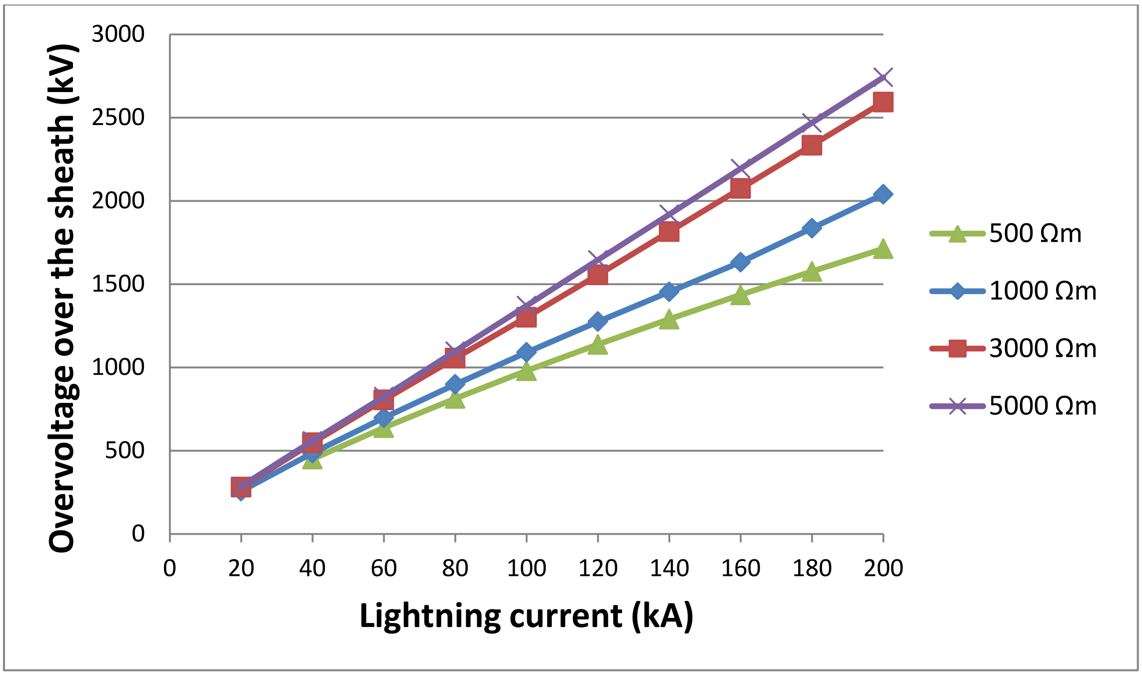

Figure 4.9. *Overvoltage between the cable shield and ground when the cable is 5 m from strike point.*

After examining the behavior of impact current and overvoltage at breakdown distance of 5 m, it seems that the channel may be formed at lightning currents of lower than 20 kA as well. Actually these are the most typical current levels of cloud-to-ground lightning strikes. Although if 5 m is very short distance it has significance for further examination because the current level of a strike of about 15 kA is an average in Finland. Figure 4.10 is a zoomed version of figure 4.8 at lightning currents ranging from 0 to 20 kA. Figure 4.11 acts as a similar version of figure 4.9. These figures indicate that the breakdown channel is formed for example at 12 kA lightning current in 3000 Ωm resistivity ground. The impact current at this point is about 11 kA and the overvoltage about 170 kV. Roughly saying lightning current of about 8-18 kA can result to an overvoltage of about 100-230 kV in 1000-5000 Ωm resistivity soil. If soil resistivity is over 5000 Ωm, the breakdown channel may form with even smaller lightning currents. In this case it results to a smaller overvoltage as well.

The formation of breakdown channel can also be seen from figure 4.12 which is an illustration of maximum breakdown distances with lightning currents ranging from 0 to 20 kA. There can be seen that with these low and moderate lightning currents the 7 m long channel can be formed only in the soil of resistivity higher than 3000 Ωm.

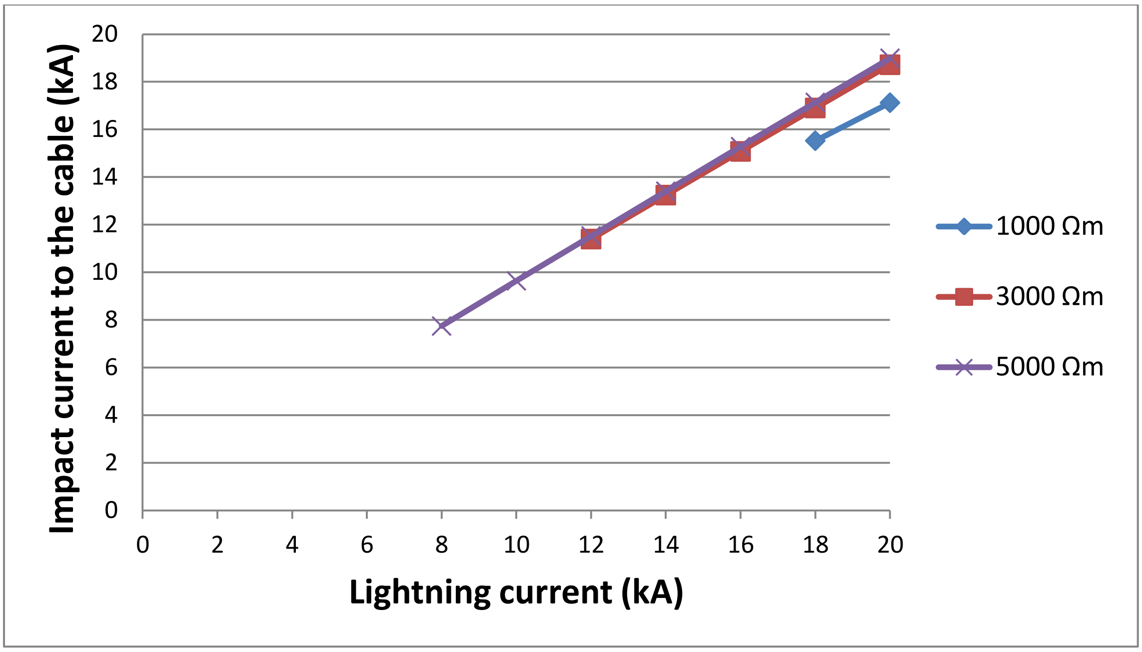

Figure 4.10. *Impact current for low lightning currents when the cable is 5 m from the strike point.*

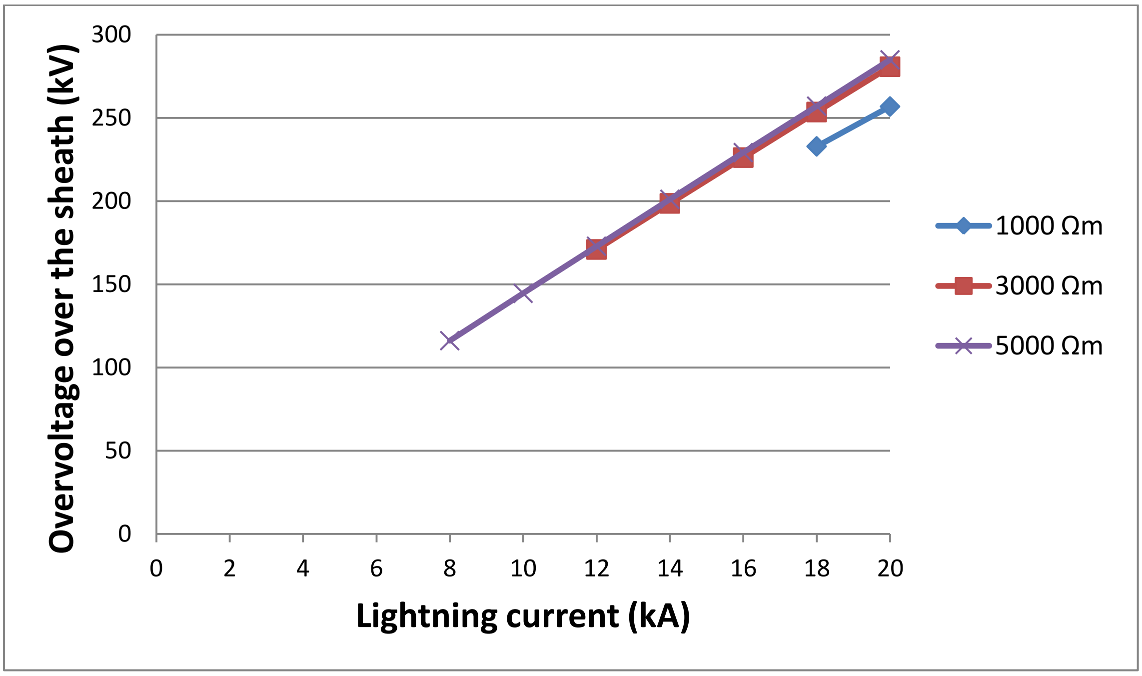

Figure 4.11. *Overvoltage between the cable shield and ground for low lightning currents when the cable is 5 m from the strike point.*

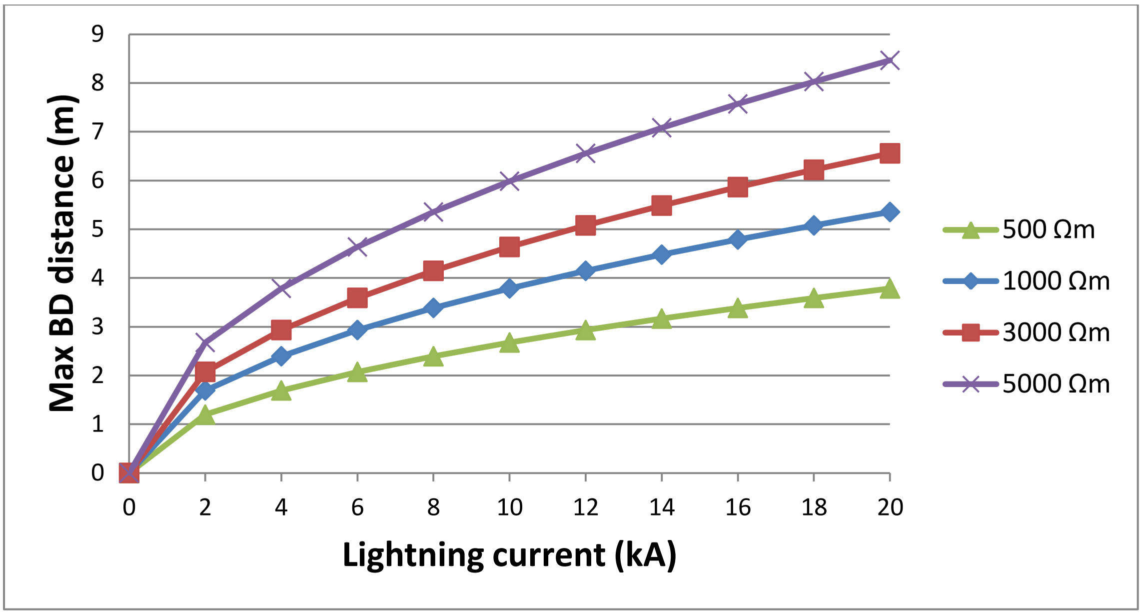

Figure 4.12. *Maximum breakdown distance with different soil resistivities as a function of low lightning currents.*

4.2.2 Restrictions and uncertainties of the model

However, there are many restrictions and uncertainties included in the model presented. The resistivity of soil is rarely homogenous when examined in the scale of few meters. Because of this the volume of ionized soil is not hemispherical like presented in the model. The volume is more or less distorted out of the hemispherical shape. This affects also the formation of actual breakdown path. Like the breakdown characteristics in general, the prediction of breakdown path in soil is a statistical process as well. Statistic prediction is not included to this simplified version of the model.

Also the selection of a valid value of critical electric field strength includes uncertainties. It becomes even more difficult when higher soil resistivity is examined. As Asimakopoulou et al. (2009) mentioned these two variables are not tied together but there are other factors of soil material affecting them. One of these is the dielectric constant of soil.

The electric breakdown model presumes that the impact current and voltage stress to the cable is generated as described forming first ionized region and then the breakdown channel if the cable lies outside the ionized region. There are other possible mechanisms as well and they are discussed in the later subchapters. In the next subchapter there is presented an experimental notions of maximum current dissolved into soil for the further evaluation of electric breakdown model results.

4.3 Limitation of the current dissolution into soil

In the previous model it is assumed that the whole lightning current can be injected to soil. However, in reality there seems to be limitations for the current penetrating the surface layers of the soil. The current is limited by the specific resistance of the upper layers of the ground (Mikhailov & Sokolov 1965, cited in Chang 1980). According to Chang (1980) significant differences have been measured between internal breakdown gradient and surface breakdown gradient. In other words, the critical electric field strength required for the breakdown to occur is not the same on surface as it is beneath the surface.

The surface breakdown gradient is probably less than internal gradient in many cases especially if the moisture content distributes only in the upmost layer of the soil. Heavy rainfall may lead into an extreme situation if upper soil layers are not coarse enough to allow the water to dissolve down into lower soil layers. In this case an extremely wet layer of soil may be formed on the ground surface which makes it very conductive. More studies should be also done to examine the behaviors of lightning current in case of extremely conductive surface layer.

If the surface layer is more conductive than lower layers it can be assumed that the current may distribute to surrounding ground surface raising the potential in a large area. However, in extremely conducting surface the potential rise is not as significant as in more resistant soil or surface of the soil. In well conducting surface of soil the current spreads into wider area resulting to smaller current density and smaller potential differences as well. The current may probably also lead to a breakdown or flashover along the soil surface and then dissolve into surrounding soil, either mainly into upper layers or into lower ones as well. This scenario is illustrated in the figure 4.13.

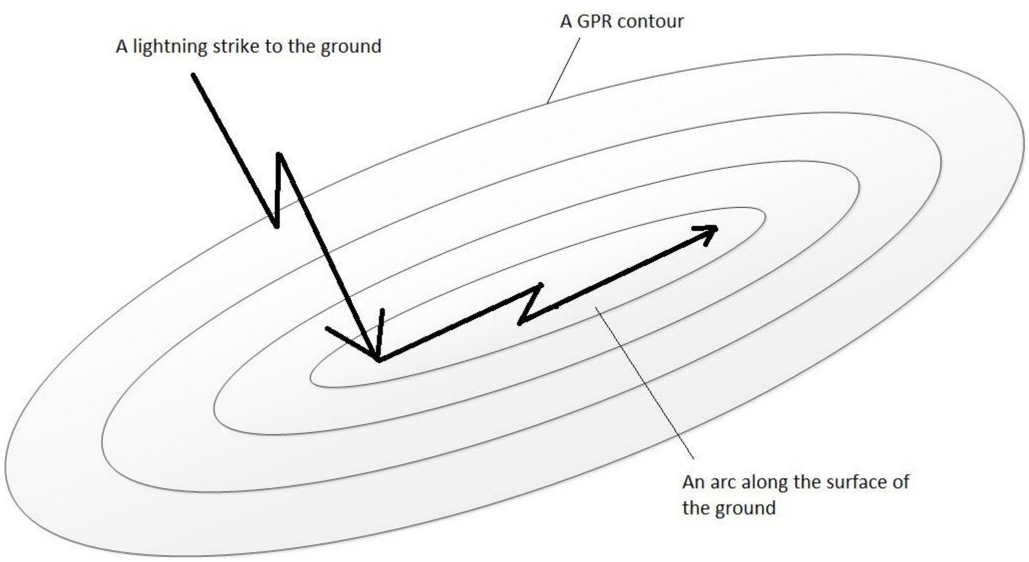

***Figure 4.13**. Soil surface breakdown.*

Chang (1980) refers to an experimental study of Mikhailov and Sokolov (1965) where the maximum lightning current injectable to soil is experimentally studied. Soil resistivity in their experiment ranged from 100 to 1100 Ωm. Based on the results of the experiment they established a formula

$$I_m = \left(16 + \frac{2*10^6}{{\rho_s}^2}\right) * 10^3\ A\ , \qquad (4.11)$$

where I_m is the maximum current injected to the soil with resistivity of ρ_s. According to Chang (1980) this equation corresponds well with measurement data up to 1100 Ωm. The validity of this equation cannot be assured with higher soil resistivity levels. However, assuming a certain level of validity the equation can be used to evaluate the effects of phenomenon also for higher soil resistivity levels. Although one has to keep in mind the assumption made when evaluating the results.

In the figure 4.14 the maximum of injected current is calculated according to experimental equation 4.11. It can be seen that in low resistivity soil the maximum current is very high and probably the total lightning current may be injected to the soil as assumed in the previous models. For example, the maximum current in 100 Ωm soil is 216 kA. However, according to equation by Mikhailov & Sokolov (1965) for example in soil resistivity of 1000 Ωm only 18 kA can proceed directly into the soil. Thus the maximum current injectable into soil is dropped very dramatically in 100 Ωm to 300 and 400 Ωm soils. After that the decrease is much lower. According to Mikhailov & Sokolov (1965) if the lightning current is especially high only minority of it is injected directly into soil. For example if a strike of 100 kA occurs into 1000 Ωm ground only 18 kA is dissolved into soil. What happens to the remaining 82 kA is that it probably causes a surface flashover on the ground surface and dissolves in the surface layer of soil over a large area. One could speculate that if the total current is now distributed over a larger area due to for example, surface flashover, the total outcome may be that the ionized area is spread over a larger area and shorter soil breakdown can occur from the ionized soil volume. In other words, larger area may suffer from the soil breakdowns but only to a depth of about 4 to 5 meters.

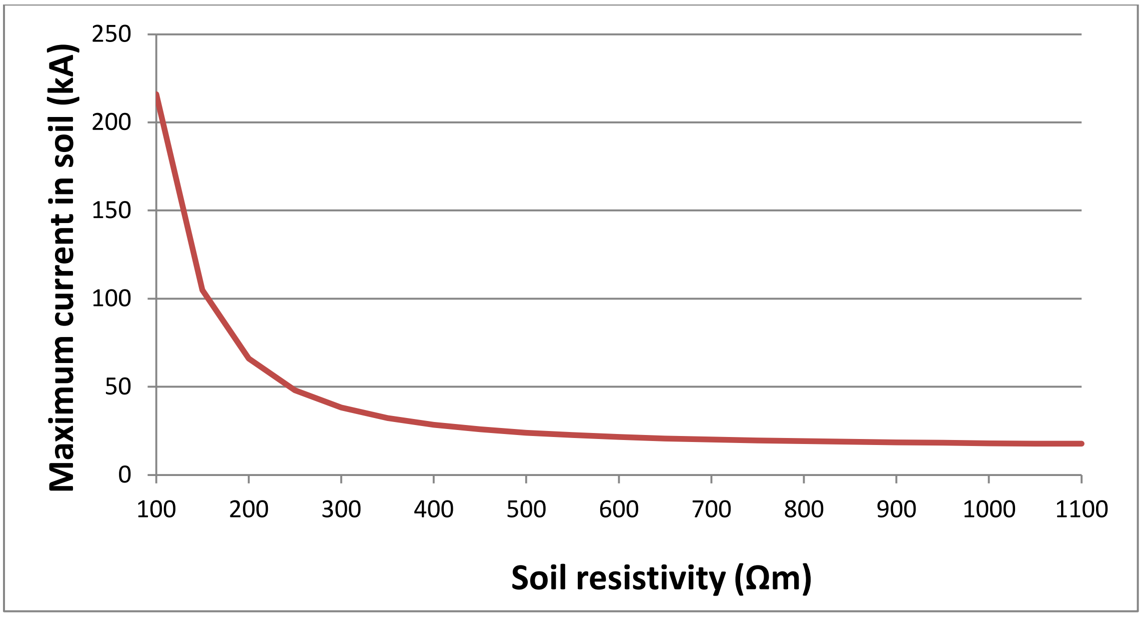

***Figure 4.14**. Maximum current injected to soil according to Mikhailov & Sokolov (1965).*

Taken a look on how this affects the ionization process in surrounding soil there are now significant differences compared to the previous models. When the maximum ionization radius is calculated with the maximum current in soil based on the equation 4.11 instead of the total lightning current it results to a much smaller radius. In the figure 4.15 the maximum ionization radius is 1.85 m in 100 Ωm soil. Equation 4.6 gives 5.5 m as the maximum value of breakdown distance in soils of 100 to 1100 Ωm resistivity (Chang 1980). This is shown also in figure 4.16. Value of 1 MV/m is still used for the value of critical electric field strength in low resistivity soils.

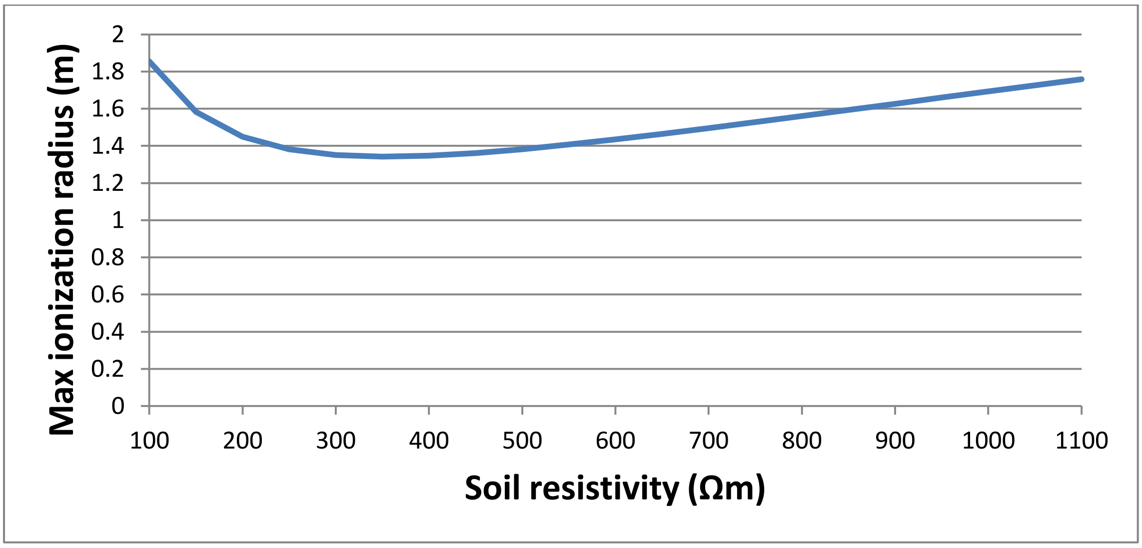

***Figure 4.15**. Maximum ionization radius according to Chang (1980)*

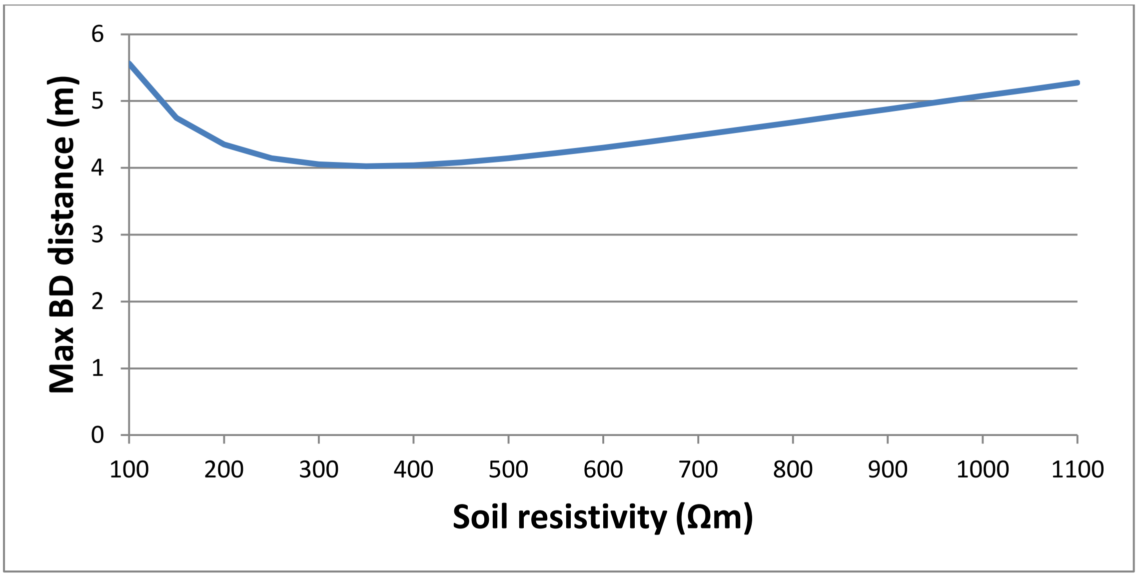

Figure 4.16. *Maximum breakdown distance according to Chang (1980).*

Chang (1980) ends up to a conclusion that a cable buried deeper than 5.5 m below the surface would have a minimum chance to suffer from a direct strike. As noticed the results differ totally from the breakdown distances calculated directly according to Song's et al model (figures 4.5 and 4.12) which are similar to their own calculations (Song et al. 2002, figure 7). The overvoltage over the sheath can be calculated using equations 4.6 - 4.10. In figure 4.17 the blue line indicates the soil resistivity levels where the breakdown channel does not reach the cable lying at 5 m from the strike point. As seen, the red points which indicate the resistivity levels where cable is struck are located in the both ends of resistivity axel, similarly with maximum ionization radii in figure 4.15. The overvoltage in 1000 and 1100 resistivity soils is now about 230 kV.

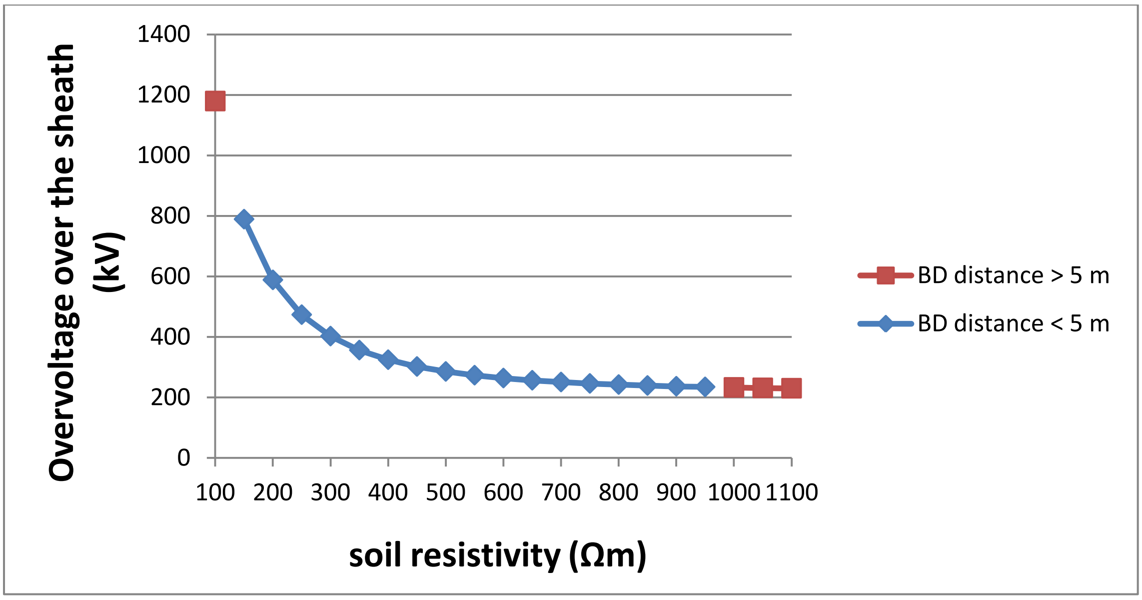

Figure 4.17. *Maximum overvoltage over the sheath if cable lies at 5 m distance from the strike point and current is limited by equation 4.11.*

As mentioned before the studies of Mikhailov & Sokolov (1965) are not directly applicable for higher resistivity soil. Next the equation 4.11 is used to approximate the phenomena for higher resistivity soils. This can be done keeping in mind that these approximations are purely hypothetical and the equation is not confirmed to be applicable for high resistivity levels above 1100 Ωm.

In the figure 4.18 the resistivity values from 2000 Ωm to 10000 Ωm are added directly to the original curve of figure 4.14. It is important to notice that the scale of horizontal axis is nonlinear. The current is clearly stabilizing towards the level of 16 kA at high resistivity values. This can be seen in the figure 4.19 where the horizontal axis covers only the values of higher resistivities.

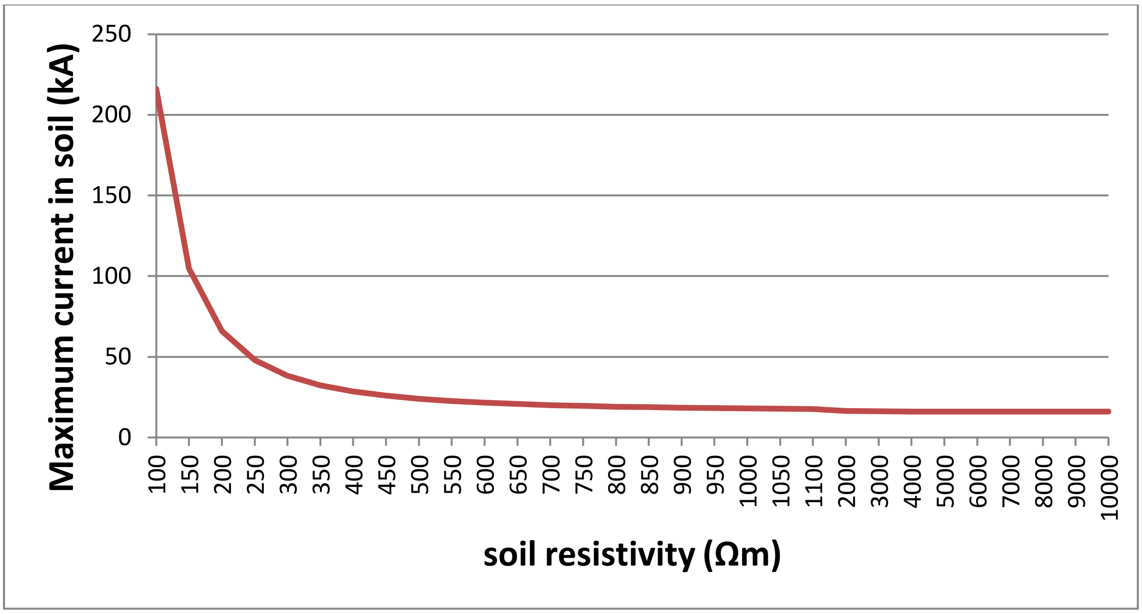

Figure 4.18. *Approximation of maximum current injected to soil in nonlinear scale.*

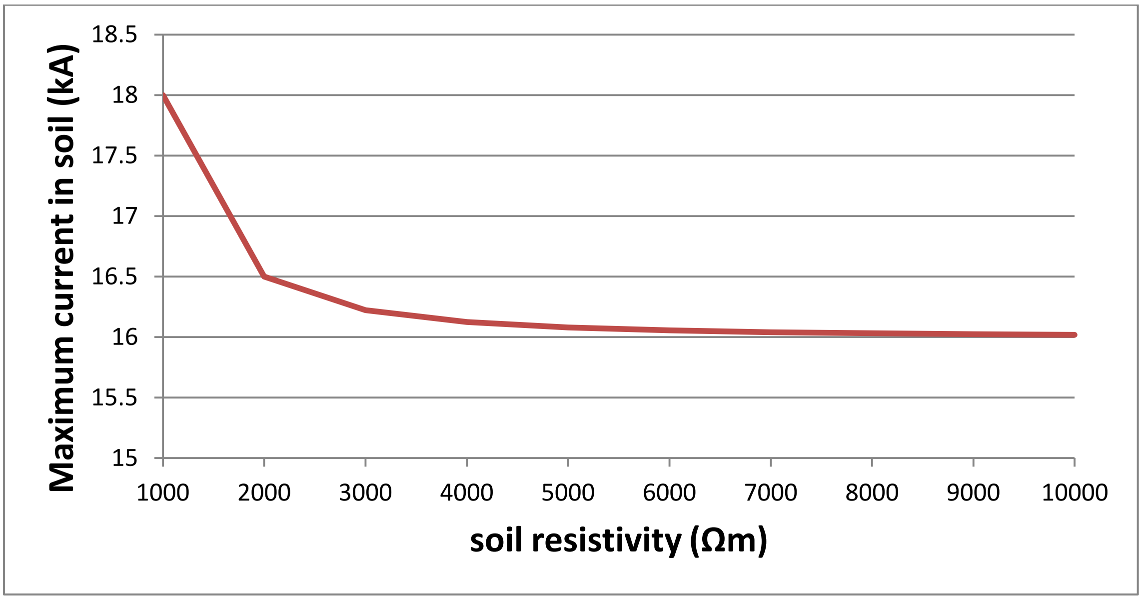

Figure 4.19. *Approximation of maximum current injected to soil in linear scale.*

The maximum ionization radius, maximum arcing distance and overvoltage in the cable lying at certain distance are approximated next similarly as they were presented before for the low resistivity values. In the figures 4.20, 4.21 and 4.22 2.0 MV/m is used as a value for critical electrical field strength for the resistivity values above 1100 Ωm similarly as in the estimations of the electrical breakdown and the ground potential rise models. In figure 4.22 it can be seen that the approximated overvoltage seems to approach the level of 230 kV as already seen earlier in figure 4.17.

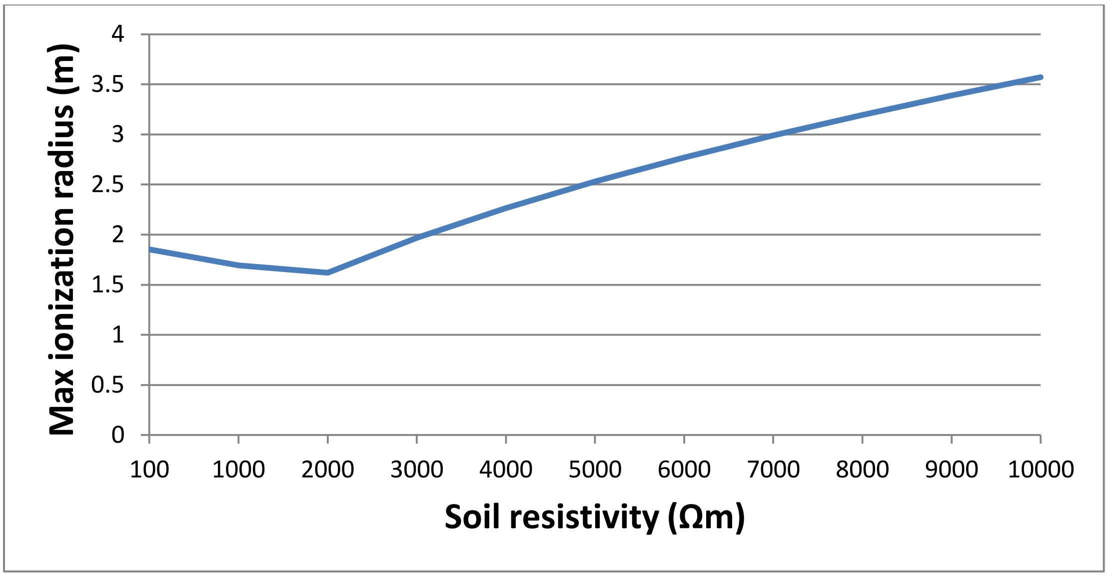

Figure 4.20*. Approximated maximum ionization radius if the current is limited by equation 4.11.*

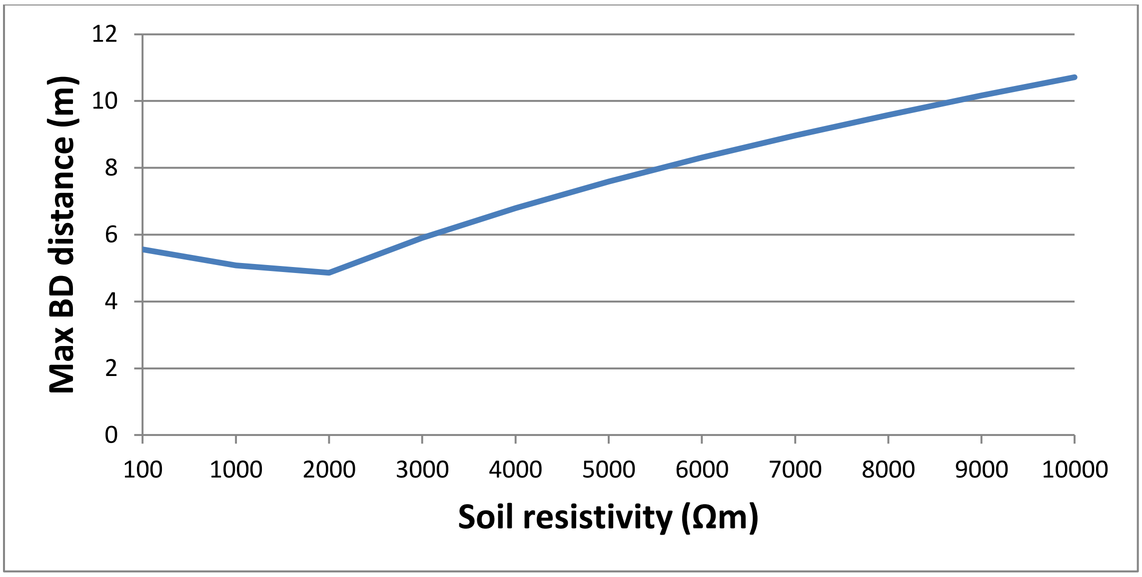

Figure 4.21*. Approximated maximum breakdown distance if the current is limited by equation 4.11.*

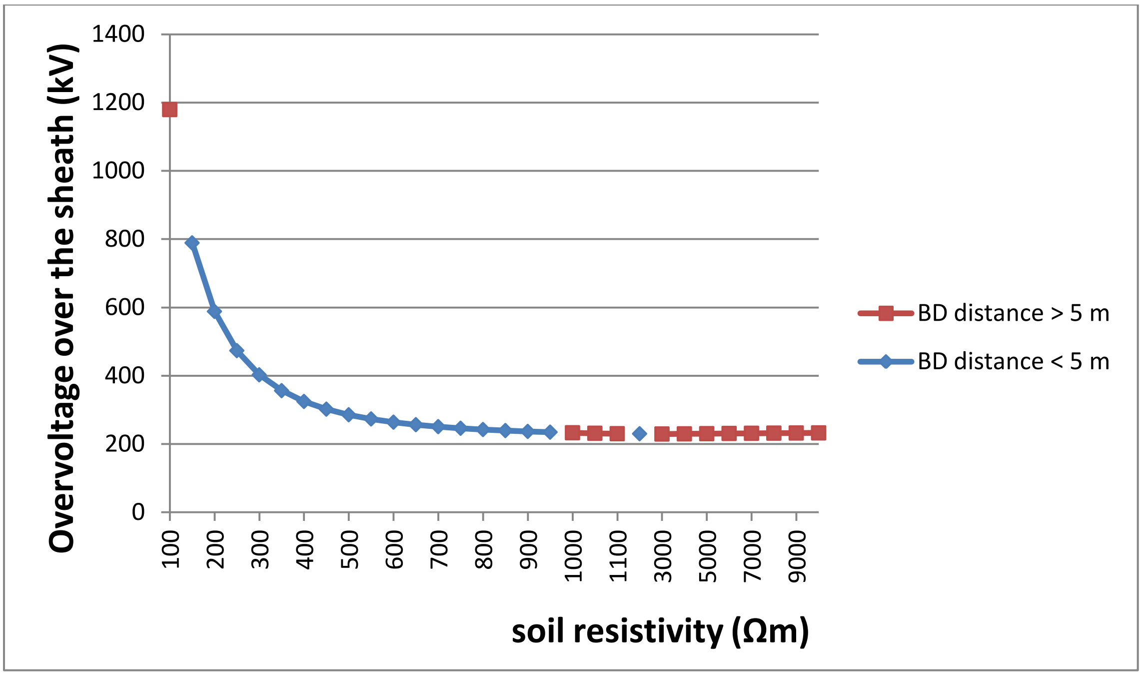

Figure 4.22. *Approximation of maximum overvoltage over the sheath if cable lies at 5 m distance form strike point and current is limited by equation 4.11.*

In figure 4.22 the data point in resistivity 1200 Ωm is an error resulted by the sudden change of the critical electric field strength. 1200 Ωm is the first approximated point and the first point where critical electric field strength value of 2 MV/m is used instead 1 MV/m. Naturally the breakdown distance there should be over 5 m as it is in the nearby values.

When these approximations are compared to the estimations got from the electric breakdown model without current limited by the equation 4.11 significant differences can be seen. Now the overvoltage in the cable is only about 230 kV for cable lying at 5 m distance from the strike point. Without the limitation of the current dissolving into soil the overvoltage was at the same level when the lightning current was 16 kA in soil with resistivity of 3000 or 5000 Ωm (figure 4.11). Otherwise the overvoltages were much higher. In figure 4.22 the level of 230 kV is reached earlier at about 1000 Ωm. If cable lies at 10 m distance the breakdown channel would not reach it in soils with resistivities less than 9000 Ωm, when calculated with limited current (figure 4.21). As discussed earlier, these results with high resistivity values are only approximations. However, there is still a significant difference when comparing the estimations of maximum breakdown distances of figures 4.5 and 4.12 to the figures of 4.16 and 4.21.

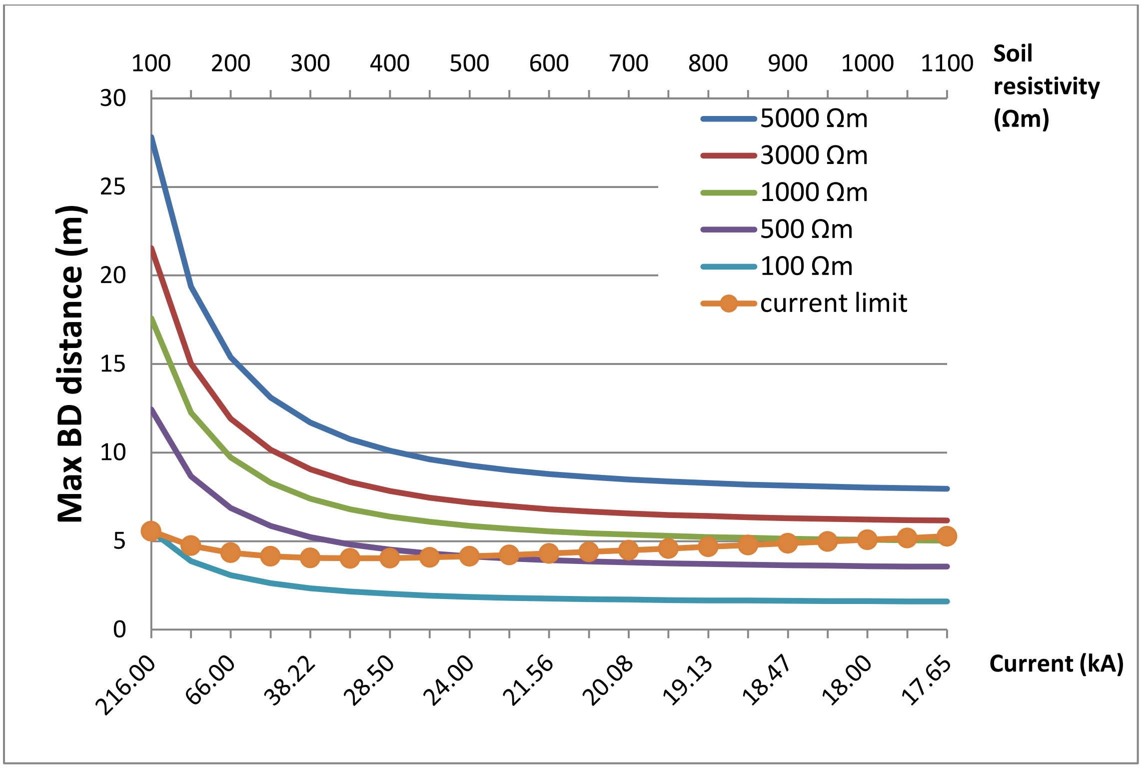

Figure 4.23. *Comparison of maximum breakdown distances with limited and unlimited currents proceeding into soil.*

In the figure 4.23 the breakdown distances estimated using electric breakdown model are shown together with some results calculated with the limited soil currents (Mikhailov & Sokolov 1965). This is done by setting on the horizontal axel the current given by the equation 4.11 when soil resistivity rises from 100 to 1100 Ωm in steps of 50 Ωm. For example in 100 Ωm the current is 216 kA and in 1100 Ωm 17.65 kA. As seen, the equation 4.11 ties the soil resistivity together with maximum current proceeding in soil. The breakdown distances are calculated for the current limit curve using the particular resistivity tied to a current in horizontal axel according equation 4.11. The rest of the curves are calculated for the current values in horizontal axel using the particular resistivity value indicated in the legend. Thus the resistivity values of the secondary horizontal axel are used only for calculation of current limit curves.

The basic idea of the figure 4.23 is to show that the higher breakdown distances indicated by the curves with fixed resistivity values are probably fairly pessimistic and exaggerated. The breakdown distance results based on the experiments of Mikhailov & Sokolov (1965, cited by Chang 1980) differ radically from the results given by electric breakdown model based on Song's et al studies (Song 2004, Song et al 2002). This can be seen directly from the publications as well. This may indicate that in the Song's model the natural limit of maximum current dissolving into soil is not taken into account. In the Song's model seems to be more like a theoretical approach maybe missing some practical aspects. In any case the experimental studies should be done more and with different soils to be able to criticize the models more. Next the effects of lightning strike on the buried cable without electric breakdown of soil are discussed.

4.4 Ground potential rise

In the previous subchapters discussed the cases where the soil breakdown is the phenomenon resulting to the puncture of the cable. However, the cable may get punctured without a soil breakdown as well due to rise of ground potential near the cable. This situation may take place if the cable locates far from the strike point. In this case the potential of the nearby soil can be compared to the voltage strength levels of cable sheaths to evaluate the possibility of the sheath puncture.

When a lightning discharge unloads its remaining energy into soil the potential difference between the point of the lightning impact and the distant ground can be several thousands of kilovolts. The potential difference can be seen as a voltage gradient along the ground, which can be several kilovolts per meter. Next the effects of lightning strike in soil are discussed with a concept of ground potential rise (GPR). (Haluza 1996.)

The potential difference on the ground surface is often called the step potential. The name refers to a hazardous potential difference through a human or animal body if their legs are spread apart in an area where there is a large voltage gradient in the ground. A ground potential difference occurs whenever a large current flows in resistive soil. It can be resulted from a power system fault, like an earth fault, or from a lightning strike to the ground. A strike can be a direct strike to the ground or it can hit a tall object that offers path to the ground for the lightning current. For humans and animals the potential difference on the ground can be lethal depending on the magnitude of the local voltage gradient. When the fault current flows to the ground via earthing wires it causes potential difference to the ground, often called ground potential rise, GPR. GPR is usually discussed related to earthing grids of an electric distribution substation or a telecommunication station. In these contexts GPR means a momentary rise of potential in the earthing grid caused by a transient overvoltage pulse. A direct lightning strike to the ground creates a similar mechanism, but since all of the lightning current is injected to the striking point, the rise of potential is locally more powerful. The magnitude of GPR in soil naturally depends crucially on soil resistivity. With other parameters kept stationary, GPR increases with increase of the soil resistivity. That is indicated also in an experimental research implemented by Jing et al. (2010).

If the soil was homogenous, the GPR contour would be a circle. However, soil is rarely homogeneous in large areas. That is why the GPR contour is nonsymmetrical in reality (Haluza 1996). The differentially small volumes in the ground, which are in the same potential, together form equipotential lines. The potential difference between two equipotential lines is constant. These lines are perpendicular to the electrical field lines, which represent the local rate of change of potential with respect to displacement. In other words field lines stand for potential gradient. Distribution of an electrical field is generally illustrated by field lines and equipotential lines in the same figure. When dielectric components are under discussion, the most interesting behavior of the electrical field is often located in interface of two different materials. (Aro et al. 2003.) GPR in homogenous soil can be demonstrated as seen in figure 4.24.

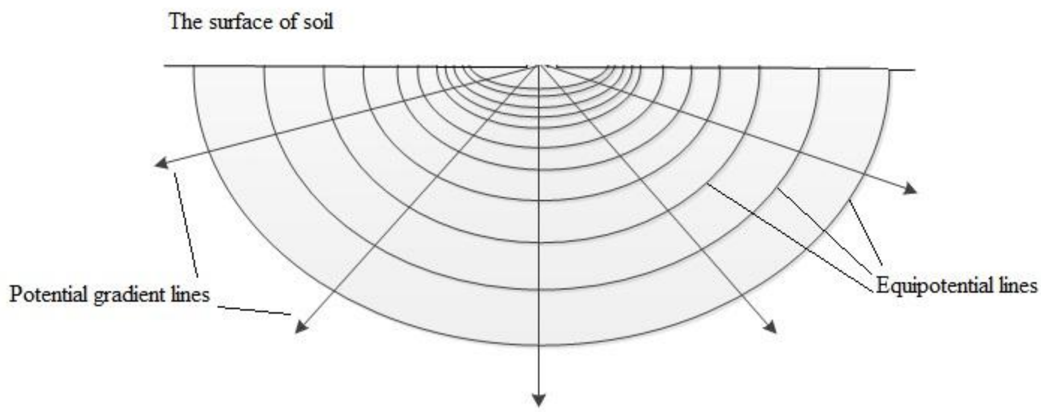

Figure 4.24. *Ground potential rise in homogenous soil.*

Potential in certain point in soil can be calculated by adding differential ground resistance elements together cumulatively. In this study the steps of 0.1 m are considered sufficient for the purpose. First the electric field strength is calculated in each radius from the strike point using the equation 4.2. The ground resistances between specific points and the strike point are then calculated with equation 4.7. Thus r is used instead of r_0 in all situations in this estimation because otherwise the calculation would give zero potential in all radii longer than the ionization radius r_0 due to ground resistance difference ΔR_g going to zero. In this straightforward estimation the potentials inside the ionized region are not equipotential as they should be. In figure 4.26 the potentials inside ionized area are fixed manually to illustrate the existence of the equipotential region. However, the most interesting potentials are in the distances outside the ionized region where the distance is greater and the potentials are lower than inside the ionized region. In figure 4.25 the ΔR_g is the resistance of the hemispherical soil layer of thickness Δr. With the lightning current I the potential difference ΔU is calculated using the equation

$$\Delta U = I \Delta R_g. \tag{4.12}$$

By summing these potential elements from the distant ground to given location at radius r from the strike point the potential at this location U_r can be estimated.

$$\sum_{i=300}^{r} \Delta U_i = U_r \tag{4.13}$$

The selection of distant ground inflicts some inaccuracy because the selected point is theoretically never distant enough to have real zero potential. In this estimation the distance of 300 m from the strike point is considered suitable. Thus the summing goes from 300 to r, the location under examination. The soil is assumed to be homogenous and the distorting effect of a buried cable is not considered in this estimation either. Because the metallic shield is again considered to be in zero potential, the voltage stress over the sheath can be estimated based on the local ground potential in the soil close to the cable.

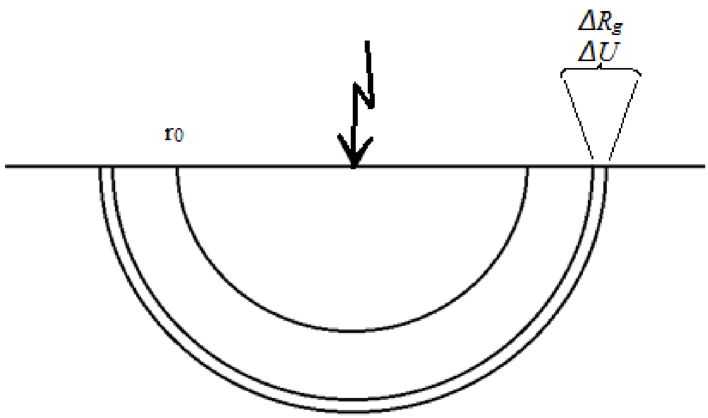

Figure 4.25. *Difference of ground resistance in GPR calculation.*

Next the GPR is estimated with 10 kA lightning current, 1000 Ωm soil resistivity and critical electric field strength in soil 1 MV/m. In the figure 4.26 the potential rise is presented at distances closer than 30 meters from the strike point. As seen, the potential rises very steeply at distances close to the strike point. The ionized area having equipotential contour can be seen in the left in the figure. The radius of ionized region in this case is 1.26 m.

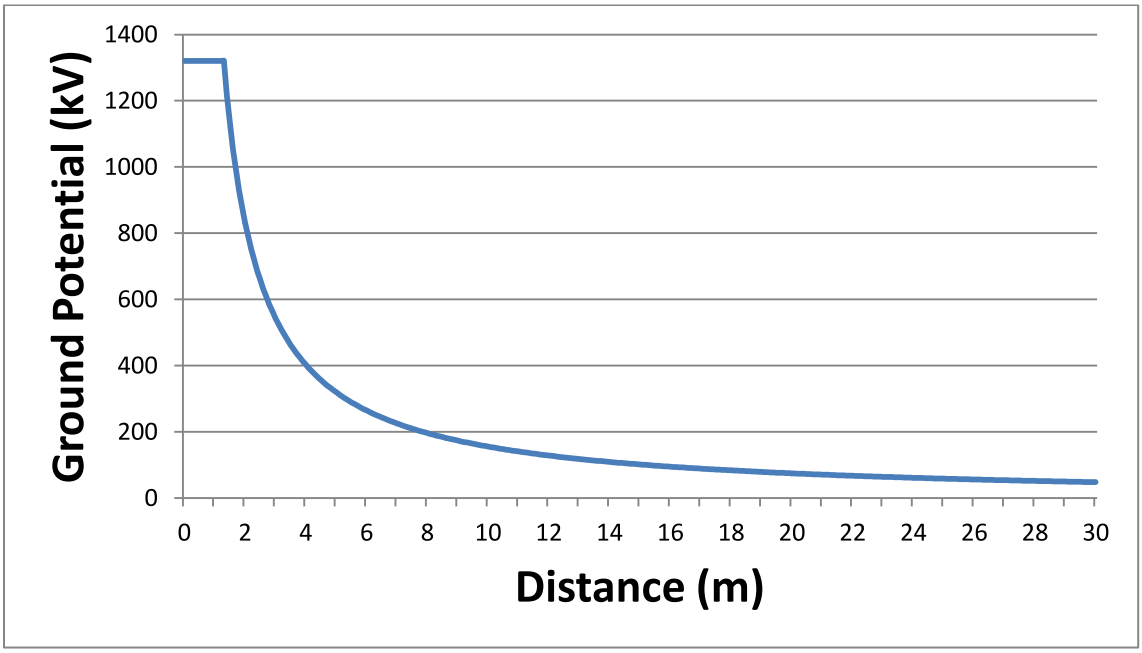

Figure 4.26. *Ground potential rise at distances closer than 30 m from the strike point when I=10 kA, ρ_s=1000 Ωm and E_0=1 MV/m.*

In the figure 4.27 ground potential levels are presented with the same current and soil parameters but now at the distances ranging from 4 to 50 m to provide a better view at the lower voltage levels. With the lightning current 10 kA and resistivity of soil 1000 Ωm the potential in the ground reaches approximately 150 kV at 10 m, 100 kV at 15 m and 50 kV at 29 m distance.

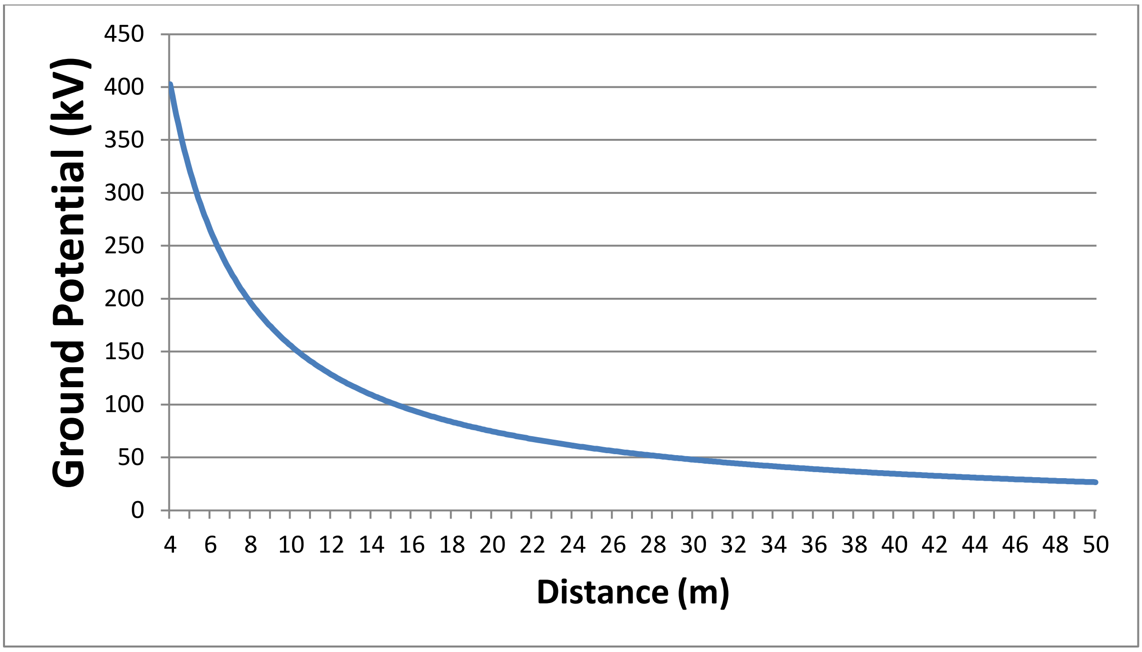

Figure 4.27. *Ground potential rise at distances from 4 to 50 m when I=10 kA, ρ_s=1000 Ωm and E_0=1 MV/m).*

Next the same examination is done for more resistive soil of 3000 Ωm while the current is kept same at 10 kA. Similarly as in the electric breakdown model the critical electric field strength is now fixed at 2 MV/m. Radius of ionized region is now 1.54 m. Soil resistivity is extremely crucial factor affecting the magnitude of ground potential rise. In the figures 4.28 and 4.29 it can be seen that the potential at same distances from the strike point are now significantly higher. Now the ground potential does not decrease to 150 kV until the distance is about 29 m. 100 kV is exceeded at the distance of about 41 m and 50 kV at about 52 m.

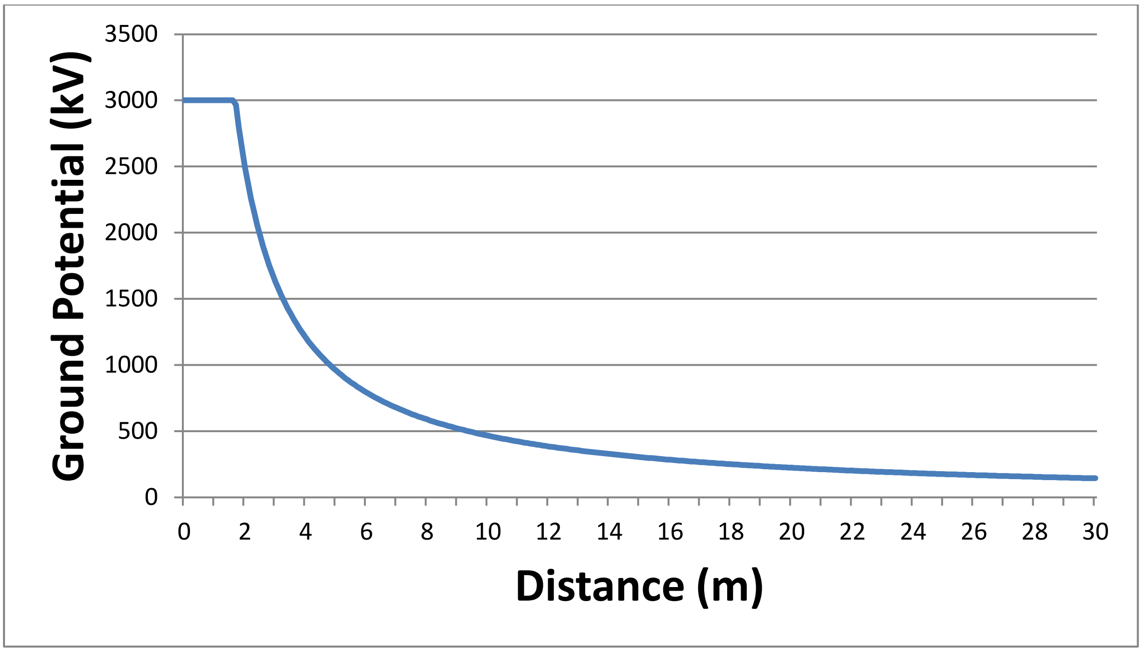

Figure 4.28. *Ground potential rise at distances closer than 30 m from the strike point when I=10 kA, ρ_s=3000 Ωm and E_0=2 MV/m.*

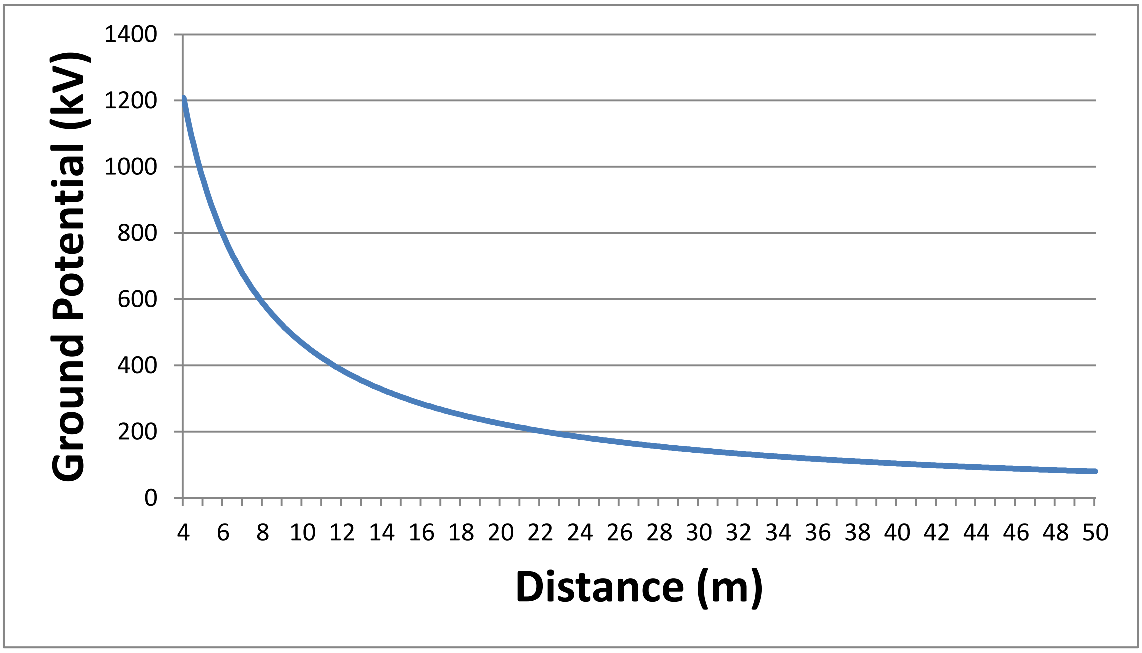

Figure 4.29. *Ground potential rise at distances from 4 to 50 m when I=10 kA, ρ_s=3000 Ωm and E_0=2 MV/m).*

Next the effect of current on ground potential rise is discussed by increasing the current value while resistivity stays stable. In this calculation the experimentally measured bond between the maximum current in soil and soil resistivity is taken into account (Mikhailov & Sokolov 1965). The value of 18 kA is chosen since it is the maximum current limited by equation 4.11 in 1000 Ωm resistivity soil. In this case the ionization radius is 1.69 m. The potential of 150 kV is now reached at about 18 m from the strike point. If the current value was increased above 18 kA it would not satisfy the limit of equation 4.11. However, smaller values like 10 kA are reasonable for examination since the equation only sets the maximum value of current.

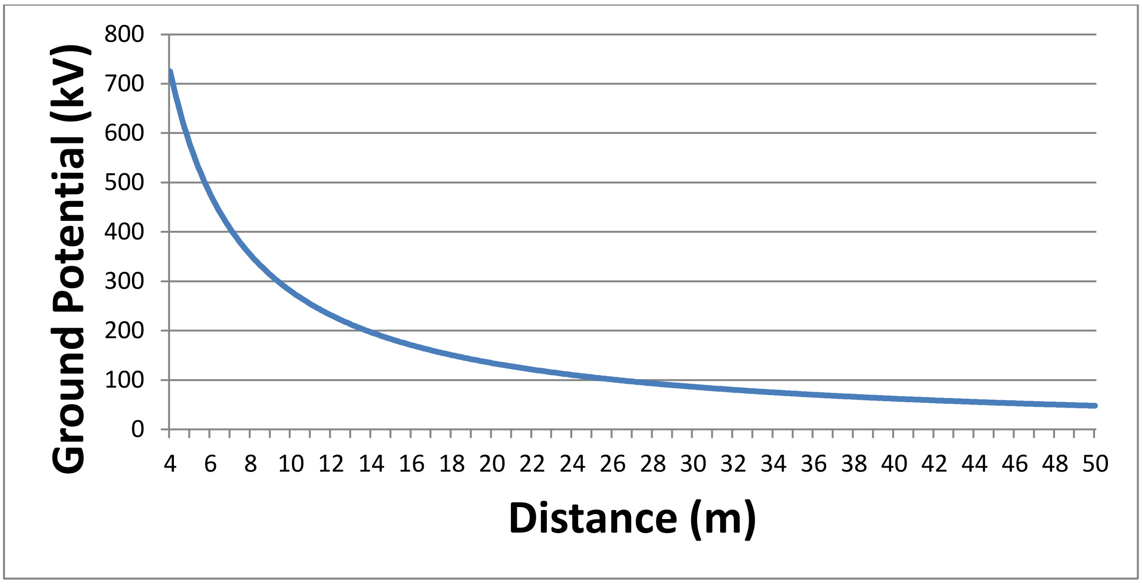

Figure 4.30. *Ground potential rise at distances from 4 to 50 m when I=18 kA,* ρ_s*=1000 Ωm and* E_0*=1 MV/m).*

As a last scenario the both current and resistivity are increased in parallel. In 3000 Ωm soil the approximated maximum current limited by equation 4.11 is about 16 kA. The level of 150 kV is not reached until at approximately 44 m. The radius of ionization is 1.97 m.

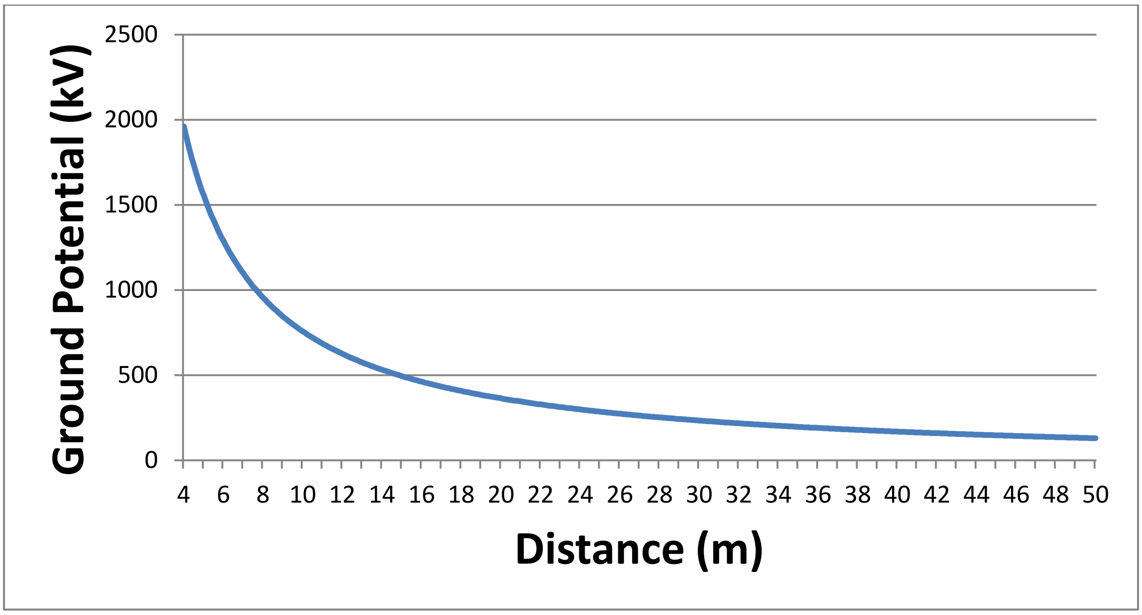

Figure 4.31. *Ground potential rise at distances from 4 to 50 m when I=16.22 kA,* ρ_s*=3000 Ωm and* E_0*=2 MV/m).*

These examples were presented to show the behaviors of the straightforward GPR-model in few different cases. The concept was discussed to show that a direct electrical breakdown is not the only mechanism for a direct strike to ground to have an effect to the buried cable. As noticed the resistivity of soil is extremely crucial factor affecting the magnitude of ground potential rise. In highly resistive soil the ground potential rise is large because the current is not easily dissolved into soil. However, like any other inhomogeneity a nearby cable distorts the electric field and the contours of ground potential rise. This adds some inaccuracy to the GPR estimations. In case of GPR estimation in long distances it is also important to notice that the changes in soil resistivity are usually more significant for greater distances.

In case of a soil breakdown reaching the cable the cable sheath is likely punctured in any case regardless of the impulse voltage strength of the cable sheath. However, in case of GPR the impulse voltage strength of cable can be compared to the potential in the soil surrounding the cable. If the local potential exceeds the voltage strength of the sheath the puncturing takes place. Due to very low current proceeding to the cable, the similar travelling wave like in case of soil breakdown is may not be probable.

4.5 Other aspects and mechanisms

Lightning strike has many ways to damage buried cables. Previously a direct strike to the ground was discussed both based on the electric breakdown in soil and ground potential rise without soil breakdown. Limitation of the current dissolving into soil was discussed as well. In addition to these there are many other possibilities of the cable to get effected by lightning current. These issues are pondered in a more lightweight manner without further calculations. At last the mechanism of soil breakdown is briefly discussed in a microstructural level.

4.5.1 Trees and conductive structures

The conductive structures provide an easy and a low resistant path for lightning currents and transient overvoltages into soil. For example utility poles, telecommunication towers and buildings usually have grounding wires buried in the soil near them. These are the ways for the lightning current to get into deeper layers of soil through the resistivity of surface level. For example, if the cable happens to be buried close to a grounding wire, it may suffer significantly from high current transients coming via that grounding wire. However, in other cases a nearby grounding may be useful while working as an additional shielding wire protecting the cable from strikes from some directions.

Trees may have a very good conductivity as well especially when wet. If struck to a tree the lightning current probably follows the roots of the tree to ground. If roots are nearby the cable they may lead into similar situations as with grounding wires. Anyway the both distort the electric field in the soil. As said earlier, soil is rarely homogenous and there are probably other conductive objects and layers in soil as well. For example, if moisture is dissolved unequally it strongly distorts the homogeneity.

4.5.2 Reflection of transient pulse in an open end of a cable

Behavior of the overvoltage transient in the discontinuity points of the cable shield can be handled with the travelling wave theory. When the travelling wave arrives to the point of discontinuity of the characteristic impedance in a cable, reflection of the wave occurs. For example, the bigger the characteristic impedance of the cable is at the other side of the point of discontinuity, the lower current will pass through it. In this case the charge is stored into the point of discontinuity. The charge raises the potential in the discontinuity point, which produces a reflecting wave directed back into the direction from where the original wave came. In figure 4.32 the dashed line represents the point of discontinuity of characteristic impedance. (Aro et al. 2003.)

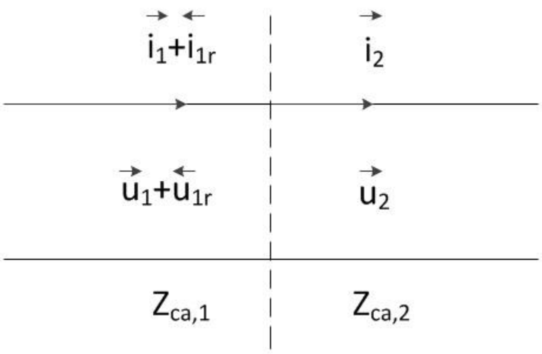

***Figure 4.32**. Reflection of a travelling wave at the point of discontinuity of characteristic impedance (Aro et al. 2003).*

The equations 4.14 and 4.15 represent the situation of the figure in general, where u_1 and i_1 are the original voltage and current in side of characteristic impedance of $Z_{ca,1}$. u_2 and i_2 are the voltage and current at the other side of the discontinuity point where the characteristic impedance is $Z_{ca,2}$. $u_{1,r}$ and $i_{1,r}$ are the possible reflections. The directions of movements in the picture are indicated with the arrows and in the equations below the quantities having the same sign have the same directions of movement as well.

$$u_1 + u_{1r} = u_2, \tag{4.14}$$

$$i_1 + i_{1r} = i_2, \tag{4.15}$$

As described earlier, the figure 4.32 stands for the reflection in general when the characteristic impedance changes.

The two extreme conditions are an open ended cable (open circuit) and solidly earthed cable (short circuit) end shown in the figure 4.33.

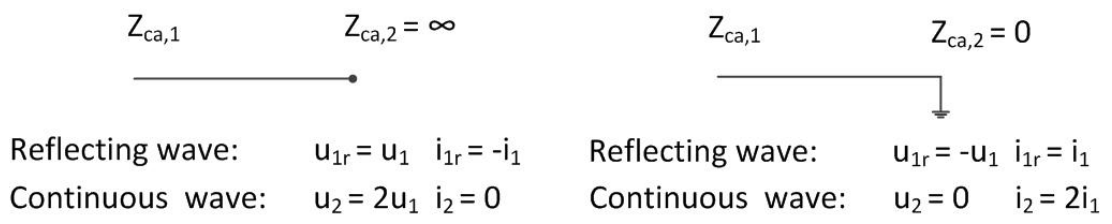

Figure 4.33. *Reflection of a travelling wave in extreme conditions.*

On the left in the figure a cable or generally a conductor has its end left open. This can be illustrated with the characteristic impedance $Z_{ca,2}$ approaching the infinity on the other side of the discontinuity point. The voltage of the open ended cable is doubled at the open end. The whole current is reflected backwards with negative polarity while total current at the open end is constantly zero. The ideal grounding of the open end on the right in the figure 4.33 instead makes the voltage drop to zero due to the negative reflection of voltage. However, in this case the current gets doubled. (Aro et al. 2003.) Naturally, in every reflection situation the total power of the travelling wave remains constant.

These reflection phenomena may have a harmful effect on the cable sheath in some cases of the lightning current traveling in the cable. Especially the doubling of the voltage may cause additional stress to the cable sheath if the ends of the cable are left open. In a long cable with both ends open the travelling wave may even reflect multiple times when the reflection waves may be superpositioned. However, when the cable is connected to the grid there is no open end anymore. It is still wise to avoid the transient reflections by grounding the open ends for the period when cable lies unconnected. As discussed later on the chapter six the temporary grounding the cable ends is useful for other reasons as well.

4.5.3 Mechanisms of soil breakdown

According to Mousa (1994), when examined in micro-structural level, most soils contain non-conducting particles and air between them. The particles are coated with water with some salts. The conductivity provided by water coating depends both on the amount of water and the amount of dissolved salt in soil. The average size of air voids between the soil particles depends on the size of the particles which usually vary in wide range. Thus a dust-like soil has smaller particles and also smaller air voids compared to for example sand with more coarse particles and larger air voids. If the soil particles are irregularly shaped the air gaps are also irregular. This makes the maximum electric field strength in soil significantly higher compared to soils with regularly shaped voids. (Mousa 1994.)

Mousa (1994) presents two possible mechanisms suggested in earlier studies for the breakdown mechanism in soil when it is subjected to a high voltage. The first one (Leadon et al. 1983, cited in Mousa 1994) is based on the idea that the electric field in the voids between soil particles grows high enough to ionize the air in the voids. Another suggestion is based on thermal heating of the water content in voids resulted from high current flowing through it. The ionization mechanism is however considered to be more convincing theory than thermal heating. Mousa (1994) lists some important proofs supporting that theory: Leadon et al. (1983) examined the ionization mechanism by replacing the air with SF_6 insulation gas which has significantly higher breakdown gradient than air. Resulting to an increase of a breakdown gradient in soil it proved that the breakdown is initiated by the ionization of the gas in the voids (Mousa 1994).

5 LABORATORY TESTS

The focus of laboratory tests was to gain information about the breakdown strengths of the outer sheaths of the chosen test cable types. Similar tests were done before for the AXAL-TT PRO by Ericsson. The idea was to use approximately similar measuring method and setup also for these tests.

By comparing the average breakdown strengths of different cable types, the vulnerability of the cables to lightning strikes can be evaluated. Some information can be achieved also from the dispersion of breakdown voltages of different samples of the same cable type with each other. This indicates how significant variations there are between the samples of the same type. Standard deviation can be used for that purpose. In this context it has to be mentioned also that breakdown events in general are of statistical nature and even in case of fully identical cable samples the results will show a statistical distribution.

The tests were done in the high voltage laboratory of Tampere University of Technology which provides safe environment and variety of equipment for research and test purposes. The test voltage sources in the laboratory are 300 kV AC voltage, 950 kV impulse voltage and DC voltage sources of 100 kV and 130 kV. There are also additional measurement devices for partial discharge, leakage current and material properties measurements. In the newly rebuilt multifunctional climate room the test samples can be exposed to extreme weather conditions. For example, temperature can be varied between -65°C and +70°C.

In this chapter there is first described the main idea and setup of the tests including a diagram of the test circuit. After that the test results are examined. Lastly the thicknesses of punctured sheath pieces are analyzed to find out the possible cross-sectional thickness variations that might have affected the breakdown strengths of the sheaths.

5.1 Facilities and test setup

In this study the breakdown strengths of the sheaths of the cable types tested were measured using the impulse voltage generator as a test voltage source. The tests were facilitated by hanging each cable one by one between the far end corners of the laboratory hall. The lengths of the samples were about 10 m. In the middle of the cable a wet piece of cloth was wrapped together with an aluminum foil on top of it. This artificial electrode was connected directly to the laboratory grounding. The structure of the electrode is show in figure 5.1. The other end of the cable was left open while the other acted as a terminal for the voltage source. The sheath of the terminal end was opened so that part of the metallic shield was revealed and could be connected to impulse generator via a copper conductor (figure 5.2). AHXAMK-W samples were tested only one phase at a time because this stranded cable type has a separate metallic shield under the sheath of each phase.

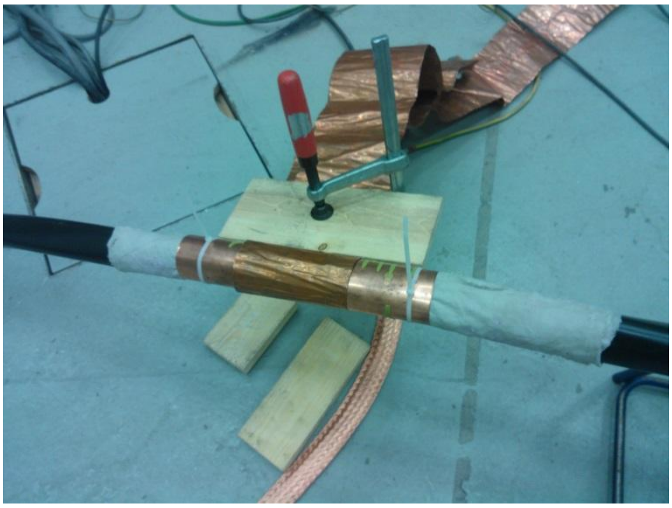

Figure 5.1. *The structure of earthing electrode connected to laboratory ground.*

Figure 5.2. *On the left: The metallic shield of a cable connected to impulse generator via a copper conductor. On the right: Open end of a cable and the grounding electrode.*

The measurement circuit used in the tests is presented in figure 5.4. The area inside the rectangle with dashed line describes the impulse voltage generator. The impulse voltage generator is so called Marx's generator consisting of ten HV capacitors, C_{HV} in the figure. Between the two terminals of each capacitor are an adjustable spark gap and a parallel discharge resistor R_D. The capacitor stages are separated from each other by internal series resistor R_I. Maximum amount of capacitors in the generator is ten. They can produce about 950 kV impulse voltage while the maximum charging voltage of the generator is 1000 kV with the energy of 50 kJ. In this series of tests three series connected capacitors were included in the test circuit. It produces about 300 kV peak voltage which was sufficient for the purpose of the test. The three capacitors in series form a capacitance of 333 nF (R_D) since each of those has capacitance of 1 µF. In the figure 5.4 all the three capacitor stages are drawn as one equivalent circuit to simplify the setup illustration. Basic idea of a multistage impulse generator is to charge all the capacitor stages in parallel through high ohmic resistors and discharge them in series by igniting the spark gaps (Kuffel et al. 2000). The discharging of the generator starts when the breakdown of the first spark gap occurs. The first gap is adjusted little shorter than the others and is ignited using a small external spark gap igniter. The other gaps will follow nearly simultaneously when the voltages in the capacitor terminals change. Charge carriers of the first arc form a breakdown channel between the next gap. Discharge resistors and internal resistors control and adjust the shape of output HV pulse. In this setup parallel discharge resistors were 3x68 Ω and internal series resistors 3x12 Ω. All the resistors are changeable as well as the number of capacitors included in the circuit.

***Figure 5.3**. Haefely SGS 1000 impulse voltage generator.*

The terminal of the impulse voltage generator is connected to external series resistor R_E which is rated 350 Ω. It connects the generator to the voltage divider. The divider transforms the output voltage to a suitable level for the measuring instrument using voltage divider ratio of 700.20. The top terminal of the divider is connected straight to the metallic shield of the cable sample via low inductance copper conductor. The impulse voltage generator of the laboratory is of type Haefely SGS 1000. In the control room the whole system is controlled by a control unit and Haefely Impulse Analyzating System DiAS 733 which is used to measure and analyze the impulses.

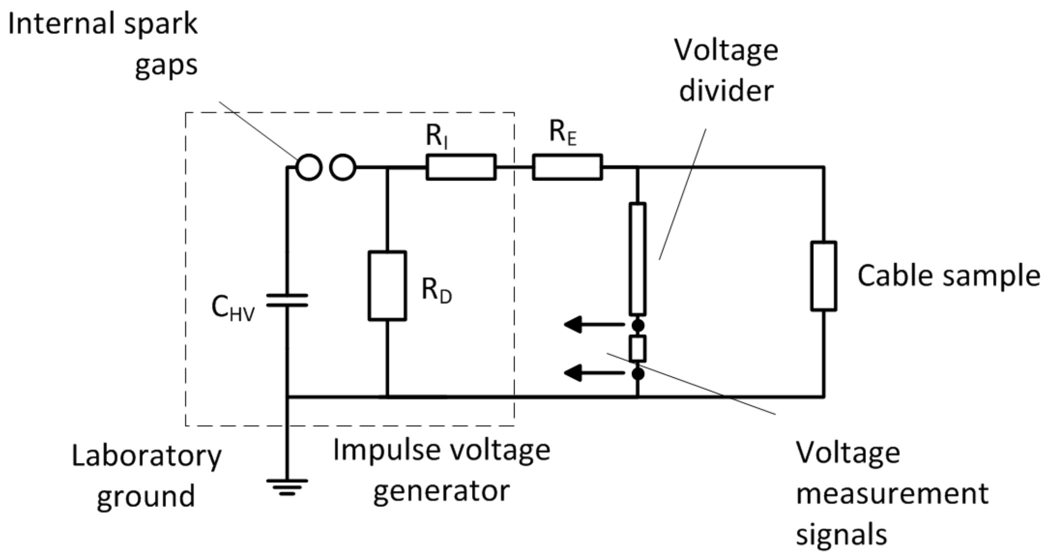

***Figure 5.4**. One stage equivalent model of the lightning impulse test circuit.*

5.2 Tests and Results

Altogether four different types of cables were originally chosen for the tests. Anyhow, AHXAMK-W and AHXAMK-WP are exactly similar cable designs the only difference being a central grounding wire stranded in the middle of the three separate phase cables in the later one and it was not possible to test the effect of the grounding wire with a reasonable test arrangements. Due to this, these cable types were tested phase by phase and since the phases are identical the number of tested cable types decreased to three and the AHXAMK-WP type was thus not tested.

Six parallel samples per cable type were considered a reasonable amount to limit the amount laboratory work but still provide statistically useful data. The charging voltage of the generator was raised in steps of 2 kV always starting from the level of about 50 kV or more below the breakdown voltage. After the voltage reached a level high enough to cause a breakdown of sheath the sample was replaced and the exact breakdown spot was examined. Before every test all dirt was removed from surface of the sample cable with a piece of cloth to prevent undesirable weak spots and distortion of electric field on the surface of the sheath.

The shape of the voltage pulse was aimed to be close to the standard impulse voltage which has a front rise time of 1.2 µs and a time to half-value of 50 µs. The tolerances of ± 30 % for the rise time and ± 20 % for the time to half value are determined in IEC standard 60060 (Kuffel et al. 2000, p. 51).

The results of the tests with positive polarity impulses injected to the cable shield are presented in the table 5.1. Below the results of every six samples there are also average, median and standard deviations calculated from the results. It can be seen from the results that the average and median of typical breakdown level was lower with AXAL-TT compared to AHXCMK-WTC/PE and AHXAMK-W. However, the standard deviation which indicates the data dispersion from the average value is the lowest with AXAL-TT. As an opposite the AHXAMK-W had the largest standard deviation of about 26 kV. Smaller SD may refer to more homogenous sheath quality between the 6 samples of this type. The statistical behavior of breakdown process has also an influence to the SD and it is obvious that with only six parallel breakdown results it is not possible to get high statistical relevance for the calculated estimations of the SD or other statistical parameters. The tests were laborious to perform and the number parallel tests is a compromise between the amount of testing time and the statistical relevance needed for usable test results.

The sheath of the sixth sample of AHXCMK-WTC/PE could not be measured. The sheath remained unbroken even with 185 kV impulse and tests with higher voltage levels led inevitable to several meters long arcs towards the open end of the cable. In most cases the flashover to the open end was be avoided by sinking the open end of the cable to insulating oil, which has significantly higher breakdown strength than air (Aro et al. 2003). However, in case of the sixth AHXCMK-WTC/PE sample the flashover occurred despite the usage of oil. This sample was not included to the calculation of average, median and standard deviation of that cable type.

A flashover on the cable surface was captured with a high exposure time photography shown in figure 5.4. All of the sheath breakdowns occurred under or close to the grounding electrode. The lengths of the samples still had to be relatively long to avoid flashovers. However, they could not be totally avoided and modifications to the test setup were required with many samples except AXAL-TT samples. These modifications included usage of longer test sample and oil insulation at the open end of the cable samples. These modifications did not affect on the actual electrical stressing of the sheet and all the results are thus comparable. Avoidance of flashovers with AXAL-TT samples resulted from the lowest breakdown strengths compared to other types.

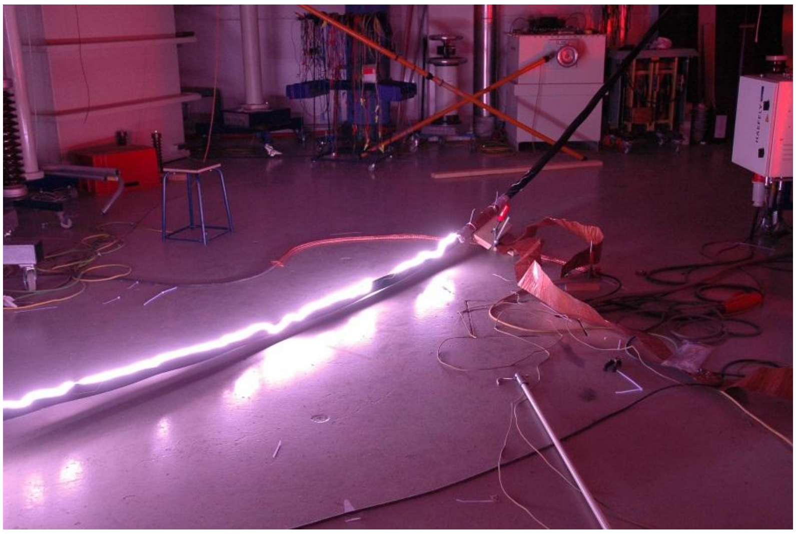

Figure 5.4. *A flashover along the surface of the cable.*

AHXCMK-WTC/PE and AHXAMK-W had higher average breakdown strength than AXAL-TT. That is probably caused by the difference in the sheath material compositions. Higher breakdown strength is an advantage but because the PE sheath is not primarily an electrical insulation, the other factors are usually at higher relevance than BD strength during the designing of the cable structure. As already discussed in the second chapter, mechanical strength, water resistivity and UV protection abilities are more important to assure the long life span of the cable in rough outdoor conditions. The difference in BD strengths is not significant when the BD levels are compared to the calculations of the fourth chapter. The results are similar to the ones gained by Ericsson in Sweden for AXAL-TT. Few verifying tests were done with negative polarity impulses to the shield. They are presented in the table 5.2 where it can be seen that they follow the results gathered with the positive polarity. Because of limited laboratory time, no more negative polarity tests were conducted.

Table 5.1. *Results of breakdown strength tests with positive polarity (kV).*

Sample	AXAL-TT	AHXCMK-WTC/PE	AHXAMK-W
1	155.2	181.5	154.5
2	164.4	171.2	146.0
3	158.2	201.1	177.8
4	137.3	176.4	186.3
5	157.3	173.4	220.8
6	163.8	not broken	171.6
Average	156.0	180.7	176.2
Median	157.8	176.4	174.7
SD	9.9	12.0	26.5

Table 5.2. *Results of breakdown strength tests with negative polarity (kV).*

Sample	AXAL-TT	AHXCMK-WTC/PE
1	160.7	173.9
2	149.6	

5.3 Sheath thickness and punctures of the sheath

After completing the breakdown strength tests and examining the results shown in table 5.1 there appeared some questions about sheath thicknesses in the punctured sections of the cables. The interesting questions were for example following ones. Does the lower breakdown strength of the sheath result from a smaller sheath thickness? Does the breakdown likely take place on the surface area with small sheath thickness?

The most reasonable way to approach these questions was to pick up the cable samples with the smallest and largest measured breakdown strengths. Since the deviation between the results is clearly the largest with AHXAMK-W cable, it was chosen for the examination. The samples 2 and 5 of AHXAMK-W represent the two extremes of the breakdown strength in this test series. The measurements were performed with a regular slide gauge. The results can be read with accuracy of about 0.05 mm using this tool. This method was accurate enough for the purposes of this small scale test. The more accurate larger scale sheath thickness monitoring can be done by cable manufacturers. The measured thicknesses of the two samples are presented in the table 5.3. The cross-sectional cylinder of the cable sample 2 used in the measurements is shown in figure 5.5. The cylinders have been cut from about 5 to 10 cm distance from the actual punctured point. However, this should give a good reference of the thicknesses at the punctured points since longitudinal variation of the thickness should be small.

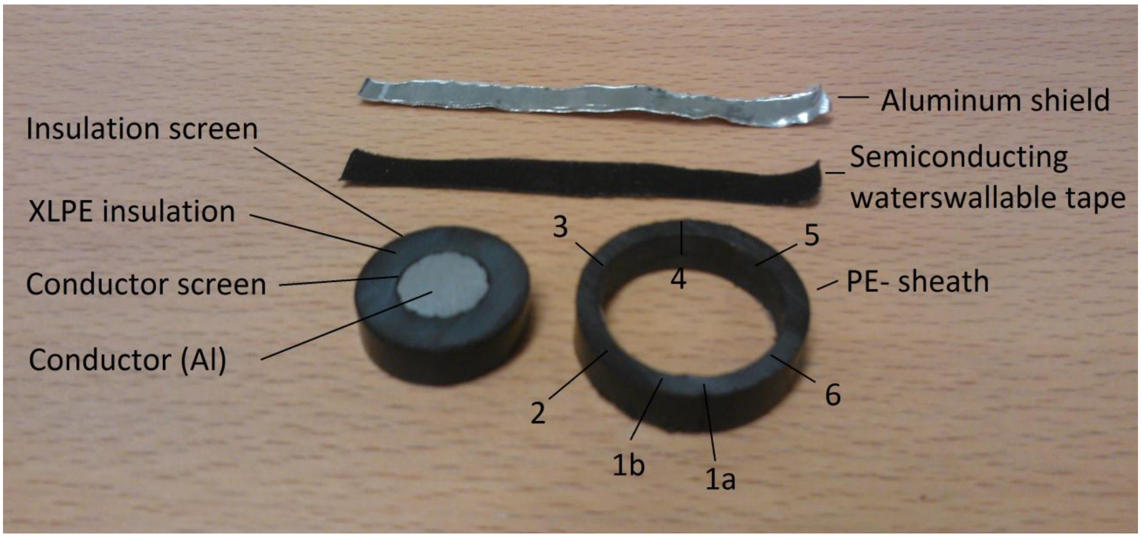

Figure 5.5*. A cross-sectional cylinder cut from AHXAMK-W sample 2. Thickness measurement points are indicated with numbers 1 to 6.*

Since according to Mutru (2013) the deviation of sheath thickness is longitudinally not as significant as cross-sectionally, the measuring points are chosen similarly with the method used by cable manufacturers. The local thickness is measured at seven points on the cross-section. Thickness 1a is measured from the spot corresponding longitudinally the punctured point in the cylinder. 1b is measured right next to 1a but other side of the PE-bulge as a checking measurement. Other measurements numbered from 2 to 6 are taken about equal distances from each other on the PE cylinder. The averages are calculated with measurement points 1a, 2 ,3 ,4 ,5 and 6. The point 1b is left out of the average because it is right next to 1a and the average is formed from 6 points with about equal distances between them.

Table 5.3*. Cross-sectional sheath thicknesses of AHXAMK-W samples 2 and 5 (mm).*

Sample	1a	(1b)	2	3	4	5	6	Average
2	3.00	(3.00)	3.10	3.15	3.15	3.20	3.05	3.11
5	3.00	(2.95)	3.10	3.10	3.15	3.20	3.15	3.12

During the measurements it appeared that the punctured point was in both samples close to the seam-like bulge on the inner surface of PE cylinder. The bulge is resulted by the aluminum foil shield layer, which has its ends superpositioned at this point like shown in figure 5.6. It means that there is about 8 mm long double layer of aluminum shield right next to the bulge clockwise. The punctured point is cross-sectionally here in both AHXAMK-W samples. It seems like there is always locally 0.1-0.2 mm thinner layer of PE on the surface of the cable in this section because of the seam point of aluminum shield. When there is the described special seam area in the cross-section interface of the shield and the sheath, it is likely that the puncture takes place here where the insulation is the weakest. However, when comparing the average and local thicknesses of the two samples there is no indication that the large margin of the breakdown strengths between them could be resulted by difference in thicknesses. It may also be possible that the sharp edge of superpositioned foil causes a locally stronger electric field.

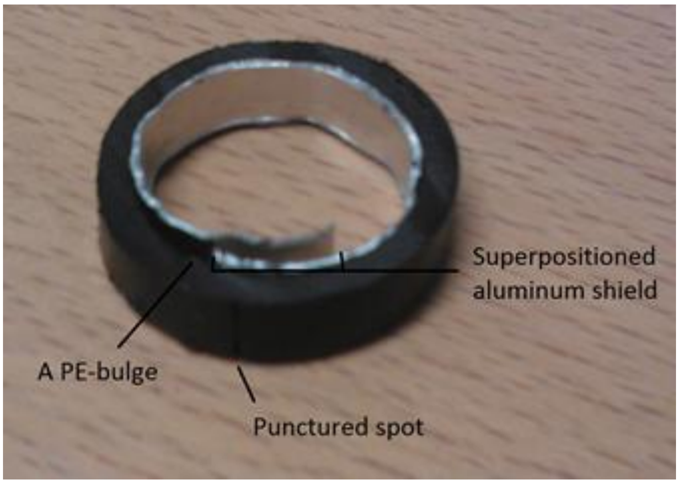

Figure 5.6*. Superpositioning of aluminum shield of AHXAMK-W sample 2.*

When considering other reasons that may have led or affected the significant difference of breakdown strengths between the cable samples, the effect of sheath thickness can practically be excluded. There are still some other factors worth examination. Even if the thicknesses are nearly indifferent, there may be still some local differences in the sheath material. For example black carbon content in the PE-sheath might be unevenly distributed. However, studying of that is not key content of this thesis and is not considered any further here. Maybe the most probable reason for the large differences between the breakdown strengths of the sheaths in general is the probabilistic nature of breakdown mechanism. Each breakdown event actually is a combination of surface arc on the sheath surface and a breakdown through the actual sheath insulation. The formation of the surface arc probably increases the deviation of the results since the formation of the arc is highly statistical as well and because the arc formation has an effect on the tested cable sheat area.

6 POSSIBILITIES TO DETECT AND PREVENT SHEATH FAULTS

Although the condition of the main electrical insulation of a cable is more crucial than the outer sheath, it is important to be confirmed that the sheath is in good condition before the cable is switched on as a part of the electricity distribution system. Possible leaks in the sheath will degrease the lifetime of the cable by allowing moisture ingress and its consequences. The sheath condition is confirmed with particular sheath fault tests described in more detail later. If the tests are performed after the required cable joints and terminations are installed, the quality of them is checked at the same time as well. This is important since handmade joints and terminals are the areas where moisture may get into the cable if the installation is not made properly. This way the proper quality of the installation work can be assured. The sheath may also get damaged by accident even if the installation is done properly. There is always possibility of manufacturing fault in the cable as well even though they are extremely unlike today. Although the most obvious purpose of the sheath fault testing is to confirm the quality of installation work, the possible damages of atmospheric overvoltages in the sheath may be pointed out as well.

In this chapter the case of a sheath damages resulted by atmospheric overvoltages is presented. After that the principles of sheath fault detection method is discussed. At last there is a discussion on preventive measures to mitigate the possibility of sheath damages caused by atmospheric overvoltages.

6.1 Viitasaari case

The interest in this study is based on the revealed sheath damages of AXAL-TT medium voltage underground cable in a rebuilt project of Elenia at Pyydysmäki-Lonnikko area, near Viitasaari in central Finland. Some other suspicions of similar cases have also come up, but no accurate data of them is available. In Viitasaari case, after the installation of new MV cable line, the condition of the sheath was tested using regular sheath fault test method introduced in the next subchapter. The first sheath fault tests were done in June 2013 as a standard measure after the installation of cables. The idea of the first tests is to ensure that the sheath remained undamaged during the installation. There were no indications of sheath faults in the first tests in June 2013 (Turpeinen 2013). Since then the cable was left unconnected to the network until the commissioning.

However the commissioning tests done in July 2013 indicated that the sheath was apparently damaged (Turpeinen 2013). Since the cable was inspected in the field and none mounting faults were found, the damages were most likely caused by atmospheric overvoltages. The damaged part of the cable is presented with a red-yellow line in the figure 6.1. In the figure the blue lines are old replaced parts of the 20 kV overhead line network. The purple lines are the remaining parts of the old network.

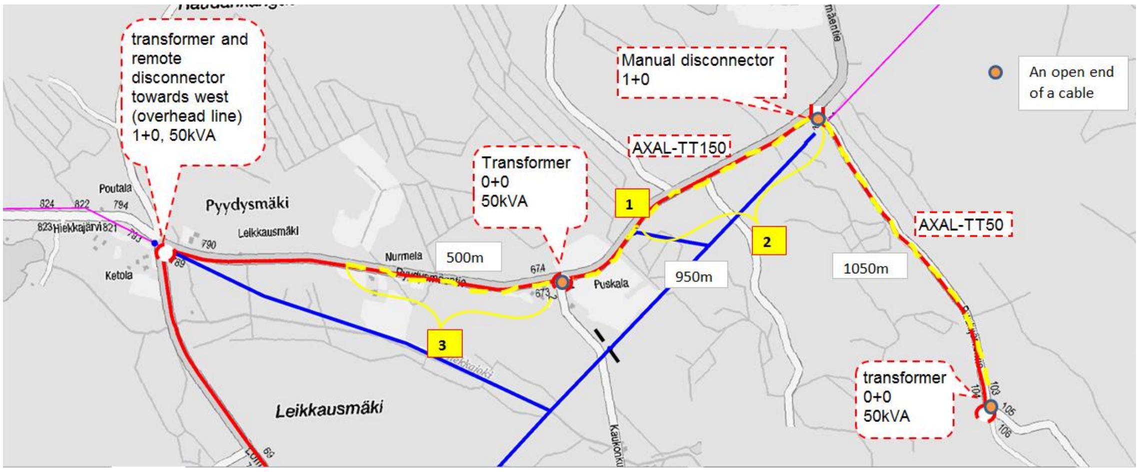

Figure 6.1. *A map of damaged AXAL-TT cable in Viitasaari.*

A view from the inside of the substation cabinet with remote disconnector and transformer in the left side of the figure 6.1 is presented in the figure 6.2. It can be seen that the cable terminals are open ended as well as the screen grounding terminals. Hence, this end of the cable was open and not grounded. The other terminals at the transformer and disconnector cabinets were likely open and not grounded as well. All of the open ends of the cables shown in figure 6.1 situated in their final locations inside the transformer or disconnector stations. The joints and terminals were also installed and completed when the faults were obtained in the commissioning tests (Turpeinen 2013).

Figure 6.2*. Open ends of AXAL-TT in the remote disconnector facility.*

After the unsatisfying results of sheath fault tests occurred, parts of the cable were dug out and examined. There were found small holes in the sheath in intervals of couple meters. One of these point-like holes is shown in the figure 6.3. Similar perforations rate of a MV cable was suspected to be caused by lightning strikes close to cable route in Austria (Muhr et al. 1997)

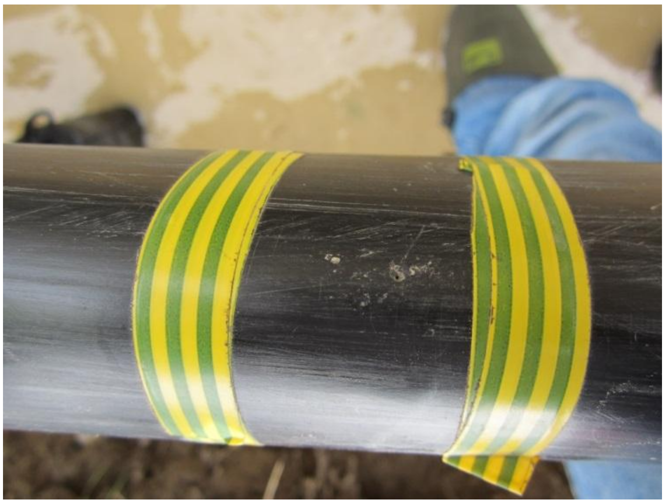

Figure 6.3*. A point-like hole in the sheath of AXAL-TT cable.*

In addition to the holes, some swellings were found in the sheath with no clear break-down marks. When the swells were removed there were found burn marks under the sheath. That refers to a high current that may have flowed in the screen under the sheath. At the site the contractor personnel tried to fix the damages using heat shrinkable plastic covers, but after realizing the continuity and amount of the damages the repair work was given up. At least one of the holes in the sheath was clearly a larger one. If the whole damaged area surrounding the hole is counted in, the diameter was even 15 mm. It may be possible that these larger holes were widened by sheath fault test because the continuous high voltage DC test voltage has enough energy to melt the sheath material. The soil material next to the hole has a major significance in the formation of the hole. However, the large hole still may be resulted fully by the lightning current and it may be speculated that the larger hole could be the point where the lightning current has entered the cable and the remaining smaller holes are caused by consequent travelling wave travelling along the cable..

The damaged cable was originally buried using mixed plowing and digging method. The geographical conditions at the site can be described rough and rocky. At some points the cable route goes over solid rock and the installation of the cable was done using concreting method. (Turpeinen 2013.)

It is very hard to describe the actual damage mechanism in the AXAL-TT case because there is no information of the striking point of the lightning. However, multiple holes in the sheath with high frequency likely refer to travelling voltage which has been injected into the shield of the cable. The soil breakdown seems more likely than ground potential rise of surrounding soil. The travelling wave and multiple punctures would not likely be possible with ground potential rise since the current injected into the cable is low. Instead, in occurrence of soil breakdown the current injected into the cable is high because of the highly conductive breakdown channel. Multiple punctures may have been avoided by use of temporary grounding in Viitasaari. However, most likely the cable had still been punctured at least once since the soil breakdown penetrates the sheath inevitably if the breakdown channel reaches the cable.

6.2 Principle of a sheath fault detection method

Sheath fault detection methods are used to obtain possible damages in the sheaths of cables. There may be different methods for the purpose, but in this case only the method used by Elenia is under further discussion.

6.2.1 Sheath fault detection according to Elenia practises

In the test used by Elenia the measuring voltage of 5 kV DC is applied for PE sheathed cables. The duration of test is 1 minute. The measurement is required for each newly installed underground MV cable in Elenia grid and it is instructed to be performed earliest at about a week after the installation of cable if cable has been plowed. This way the soil has time to become tighter around the outer sheath of the cable. If the phases of the cable are separately sheathed, every sheath must be also tested separately. Since 5 kV is considered as high voltage the required safety aspects during the testing must be carried out. The cable joints and terminations must be finished before the testing. This way their conditions are checked as well at the same time. Every buried cable length has to be tested and documented. The measurement records are archived and presented to the orderer of the work. (Vattenfall 2008.)

Elenia includes this test into the general commissioning tests that are done for every new cable installation. The sheath fault test is done in parallel with an insulation resistance test, which is used to measure the resistance between live parts and electrical ground. Phase conductors represent live parts and electrical ground is available in earthing conductor connected to the ground. While insulation resistance testing is a way to detect faults in the main insulation, the sheath fault detection is made to spot the faults in the outer sheath. Faults in the main electrical insulation are more critical for the system and the cable because they lead quickly to interruption of electricity distribution. In case of a fault in the sheath instead, it may take several months or years until the fault leads to distribution interruption. This is maybe one reason why the sheath fault tests have not been performed much in the past. Also the plowing is relatively new method and at least during the first years of the implementation the method increased the risk of sheath faults Before the implementation plowing method, the need for sheath fault tests was probably lesser. Since the MV underground cables are becoming more and more common in distribution network, the knowledge and usage of sheath fault testing is spreading wider among the utility companies in Finland.

In Elenia it is noticed that since the contractors have gained experience on the testing method through years of working with it, the rate of installations where the fault indication limit is exceeded is dropped as well (Vähäkuopus 2013). The drop is likely resulted by constant learning process which leads to improvement in the quality of cable installation. Generally, this is a win-win situation for both the network owner and the contractor.

The sheath fault testing is generally based on measuring of leakage current from the shield to the ground. If the leakage current through the sheath is high enough, it indicates that the sheath is faulty. The test voltage is injected to the metallic shield or screen of the cable. The resistance between the shield and earth can then be calculated by measuring the leakage current from shield to earth. However, the tolerances in current levels indicating a fault are not very clear. In the figure 6.3 there is presented the recommended interpretation of the leakage current levels through a PE sheath according to Elforsk (1997). The figure would be different for the PVC sheathed cables or cables manufactured of some other sheath material. The test voltage of PVC (2 kV DC) cables differs also from the one used for PE sheathed cables. However, since PE is the most used sheath material of modern MV power cables in this study only the leakage current through PE sheath is discussed.

In the figure 6.3 the Elforsk (1997) guide for interpreting sheath fault test results is given. Results for faulted sheath is indicated with red and the non-faulted one with green color. A slightly problematic feature is that there is a blank area between unbroken and broken sheath in the leakage current levels. Leakage current of 1 mA per kilometer refers clearly to a sheath fault, as well as 1 or few µA/km refers that there is no fault in the sheath. If the current still lies between these boundaries, the interpretation of fault existence is not totally clear. However, in practice the results where the measured leakage current remains in the blank area have been relatively rare (Kalliorinne 2013). In most of the cases the resistance is several dozens or hundreds of GΩ if the sheath is not harmed. The figure 6.3 is based on the picture in the Elforsk report (1997). The resistance values are added to the figure for the measured cable with length of 1 km.

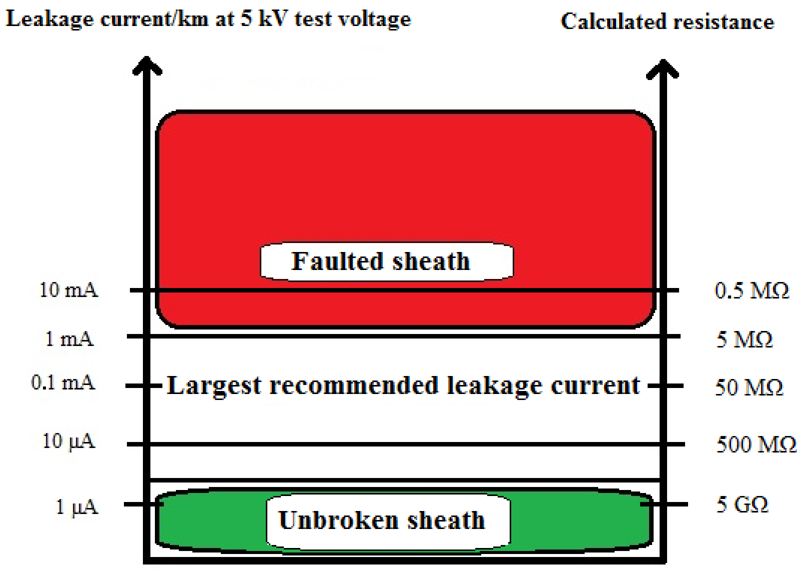

***Figure 6.3**. Interpretation of measured leakage current through the PE-sheath for 1000 meters long cable (Elforsk 1997).*

6.2.2 Evaluation of fault indicators

According to instructions of Elenia (Vattenfall 2008) the resistance over the sheath must be more than 500 MΩ (leakage current less than 10 µA/km) with 1 km cable length. If the resistance is less than 5 MΩ, the fault location must be found out and fixed using proper methods confirmed by the cable manufacturers (Vattenfall 2008). However, there are sheath fault cases in which the resistance was between 5 and 50 MΩ and even between 50 and 500 MΩ and the sheath was found evidently damaged. In Viitasaari case for example, in the faulted cable length of 700 meters a resistance of 155 MΩ was measured while the other stretches of cable had resistances of about 100 or 50 GΩ. The resistance over the sheath can be calculated using the equation

$$R_{sheath} = \frac{U_{sheath}}{I_{leakage} * l_{cable}}, \qquad (6.1)$$

where R_{sheath} is the resistance over the sheath, U_{sheath} is the test voltage over the sheath, $I_{leakage}$ is the leakage current per kilometer and l_{cable} is the length of a measured part of the cable in kilometers. The corresponding leakage current of the faulted cable length

(155 MΩ and 700 m) was about 46 µA/km. It shows that values of leakage current above 10 µA/km may indicate the existence of a sheath fault. Although the uncertainty of blank area in the figure 6.3 is presented in the Elforsk report (1997), the leakage current of 10 µA/km is still simply stated as a limit of fault indication in the report as well. Based on these issues the interpretation could be like illustrated in the figure 6.4. The resistances on the right are calculated for few cable lengths typical in the sheath fault testing. During the measurements the resistance given by the tester device should be compared to the cable length, especially if the resistance stands close to the limit of 500 MΩ or cable length is significantly greater or smaller than 1000 meters. However, if the measured resistance is several tens or hundreds of GΩ, the sheath is clearly healthy.

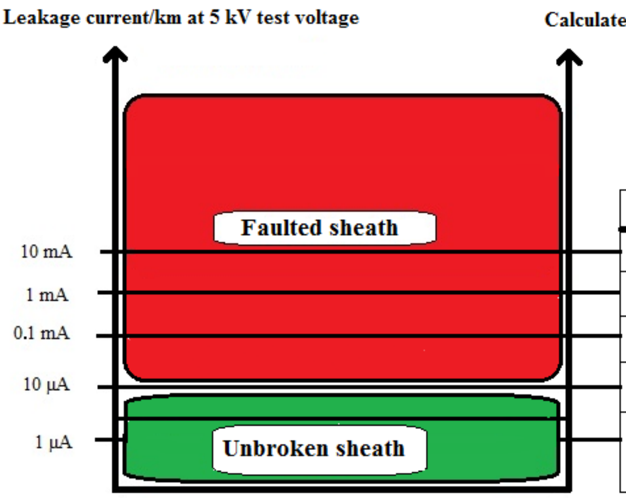

Calculated resistance

1000 m	750 m	500 m	250 m	100 m
0.5 MΩ	0.67 MΩ	1 MΩ	2 MΩ	5 MΩ
5 MΩ	6.67 MΩ	10 MΩ	20 MΩ	50 MΩ
50 MΩ	66.7 MΩ	100 MΩ	200 MΩ	500 MΩ
500 MΩ	667 MΩ	1 GΩ	2 GΩ	5 GΩ
5 GΩ	6,67 GΩ	10 GΩ	20 GΩ	50 GΩ

***Figure 6.4**. Suggested interpretation of measured leakage current through the PE-sheath for few different cable lengths.*

6.3 Preventive measures

Since the huge number of variables and differencing factors like the soil characteristics make every sheath damage case a little different from each other, the effectiveness of preventive measures might be hard to measure or evaluate. However some preventive measures can be carried out as an attempt to protect the sheath from lightning strikes. Attempt is a good term here because there is no method available that would protect the sheath fully for lightning strikes.

The total amount of sheath damages caused by atmospheric overvoltages in Finland is unknown. Since the rate of cable laying has accelerated there can be excepted more of these problems as well in the future. Naturally, the frequency of these kinds of damages defines how much intention the distribution network owners are willing to implement. From this point of view it might be useful to gather statistics of annual sheath fault cases. If compared, for example, to annual lightning statistics, increase of cabling rate, and applied preventive measures, the trends in the change of sheath fault frequency could be surveyed. At the moment the fault frequency seems to be at the level in which only the preventive measures having relatively low investment costs are worth further consideration.

6.3.1 Shielding ground wires

According to Haluza (1996) the probability of a direct strike to buried cables can be mitigated by laying bare earthing conductors beside the cables. These provide an alternative path for lightning current and prevent formation of harmful overvoltages over the sheath. Chang (1980) proposed this kind of implementation of metallic ground wires for the extra protection against lightning strikes. He also calculated theoretically optimal locations in proportion to the object under protection. However, the additional cost of extra protection like this would be probably too large because of material and installation costs to be used in large scale. However, for some special cases this might be useful preventive method as well. These could be for example areas with exceptionally high frequency of lightning strikes. In the case if there appears a need to increase the protection of buried cables in future, the shielding ground wires may be an effective way to do it. However, the efficiency of the shield wires should be somehow studied in practice if they are intended to be applied in large scale. By acting as a potential guiding electrodes the this kind of conductors would also prevent the failure risk arising by the ground potential rise.

As presented in the second chapter, there is a pale earthing conductor included in a normal AHXAMK-W cable. The sheathed individual phase conductors of the cable are stranded around it. It would be interesting to know if it could work as a preventing protection against overvoltages over the sheath. It would mean that structure of AHXAMK-W is less vulnerable to voltage stress over the sheath. Unfortunately, that could not be pointed out in this study since it would have required additional laboratory tests with the AHXAMK-W cable buried in soil sample. This experimental comparison of sheath vulnerability between a stranded cable type with pale earthing conductor like AHXAMK-W and a solid structured type like AXAL-TT and AHXCMK-WTC/PE would be especially useful today when network companies are investing significantly to underground electricity distribution. However, the effectiveness of the central grounding wire of stranded cable types should be compared to the version in which the grounding wire has been laid for example 10 to 30 cm above the cable. This kind of arrangement would probably offer more effective protection than the central grounding wire does. If the central grounding wire was replaced like this, it would not increase the material costs. Anyhow, it is most probable that even the central grounding wire will act as a potential guiding electrode and thus prevent at least partly the possible sheath failures due to ground potential rise in cases where the cable is far enough from the lightning strike point so that a direct soil breakdown to cable will not take place.

6.3.2 Temporary grounding of open ends

In Viitasaari case the cable joints and terminations were completed but the sheath was broken before the utilization of the cable line. As previewed before in the fourth chapter, the travelling wave caused voltage stress can be doubled at the open ends of a cable due to reflection of overvoltage pulse. This can be prevented by direct grounding of the open cable ends before the cable is connected to the grid. This method is already applied by Elenia. Suitable temporary grounding of a cable end is presented in the figure 6.5.

Figure 6.5*. Temporary grounding of an open end (Ericsson 2013b)*

First a screw is inserted into every phase conductor and metallic shield or screen. The screws are then connected together electrically with grounding wire. A rubber cap and electrical tape in the middle picture provide water tightness of the installation. The grounding wire is then attached to the grounding rod using a jubilee clip. This method prevents formation of harmful potential differences inside the cable structure as well as between the cable shield and earth.

During this study it was noticed that the completed cable terminations should make no exception in case of the temporary grounding instructions. They are open ends also until the connection or grounding is done. The figure 6.6 was added to the Ericsson grounding instructions (2013b) to improve the practices of temporary grounding and ensure the occupational safety during cable network construction.

The temporary grounding is clearly not as effective protection against soil breakdown or ground potential rise as shielding ground wires. It may only prevent from sheath failures in a case when a travelling surge due to lightning incident is low enough not to cause directly sheath breakdowns but would cause them due to reflections at the cable ends. However, it is a cheap and fast installation that should prevent reflections of travelling waves and it is especially important in enhancing occupational safety during cable network construction. An unconnected cable is in practice a capacitor which may be charged due to lightning activity or other abnormal electrical transient. Temporary earthing will fully prevent for this occupational safety risk.

***Figure 6.6**. Temporary grounding of terminated open ends (Ericsson 2013b)*

The grounding rod is not a low resistance grounding method but it is considered to be sufficient for a temporary grounding structure. However, if there is a low resistance grounding point available nearby like in figure 6.6, it should be always preferred over the grounding rod. However, it is important to notice that the given suggestions do not provide a total protection and such arrangement would likely be far too expensive or even impossible to construct.

7 CONCLUSIONS

The focus of this study was to evaluate the vulnerability of medium voltage underground cables to sheath damages caused by atmospheric overvoltages. Special interest was towards the buried but yet not utilized cables. However, during the study it appeared that the most likely failure mechanisms are not restricted to unconnected cables only. Lightning caused electric breakdown in soil and ground potential rise affect similarly on utilized cables as well. The reflections of travelling wave are still mitigated or avoided if the cable is utilized or temporary grounded. The open ends of the damaged cable in Viitasaari may have contributed to the puncture frequency in the cable sheath.

At the beginning of the study impulse voltage breakdown strengths of the cable sheaths were measured from the selected cable types. These levels were then compared to the results of theoretically calculated estimations discussed in the fourth chapter. As mentioned before the PE sheath of a modern underground cable is developed primarily to protect the cable against mechanical and chemical stress, moisture and UV degradation. Since electrical insulation is not the first ranked function of the sheath, there are no standardized maximum limits for the variation of breakdown strength of sheath.

7.1 Sheath punctures

The average breakdown strengths of the sheaths in the laboratory tests were about 150 kV or more. This level can be compared to the ground potential rise calculations to evaluate if the sheath punctures. The calculated estimations of the fourth chapter covered three different aspects. At first the effects of a soil breakdown on a buried cable were calculated based on the model of Song et al. (2002). In case of the soil breakdown, the breakdown strength of the sheath can be compared only to the voltage of the travelling wave proceeding in the shield after the sheath is already once punctured. When the soil breakdown channel reaches the cable the sheath is inevitably punctured as a result of the high voltage over the sheath. The results indicate that the breakdown distances in soil are usually approximately 10 meters or less in average Finnish conditions. An average maximum breakdown distance could be about 6 meters since that is resulted by an average 15 kA strike in a typical 3000 Ωm soil (figure 4.12). However, distances of 20 m or even 25 meters are not totally impossible either but they require a very high lightning current combined to high soil resistivity to happen.

If a cable buried at 10 m distance of the strike point is examined, the overvoltage of the travelling wave in the shield is about 500 kV in minimum if the breakdown channel extends to the cable. This is happened in soil resistivity of 5000 Ωm (figure 4.7). In this case the measured breakdown strengths of the cables are not enough to withstand the voltage stress. This may take place only with a high current lightning strike of at least 40 kA. The formation of lower overvoltages is not possible in this case because the breakdown channel of lower lightning currents will not even reach the distance of 10 m. If the cable lies at 5 m, the level of overvoltages of about 100-300 kV are possible. This is because the breakdown channel is now short enough for low lightning currents of about 8-20 kA to reach the sheath (figure 4.11). At this distance the sheath may be capable to withstand the voltage stress without multiple punctures if the lightning current is low enough.

The calculated breakdown distance results based on the model of Song et al. were similar to ones of their own (Song et al. 2002, figure 7.) However, the results of maximum breakdown distances based on Song's model (Song et al. 2002) change significantly if the experimental results of Mikhailov and Sokolov (1965, cited in Chang 1980) are counted in as the second aspect. They discovered that the resistivity of upper layers of soil limits the maximum current that can be injected into soil (figure 4.14). The results are anyhow confirmed only for soil resistivities between 100 and 1100 Ωm. While keeping this uncertainty in mind, the maximum breakdown distances may still be approximated for higher resistivities as well. The approximation in the figure 4.21 states that the breakdown distances of 10 meters and longer are very unlikely since they would require conditions with extremely high soil resistivity. In the confirmed conditions (100-1100 Ωm) the maximum breakdown distance with the limited current is about 5.5 meters. Based on that, Chang (1980) came up with a conclusion that a cable buried deeper than 5.5 m would be in safe from the lightning strikes. This conclusion has no relevance in the field since it is not a reasonably practicable suggestion in case of electricity distribution cables. The safety margin however is not the same if the distance is calculated in direction of ground surface because the current is not this way limited in case of a surface flashover. This is because the surface breakdown gradient of soil is lower that the internal soil breakdown gradient. When the long distances between the cable and strike point are discussed the role of current limitation is likely relatively small. This is because if the cable is buried in 0.7 meters and the distance to the lightning strike point is 5.5 meters, the breakdown channel likely proceeds along the surface of the soil at first and then goes into deeper soil layers. Based on this presumption the breakdown distances of 10 m and more can be possible again. The flashover over the surface of the soil should be studied more to give a proper estimations of the maximum breakdown distances in case of the channel forming along the surface.

The third aspect, ground potential rise, is the formation of voltage stress over the cable sheath without a soil breakdown. If the potential of the soil surrounding the cable momentarily rises higher than the measured average impulse voltage breakdown strength of the sheath, the sheath will be punctured. However, in this case the multiple punctures over longer cable distance unlikely occur since there is no high current going into the cable shield because of lack of the well conducting breakdown channel. With 10 kA lightning current in soil of 1000 Ωm the potential of 150 kV is reached at the distance of 10 m (figure 4.26). With the same current in the soil of 3000 Ωm the level of

150 kV is located at about 29 m. With higher currents the potentials are higher as well. However, the current limitation in the upmost layers of the soil affects the ground potential rise as well. In other words, it is not reasonable to calculate the potential rise with the currents of 30 kA and higher because that would require a very conductive soil to satisfy the terms of Mikhailov and Sokolov (1965, cited in Chang 1980) (figure 4.14).

It is important to notice that the soil breakdown and the ground potential rise are closely related to each other because the potential rises in the soil surrounding the breakdown channel. If a soil surface flashover occurs and then affects the cable in form of a soil breakdown or ground potential rise, the situation is more complicated and is not evaluated in this study. However, these kinds of combined processes may be usual and should be studied more together with the detailed electrical properties of soil surface.

Based on the models applied in this study, the length of soil breakdown may be 10 m and more only if the current limitation is not taken into account. If the soil surface flashovers occur, the extreme distances like 20 m might be possible, but as seen in the figure 4.5 they require extreme conditions as well. With ground potential rise the puncture seems to be possible even at distance of 30 m. However, while very long distances between the cable and the strike point are discussed, the uncertainty resulted by the assumption of homogenous soil becomes severe. As a rough estimation it could be said that cables lying at a distance of about 10 m are in the active danger zone. If the current limitation is not considered, the half of the lightning strikes will lead to soil breakdown to the cable at about 4.5 meters distance in typical Finnish resistivity conditions of 3000 Ωm. This is shown in figure 4.12 when keeping in mind that the median of lightning current in Finland is about 10 kA. A median lightning current is thus not high enough to cause a soil breakdown to 10 m distance. Instead, 50 kA current, which is carried by about 5 % of the negative strikes (figure 4.2), will lead to approximately 6 – 10 m soil breakdowns in 500 – 3000 Ωm soil, while in 5000 Ωm soil 10m breakdown distance may be caused by approximately 30kA current strike (figure 4.5).

The estimations of the breakdown lengths and levels of overvoltages in this study have many restrictions and uncertainties. The restrictions and uncertainties of the soil breakdown model were discussed in the chapter 4. The inhomogeneity of real soil adds uncertainties to the ground potential calculations as well.

7.2 Preventive measures and future research

As a preventive measure temporary grounding of shield or screen is a reasonable act. In the method the phase conductors and the shield are connected to each other and grounded together. The temporary grounding is especially important due to occupational safety because it ensures discharging of the cable capacitance in case it is charged due to some reason like lightning transient. The reflections of travelling waves are prevented as well when the effect of discontinuation point of the characteristic impedance is avoided or at least mitigated. The grounding should always be done to a large area grounding grid if it is available instead of separate grounding rod.

Use of additional shielding ground wires in soil parallel to the cables as a preventive measure would likely be too expensive in large scale when compared to the relatively low frequency of sheath faults. The supposed increase of sheath fault frequency should be monitored while the cabling rate is increased. Also sheath conditions of some cables that have been buried in high flash density area could be studied, since their sheath conditions are unknown and sheath faults can be hidden faults. The efficiency of shielding ground wires should also be studied in field conditions to evaluate the usefulness of the method. Possible benefits of ground wire already included to the structure of stranded cable types like AHXAMK-W are also worth some further research. It most probably mitigates at least to some degree sheath punctures due to ground potential rise in the cases where cable is far enough from the strike point not to cause a direct soil breakdown to cable. Vulnerability of the sheath would be one of the factors affecting whether the solid or stranded cable type was more reasonable choice to be applied in large scale distribution network investments. Also the difference in the shielding abilities of the central grounding wire and the shielding grounding wire above the cable is an interesting topic. The effect of current limitation of the upmost soil should be studied more in Finnish soil conditions as well. For the purpose of underground distribution network design the lightning effects in the soil from the surface to about one meter deep are the most interesting ones and should be focused in the future studies.

REFERENCES

Asimakopoulou, F. E., Gonos, I. F., & Stathopulos, I. A. 2009. Experimental investigation on soil ionization. Proceedings of the 16th International Symposium on High Voltage Engineering. pp 5.

Aro, M., Elovaara, J., Karttunen, M., Nousiainen, K. & Palva, V. 2003. Suurjännitetekniikka. Helsinki, Gaudeamus Helsinki University Press. pp 520.

Bogatin, E. 2000. What is characteristic impedance? [WWW]. [accessed on 3.9.2013]. Available at:
http://www.speedingedge.com/PDF-Files/BTS002_Characteristic_Impedance.pdf

Chang, H. T. 1980. Protection of Buried Cable from Direct Lightning Strike, Electro magnetic Compatibility, vol. EMC-22, no. 3, pp. 157-160.

Cooray, V. 2010. Lightning Protection. The Institution of Engineering and Technology, London, United Kingdom. pp. 1018

Energiateollisuus ry. 5.9.2013. Sähkönjakeluverkkoon investoidaan lähivuosina miljardeja [WWW]. [accessed on 10.9.2013]. Available at:
http://energia.fi/ajankohtaista/lehdistotiedotteet/sahkonjakeluverkkoon-investoidaan-lahivuosina-miljardeja

Elforsk. 1997. Mantelprovning av 12 och 24 kV polymerkablar: handbok. Stockholm. Elforsk rapport, 97:26.

Ericsson. 2013a. AXAL-TT PRO 12/20(24) kV Product Information

Ericsson. 2013b. AXAL-TT grounding instructions

Jing, Y., Jian-Guo W., Yang Z., Qi-Lin Z., Tie Y., Yun-Jun Z. &
Gui-Li F. 2010. Observation of ground potential rise caused by artificially triggered lightning, 2010 Asia-Pacific Symposium on Electromagnetic Compatibility (APEMC). pp. 1297-1300.

Haluza, D. 1996. Lightning, Ground potential rise, and electrical damage: Protecting Wayside Equipment on the MTA Long Island Rail Road. IEEE. 135 pp.

Hays, J. B. and Bodle, D. W., 1958. Electrical protection of tactical communication systems, Bell Telephone Lab. New York.

IEC.2006. International standard IEC 60071-1. Eight edition. pp 69.

IEEE. 2002. IEEE standard 1585 Guide for the Functional Specification of Medium Voltage (1-35 kV) Electronic Series Devices for Compensation of Voltage Fluctuations. pp 16.

Jolly, D.C. 1972. Contamination Flashover Part II, Flat Plate Model Tests. IEEE Trans. Vol. PAS-90, No. 6. pp 2443–2451.

Jägerskiöld, Claes. Sales Manager. Cables and Interconnect, Ericsson. E-mail conversations during 2013.

Kalliorinne, Turkka. Trainee, Construction and Materials, Elenia. Discussions during 2013.

Klairuang, N., Pobporn, W. & Hokierti, J. 2004. Effects of electric fields generated by direct lightning strikes on ground to underground cables, International Conference on Power System Technology, 2004. pp 1117-1121.

Kuffel, E., Kuffel, J., Zaengl, W. S. 2000. High Voltage Engineering Fundamentals. 2. edition. Butterworth-Heinemann Limited. pp 539.

Leadon, R.E., Flanagan, T.M., Mallon, C.E., and Denson, R. 1983. Effect of Ambient Gas on Arc Initiation Characteristics in Soil, IEEE Trans. on Nuclear Science, Vol. NS 30, No. 6. pp 4572-4576.

Mikhailov, M. I., Sokolov, S. A. 1965. Reducing the cost of protecting cable mains from direct lightning action, Telecommun., USSR, no. 6, pp. 50-53.

Mousa, M. Abdul. 1994. The soil ionization gradient associated with discharge of high currents into concentrated electrodes. IEEE transactions on Power Delivery, Vol. 9, No. 3, July 1994. pp 9.

Muhr, M., Pack, S., Haidvogl, H. & Kreyca, F. 1997. Effects of lightning strikes on 20 kV earthcables, Electricity Distribution. Part 1: Contributions. CIRED. 14th Interna tional Conference and Exhibition on (IEE Conf. Publ. No. 438), pp. 28/1.

Mutru, Mika. Recearch and Development Manager, Power Cables, Reka Cables Ltd. E-mail conversations during 2013.

Mäkelä, Antti. 2012. Lightning observations in Finland 2012. Finnish meteorological institute. pp 62.

Mäkelä, Antti. 2011. Lightning observations in Finland 2011. Finnish meteorological institute. pp 62.

Mäkelä, Antti. 2010. Lightning observations in Finland 2010. Finnish meteorological institute. pp 62.

Perala, R.A. 1982. The effect of soil conductivity and insulation dielectric strength upon lightning damage to buried insulated cables. Proceeding of International Aerospace Conference on Lightning and Static Electricity. Oxford, England. pp. F 1.1-F 1.8

Reka Cables. [WWW]. [accessed on 3.9.2013]. Available at:
http://www.reka.fi/products

SFS. 2009. SFS 6001+A1+A2 High-voltage electrical installations. Helsinki, Finnish Standards Association. pp 120.

SFS. 2008. SFS 5636 XLPE-insulated Al and Cu power cables. Design and testing. Helsinki, Finnish Standards Association. pp 69.

Simonen, Vesa-Matti. 2009. Keskijännitekaapeleiden terminen kuormitettavuus, Master of Science Thesis, Tampere University of Technology. pp 89.

Song, Z. 2004. A Numerical Model to Evaluate Characteristics of Lightning Break down Channels in Soils and Current Intercepted by Buried Cables. Doctoral thesis. pp 111.

Song, Z., Raghuveer, M.R. & Jingliang, H. 2002. Complete assessment of impact of lightning strikes on buried cables, 2002. IEEE CCECE 2002.
Canadian Conference on Electrical and Computer Engineering. pp. 30.

Sunde, E. D. 1968. Earth Conduction Effects in Transmission Systems. New York, Dover.

Sunde, E. D. 1945, Lightning protection of buried toll cable, Bell
Syst. Tech. J., vol. 24, pp. 253-300

Thue, W. 1999. Electrical Power Cable Engineering. Washington D.C. Marcel Dekker, Inc. pp. 307

Tiainen, E. 2001. Maadoitusresistanssien mittaukset. Sähköala 4/2001 pp. 3

Turpeinen, Pentti, Supervisor, Voiman Oy, Interview 10.5.2013

Vattenfall Verkko Oy. 2008. Kaapelin vaipan eheyden mittaus, Työohje. pp 3.

Vähäkuopus, Santtu. Specialist, Strategic Network Planning, Elenia. Discussions during 2013.

APPENDIX 1 :

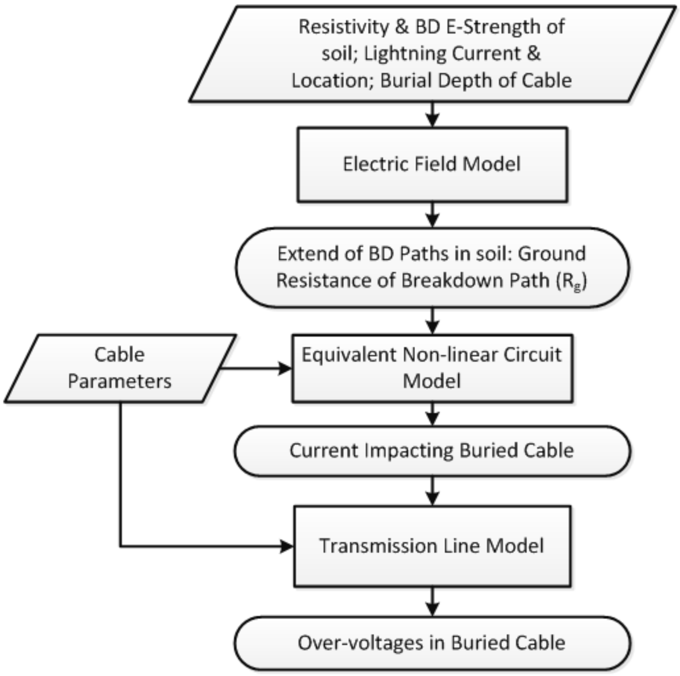

The combination of models used in evaluation of lightning strike caused cable stresses according to Song et al. (2002)